Order Number 9325164

The interactions of G-proteins with nucleotides probed by classical Raman difference spectroscopy

Weng, Gezhi, Ph.D.

City University of New York, 1993

U·M·I
300 N. Zeeb Rd.
Ann Arbor, MI 48106

The Interactions of G-Proteins with Nucleotides Probed by Classical Raman Difference Spectroscopy

by

Gezhi Weng

A dissertation submitted to the Graduate Faculty in Physics in partial fulfillment of the requirements for the degree of Doctor of Philosophy. The City University of New York.

1993

This manuscript has been read and accepted for the Graduate Faculty in Physics in the satisfaction of the dissertation requirement for the degree of Doctor of Philosophy.

Feb. 8 1993
Date

Robert Alfano
Chair of Examining Committee

March 30, 1993
Date

Joseph B. Krieger
Executive Officer

Frederick W. Smith

Supervisory Committee

The City University of New York

ABSTRACT

The Interactions of G-Proteins with Nucleotides Probed by Classical Raman Difference Spectroscopy

by

Gezhi Weng

Advisor: Professor Robert H. Callender

We explored the ligand binding pocket of two proteins, Elongation Factor Tu (EF-Tu) and *ras*-p21, both belong to the G-protein super family, by using ultra sensitive difference Raman techniques.

The Raman difference spectra of GDP minus 8D-GDP revealed that the conformations of bound GDP are both *c-2 endo anti* in the two proteins. The hydrogen binding status at 7-N position of the nucleotide are the same in proteins than in water.

The successes of incorporating nucleotide analogs IDP and 6-thio-GDP into the proteins made it possible to investigate the roles of the two polar "binding handles" of the guanine base, namely the 2-amino and 6-carbonyl groups. Raman results show that the 2-amino and 6-keto groups form strong hydrogen bonds with the protein. The interaction of the 2-amino group with p21 is stronger than with EF-Tu, while the interaction at 6-keto position is weaker in p21 than in EF-Tu. The binding pocket of p21 is more hydrophobic than that of EF-Tu. The difference spectra formed between GDP and 6-^{18}O-GDP confirmed these results obtained by using chemically modified nucleotides.

Isotopically labeled nucleotide, β-$^{18}O_4$-GDP, is used to study phosphate bindings to the proteins. Phosphate vibrations of GDP are found to be strongly affected by protein binding.

The results of the difference Raman spectra of the active form of the proteins (the GTP binding forms) and the inactive form of proteins (GDP binding forms) show that protein conformations of the two forms are different, at least part of the hydrogen bonded peptide back bone has been changed during protein activation. Tyrosine residue(s) and a cysteine residue of EF-Tu are involved in the conformational changes. The phosphate vibrational band, which is present in the difference spectrum of GDP minus GTP, is buried under protein changes in EF-Tu, but can be observed in the p21 difference spectrum. The data seem give evidence that the triphosphate back bone of GTP has the same conformation in protein than in solution.

Most of results obtained from difference Raman spectroscopy, such as the conformations of the nucleotide and the existance of the hydrogen bonds and are consistant with the x-ray studies. However, our Raman studies are able to give the relative strength of the hydrogen bonds, which is hard to get from x-ray results.

In the process of finding week nucleotide peaks using difference Raman spectroscopy, it was found that this technique is also very sensitive to protein hydrogen-deuterium exchanges, A few un-exchanged protons may obscure the weak nucleotide peaks of the difference Raman spectra formed between different protein-nucleotide complexes in amide I region.

I dedicate this thesis to my parents

ACKNOWLEDGMENT

I like to express my deep gratitude to Professor Robert Callender for his guidance and inspiration. The pleasant atmosphere that he and all the other people in the lab created, made it possible for me to be able to devote my all attention to my research project during these years. His style of research has had a great influence on me.

I thank Dr. Danny Manor for leading me, after one year of unsuccessful protein purification, into an active research field which was new and exciting to me. I thank him for sharing those happy and frustrating moments of my experiments. I have been benefited a lot from his advice and helps.

I thank Dr. Hau Deng for many valuable advices and fruitful discussions. His extensive experiences and clear discernment were always good guidance for my research.

I like to thank Dr. James Ball for his efforts to improve the instruments in the lab, which made many of these measurements possible.

I feel grateful to Dr. Sharon Cosloy and Dr. Valeria Balogh-Nair for the advice and the help that they offered me in my research.

I like to give thanks to Chunxiang Chen and Zhenjia Chen for synthesizing the compounds used in my experiments. I also like to thank Dongguang Xiao, Yongqing Chen, Lewen Huang and Dr. Jeron Van Beek for their constant help in my routine laboratory work.

Finally I like to thank my parents for their encouragement, patience and tolerance over the years. It was, partly, for their expectations, that I have worked very hard trying to finish my work.

CONTENTS

Abbreviations

p21,	gene product of the human *c-H-ras* proto-oncogene;
EF-Tu,	Elongation Factor Tu from *E. coli;*
EF-Ts,	Elongation Factor Ts from *E. coli;*
GDP,	guanosine 5′ diphosphate;
8D-GDP,	8-deuterium GDP
GDPβS,	Guanosine 5'-*O* -(2-Thiodiphosphate);
IDP,	inosine 5'diphosphate;
6-thio-GDP,	6-thioguanosine 5' diphosphate;
6-hydro-GDP,	2-amino purine ribose 5' diphosphate;
6-^{18}O-GDP,	guanosine 5′ diphosphate with ^{18}O label at 6 position;
β-$^{18}O_4$-GDP,	guanosine 5′ diphosphate with tetra ^{18}O labels on β phosphate;
GDP-NH_2,	guanylyl(β–amino)-diphosphate;
GMP-PCP,	guanylyl(β,γ-methylene)-triphosphate;
GMP-PNP,	guanylyl(β,γ-imido)-triphosphate;
Tris,	tris(hydroxymethyl)aminoethane;
dGDP,	deoxy-guanosine 5′ diphosphate;
PMSF,	phenylmethylsulfonyl fluoride;
EDTA,	(ethelenedinitrilo)-tetracetic acid;
RP-HPLC,	Reverse phase high performance liquid chromatography;
DMSO,	Dimethyl Sulfoxide;
DTE,	1,4-dithioerythritol;
DTT,	dithioreitol;
IPTG,	isopropylthiogalactoside

LIST OF TABLES

LIST OF FIGURES

CHAPTER I

INTRODUCTION

A number of key cell functions (proliferation, hormone response, neurotransmission, and protein biosynthesis) are regulated *in vivo* by members of a family of guanine nucleotide binding proteins, so called G-proteins. These proteins share strong functional and structural homologies ([1-4]). G-proteins act as molecular switches that turn on and off certain biological processes. These switching functions are tightly controlled by the nature of the bound nucleotides. Normally, a G-protein contains GDP in a specialized binding site and has no biological activity associated with it. A particular stimulus triggers the exchange of bound GDP to GTP, and thereby alters the conformation of the protein and activates its biological function. Intensive research has been carried out to understand how these biological functions are stimulated by G-protein systems and how the GTP and GDP forms can cause such dramatically different biochemical processes. It is thus of considerable interest to explore the interactions between the bound nucleotides and these proteins.

The G-proteins we have chosen to study are bacterial elongation factor protein EF-Tu and the *ras* p21 protein. These two proteins are the best studied G-proteins to date. Their high resolution X-ray structures have been obtained, providing useful guidances to the spectroscopic studies on molecular interactions.

Elongation factor Tu (EF-Tu) is involved in the chain elongation step of bacterial protein synthesis (Figure 1.1). When GDP is exchanged by GTP, a reaction catalyzed by EF-Ts, the "quiet" EF-Tu complex, becomes activated. EF-Tu•GTP binds aminoacyl-tRNA and carries it to the protein synthesis site on the mRNA-programmed ribosome. GTP is then hydrolyzed, the aminoacyl-tRNA is positioned at the A site of the ribosome prior to subsequent peptide bond formation, and a binary complex of EF-Tu•GDP is released ([5]).

EF-Tu's 393-amino acid polypeptide chain is folded in three distinct domains (Figure 1.2a). The N-terminal domain (residues 1-200) binds GDP or GTP, the middle and C-terminal domain play essential roles in regulating the activity of the N-terminal domain of the intact molecule as well as in the interactions of EF-Tu with aminoacylated tRNA, elongation factor Ts, and the antibiotic agent kirromycin ([6]). The GDP molecule binds to the surface of N-terminal domain (also called G-domain) of EF-Tu. The guanine ring is partly buried in a cavity defined by the residues Leu175, Thr26 and the side chain of Lys136. With an acceptor to donor distances of 2.7 Å, the main chain nitrogen of Asn135 can form hydrogen bond to 6-O of guanine. Asp138 can form hydrogen bonds to 1-N and 2-N of guanine, both of which are located 2.9 Å away from the carboxyl oxygens of Asp138.

Ras-p21 is a small protein (~21kd), which has been found to be mutated in approximately 30% of human tumors. The cellular roles of this protein are unclear, but it is believed to be involved in a growth-promoting signal-transduction pathway. The intrinsic GTPase activity of p21 is relatively low. In the active GTP-bound form, *ras*-p21 interacts with the GTPase activating protein (GAP) ([7]), which is either an effector of *ras* action or its negative regulator. The interaction between p21 and GAP ensures that p21 is maintained in the GDP bound conformation. Single mutations at certain positions (i.e. position 12, 13, 35 or 61) of p21 reduce its intrinsic and GAP-induced GTPase activities, thereby allowing these mutants to stay in the active GTP-bound state over prolonged time ([8]), which lengthens the transmission of the growth signal, resulting in unregulated cell growth. Two other cytosolic proteins, *Ras*-GNRF (Ras-guanine nucleotide-releasing factor ([9]) and an inhibitor of GTPase activity ([10]), were found also to interact with *ras*-p21.

The topological order of the secondary structure elements of *ras*-p21 is found to be the same as the N-terminal domain of EF-Tu (Figure 1.2b). The roles of Ala146 and Aps119 in p21 are similar to those of Asn135 and Asp138 in EF-Tu. The carboxylate group of Asp119, which is located in the guanine-specificity region, contacts with the exocyclic 2-amino group and the endocyclic 1-N of guanine. Asp119 is also close enough to interact with the side chain hydroxyl of Ser145 and with the amino group of Lys147. Similar to Asp138 in EF-Tu, mutation of Asp119 drastically reduces the affinity for guanine nucleotide ([8]). The conserved sequence motifs Asn116-Lys-X-Asp119 and Ser145-Ala-Lys147 of guanine binding pocket are identical in the great majority of guanine nucleotide binding proteins ([11]).

X-ray studies also show that there are several hydrogen bonds between phosphate groups and the conserve consensus sequence Gly-X-X-X-X-Gly-Lys-Ser/Thr motif of the phosphoryl binding loop. As is generally the case for dinucleotide binding proteins, the phosphate binding site of these G-proteins is stabilized by the positive dipole moment of this helix, of which the carbonyl oxygen atoms in the loop all point in a direction away from the β-phosphate.

Vibrational spectroscopy provides a wealth of information on the conformations and structures of molecules, particularly small molecules, as well as protein-ligand interactions, like hydrogen bonding which perturb a molecule's electronic distribution. In this latter case, the modified electronic distribution results in modified vibrational force constants, sometimes along quite well defined and important coordinates. Thus, the changes observed in the vibrational spectra of a bound ligand are a direct measure of how a protein acts upon it. In contrast to x-ray crystallography, which provide coordinates of atoms in a molecule, Raman frequencies are directly related to the force field. An important experimental constraint, however, in the use of vibrational spectroscopy has been that the signals from proteins are generally much greater than those from bound ligand. The signals of the bound ligand, or other small protein molecular moieties, are difficult to isolate. One approach in overcoming this difficulty is to employ resonance Raman spectroscopy (cf. [12, 13]). In this case, the exciting laser light is in resonance with a chromophore, thus, yielding greatly increased Raman cross sections. A number of very important chromophoric protein systems have been so studied. Unfortunately this approach is limited to proteins which contain relatively isolated chromophores.

Our group has succeeded previously in describing complex formation between enzymes, their substrates and co-factors in a family of dehydrogenases (cf. [14-17]), to a level of quantitating hydrogen bonding patterns ([18]) and *in situ* protonation states ([19, 20]), using ultra sensitive non-resonance Raman difference techniques. This thesis work is focused on the efforts of enlarging and applying this technique to EF-Tu and p21 as representatives of the GTPase super family. We were trying to answer questions such as what are the specific interactions that anchor the nucleotide in the active site of these G-proteins, how strong are these interactions, and what kind of protein changes may switch the proteins from their "off" states to their "on" states. In earlier studies of our group, the non-resonance Raman spectrum of a enzyme-substrate complex was measured as was that of the enzyme itself. The difference spectrum between these two was obtained by subtracting the two spectra numerically, and it contains ligand bands which arise from the bound substrate as well as protein bands which arise from protein changes induced by substrate binding. This procedure can not be used for G-proteins, because these proteins are unstable without bound ligand. We therefore have taken somewhat different approaches in this study. The bound nucleotide is replaced by a nucleotide derivative, which has been either isotopically labeled or chemically modified at a selected position, and the spectra of the protein-nucleotide and protein-nucleotide derivative are taken. The difference spectrum formed between these two then arises from modes which are affected ("edited") by the labeling or modification, and all other parts of the Raman difference spectrum subtract to zero.

We report here our results on the Raman spectra of EF-Tu and *ras*-p21 containing GDP, GTP or other nucleotide analogues. Some spectral assignments are made, and protein influences on ligand binding, as well as possible protein conformational changes, are discussed. The analysis is compared to high resolution X-ray results for the GDP ([21]) and GTP ([8, 22, 23]) forms of p21 and the GDP form of EF-Tu ([24-26]). This is of interest because an X-ray diffraction analysis of the GTP conformation of EF-Tu is as yet unavailable. Moreover, the procedures used here may be employed to obtain vibrational data of membrane bound proteins, a very substantial class for which X-ray diffraction studies may be far in the future.

Figure 1.1: A cartoon of the biological function of EF-Tu ([27]).

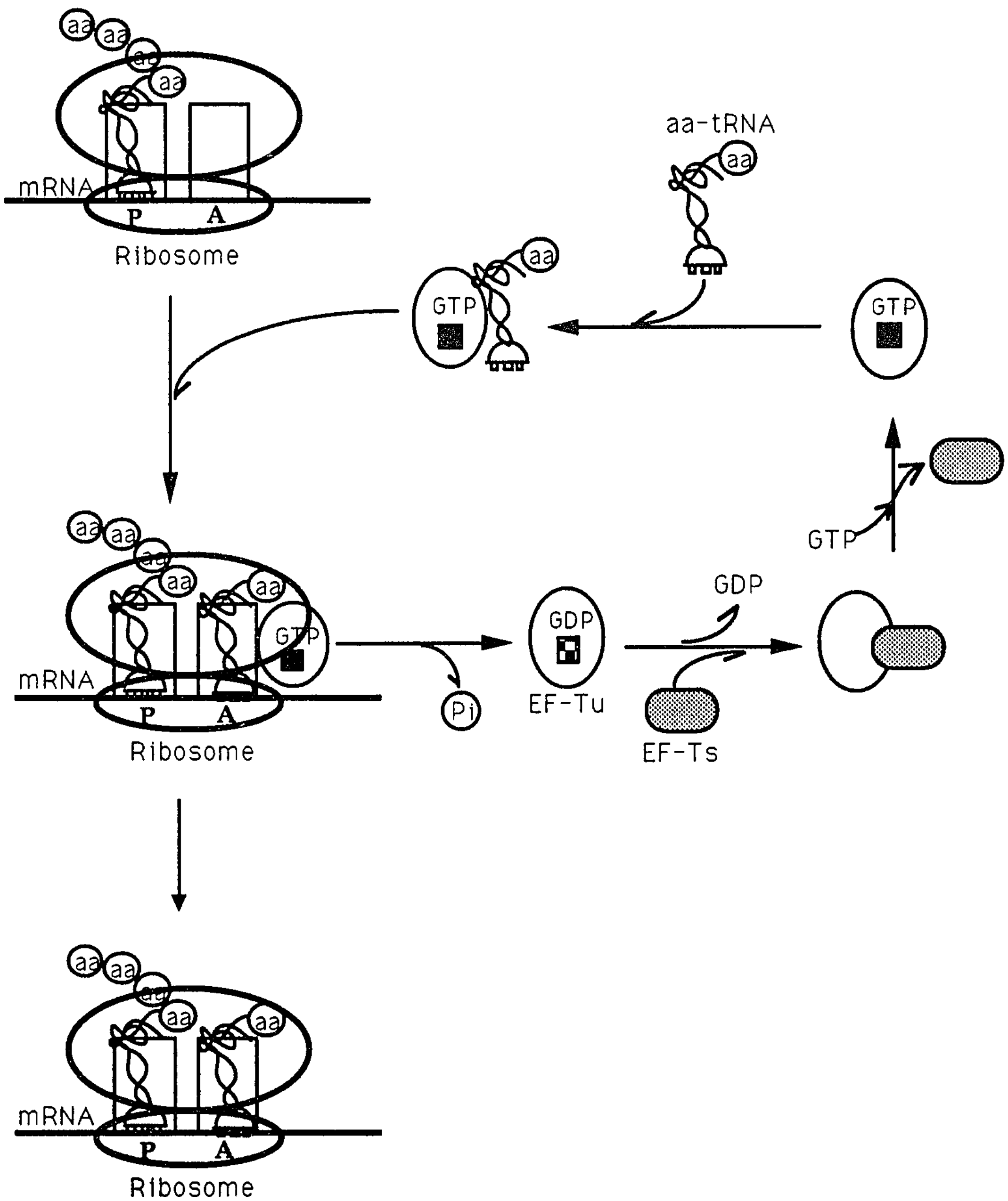

aa
aa
aa
aa
mRNA
P
A
Ribosome
aa-tRNA
aa
GTP
aa
GTP
GTP
GDP
GDP
EF-Tu
Pi
EF-Ts
mRNA
P
A
Ribosome
aa
aa
aa
aa
aa
mRNA
P
A
Ribosome

Figure 1.1

Figure 1.2: (a) Three dimensional model of the three domains of the EF-Tu. Domain I (G-domain) is the nucleotide binding domain (amino acids 41-59 were not shown, [28]). (b) Structure cartoon of the G domain of *ras*-p21 ([29, 30]). β-strands are drawn as arrows, α-helices as curled ribbons, and loops as double lines. The GTP locations is approximate, known and hypothetical interaction sites are labels.

(a)

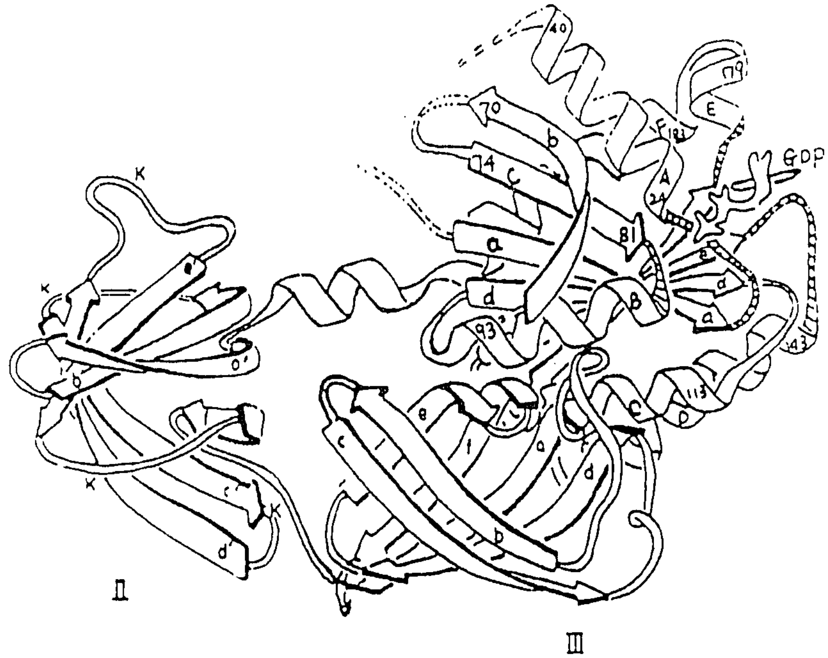
GDP
I
II
III

(b)

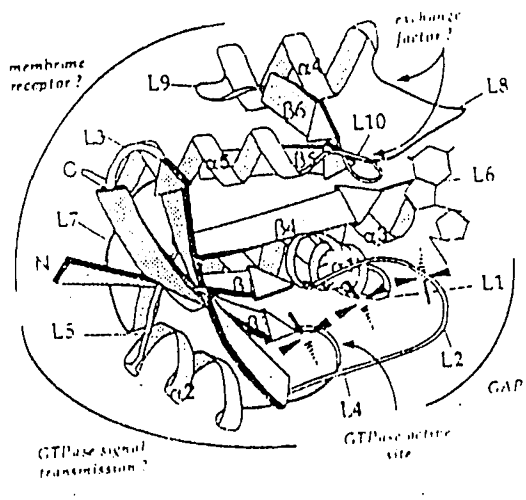
membrane
receptor ?
exchange
factor ?
L9
L8
L10
L3
L6
C
L7
N
L1
L5
L2
L4
GAP
GTPase signal
transmission ?
GTPase active
site

Figure 1.2

CHAPTER II

CLASSICAL RAMAN DIFFERENCE SPECTROSCOPY

A. Raman Scattering

The physical origin of Raman scattering lies in the inelastic collisions between molecules and photons. The frequency of scattered light is shifted relative to the incident light by the amounts corresponding to the normal mode frequencies of the molecular vibrations. In each normal mode, all the atoms in the molecule vibrate with same frequency, and all atoms pass through their equilibrium positions simultaneously. Figure 2.1 shows some of the possible consequences of a photon-molecule interactions, including Raman process, in which the upward-pointing arrows indicate the combination of a photon with the molecule, the downward-poiting arrows indicate the release of a photon after a very short time interval ($<10^{-13}$ second for Raman process). The lengths of the upward-pointing arrows are proportional to the frequencies of the incident light while the lengths of the downward-pointing arrows are proportional to the frequencies of scattered light. In the normal Raman scattering process, the incident light brings the molecule up to a virtual energy state, the molecule scatters light and returns to a different vibrational level on the ground electronic state. The frequency of the scattered light is, thus, shifted from that of incident light.

The positions of Raman peaks are properties solely of the electronic ground state, while the Raman amplitudes are functions of both ground- and excited-state electronic structures.

B. Group Frequencies

Because of their high molecular weight, Raman spectra of proteins, protein-ligand complexes or even large ligands themselves are usually very complicated. It is very hard to understand and interpret Raman spectra of these molecules by normal mode calculations, which attempt to solve the equations of motion for all the atoms in the molecule using normal coordinates. For most compounds, some characteristic vibrational frequencies are found to be correlated with certain chemical functional groups. These vibrational modes are called group frequencies. The existence of group frequencies is attributable to the fact that the force constant for a given chemical bond is, to a degree, transferable form one molecule to another. Group frequencies find their maximum usability when they are relatively easy to be identified from other Raman bands and when they vary with environmental interactions. We will use mainly the concept of group frequencies to interpret our Raman results.

Proteins and synthetic polypeptide consist of amino acids joined together by peptide bonds. These peptide bonds give rise to many different types of vibrational modes. Among them the most important group vibrations are amide I and amide III in-plain vibrational modes (Figure 2.2). These modes are correlated with structure properties of protein molecules ([31]).

C. Instrumentation

Figure 2.3 shows the typical instrumental set up of our Raman experiment. A laser beam is introduced through the sample. The scattered light is collected in 90 degrees and focused on the entrance slit of a spectrometer. The gratings in the spectrometer disperse the incoming light into a spectrum of frequencies. This spectrum is transformed into electronic signal by a detector, and then sent to a computer for analysis.

The laser sources available in our laboratory are a 4-Watt argon ion laser from Spectra Physics (model 165), a 5-Watt krypton ion laser (model No. CR-2000, Coherent Radiation Inc.) and a 25-Watt INOVA-200 argon ion laser (Coherent Radiation Inc.). The sample holder can hold a double or a triple split cuvette specially designed for measuring several spectra under the same conditions, and each sample space of the split cell has a dimension of 2.5x2.5mm. The cuvette is set on a computer controlled stage which can be moved to within 1 μm accuracy. Raman spectra are measured by a Triplemate spectrometer (Spex Industries), equipped with a solid state detector system (model DIDA-1000 water cooled photodiode array and a model ST-100 detector controller; Princeton Instruments), or a charge coupled detector (CCD) system (CCD model LN/CCD-1152UV liquid nitrogen cooled and a model ST-135 detector controller; Princeton Instruments). Data are acquired, stored and analyzed on a Mac-II computer (Apple, Cupertino CA). Spectral lines are calibrated against known Raman lines of toluene or benzene and are accurate to within ± 2 cm^{-1}. The spectral resolution of the instruments is typically set to 6 cm^{-1} full width at half maximum.

D. Difference Raman Spectroscopy and Its Resolution

To study protein-ligand interactions we intend to measure the Raman spectrum of bound ligand or other small protein molecular moieties. An important experimental constraint, however, in the use of vibrational spectroscopy has been that the signals form these part of the complex are difficult to isolate. Because of the smaller mass of the ligand, compared to that of the protein, signals from the former are generally overwhelmed by background vibration bands form the protein itself. This difficulty has been largely overcome in recent years using Raman difference spectroscopy ([14, 17, 32]). The Raman spectra of protein-ligand complex as well as that of apo-protein are measured under same conditions. The protein spectrum is numerically subtracted from the complex spectrum after the measurements. The difference spectrum thus obtained, contains the signals of bound ligand, as well as protein changes induced by ligand binding. The operation can be represented by:

Spectrum (enzyme•L) - Spectrum (enzyme)

= Spectrum (L in enzyme) + Spectrum (protein changes) .... (1)

where L represent a cofactor, inhibitor or substrate of the enzyme.

This procedure, however, is not suitable for proteins like EF-Tu and p21, which are unstable without bound ligand. An alternative route we have taken to get the difference spectra of these proteins is represented by the following:

Spectrum (G•L1) - Spectrum (G•L2)

= Spectrum (L1-L2 in protein) + Spectrum (protein changes) .... (2)

The bound nucleotide (L1) is replaced by a nucleotide derivative (L2) either isotopically labeled or chemically modified at a selected position, and the spectra of the protein-nucleotide and protein-nucleotide derivative are taken. The difference spectrum formed between the two complexes, G•L1 and G•L2, arises from modes which are affected by the specific labeling or modification. If L2 is L1 molecule isotopically labeled at certain position, the protein changes at right side of the Equation (2) should be zero, since G•L1 and G•L2 have same chemical properties. If L2 is chemically modified L1 molecule, the second term at right side of Equation (2) is, generally, not zero. We have found that the signal from the protein changes generally has a magnetite of 0.5 to 1% of amide I intensity.

To get accurate difference spectra and to avoid artifacts, we use a split cell (Figure 2.3) to measure several samples. The temperature and humidity in the room, where the measurements are taken, are controlled to be nearly constant. Arrangements like these are used to reduce the influences of different optical properties for the different samples and to control the environment fluctuations which may affect accuracy of the measurements. The long term drift of the optical system can be canceled out if we take the spectra in a sequential way and line up the spectra before adding them together. A detailed procedure of the alignment is described as follows: assume sample A is a stable protein-ligand complex, sample B is another stable protein-ligand complex different from A. The spectra of A and B are measured in a $A_1B_1A_2B_2....A_nB_n$ fashion, each run taking 10 to 20 minutes. The sets of data are then checked by the subtraction A_n-A_{n-1}, A_n-A_{n-2}, ..., A_n-A_1 and B_n-B_{n-1}, B_n-B_{n-2}, ..., B_n-B_1. All the results of the subtractions should give a flat featureless background. If the difference spectrum shows features of derivative-like signals, the subtracted spectrum may be shifted first and then subtracted (Figure 2.4). The amount of shifting, usually 0.01 cm^{-1} to 0.8 cm^{-1}, is determined by the disappearance of the derivative peaks in the difference spectra. The amount of the shift can also be calculated from band shape. Assume $I(\nu)$ is the Raman intensity of a spectrum, δ is a small amount, then

$$\Delta I(\nu) = I(\nu+\delta) - I(\nu) \approx \delta\, \partial I(\nu)/\partial\nu \qquad \text{.... (3)}$$

If a band is Lorentzian with a intensity at the center I(0) and the full width at half-maximum Γ, we find that

$$\Delta I_{max} / I(0) = 1.9\, \delta / \Gamma \qquad \text{.... (4)}$$

therefore, the amount of shifting is

$$\delta = \Gamma\, \Delta I_{max} / (1.9\, I(0)) \qquad \text{.... (5)}$$

If the spectroscopic features can not be corrected by shifting, the corresponding spectrum should be discarded. All the spectra taken for the same sample are then added together as A or B. To get the difference spectrum, B is subtracted from A. The disappearance of protein characteristic bands, i.e. bands from phenylanaline around 1000 cm^{-1}, methylene band around 1450 cm^{-1}, amide III band at 1200-1300 cm^{-1} region and amide I band at 1600-1700 cm^{-1} region should be taken as the criteria of the extend of the subtraction. Sometimes, the phenylanaline peak does not be subtract out, and a small spectrum shift may be necessary in this case.

Figure 2.4 and 2.5 show two examples of the data manipulation mentioned above. The difference spectra is formed between two different runs of the EF-Tu•GDP complexes (Figure 2.5a,b). Before shifting, the difference spectrum shows number of derivative-like features (Figure 2.4c). From the intensity and width of the original peak, and the intensity of the derivative peak, the amount of shift calculated according to Equation (5) is about 0.65 cm^{-1}. After 0.63 cm^{-1}

right shift (Figure 2.4d), not only phenylanaline peak, but all the derivative-like features, are subtracted out, leaving only the short noise.

Figure 2.5 shows the difference spectrum formed between EF-Tu•GDP and EF-Tu•6-^{18}O-GDP. The phenylanaline peak shows up as a strong derivative-like peak at around 1000 cm^{-1} (Figure 2.5a). The amount of shifting necessary to get rid of this derivative-like peak, according to Equation (5), is calculated to be 0.061 cm^{-1}. The difference spectrum formed after shifting the spectrum of EF-Tu•6-^{18}O-GDP by 0.06 cm^{-1} (Figure 2.5b) has almost the same features as the unshifted difference spectrum. The phenylanaline peak disappeared, while the positions and intensities of all the other major peaks are not affected by the shifting.

For the G-proteins studied here, the intensity of the highest nucleotide peak is about 3% (for EF-Tu) to 6% (for ras-p21) that of the protein amide I peak. With careful measurement, intensity differences as little as 0.1% of the most intense Raman peaks can be detected by our experimental system.

Figure 2.1: The energy diagram of photon-molecule interactions. The lengths of the upward-pointing arrows are proportional to the frequencies of the incoming light while the lengths of the downward-pointing arrows are proportional to the frequencies of the scattered light. The curled lines represent non radiation relaxing process. The vibrational quantum numbers in the upper and lower electronic states are n and n' respectively. The frequencies of incident light are υ_0, while that of the scattered light are υ_1. The energy gap between the lower vibrational levels is υ_{vib}.

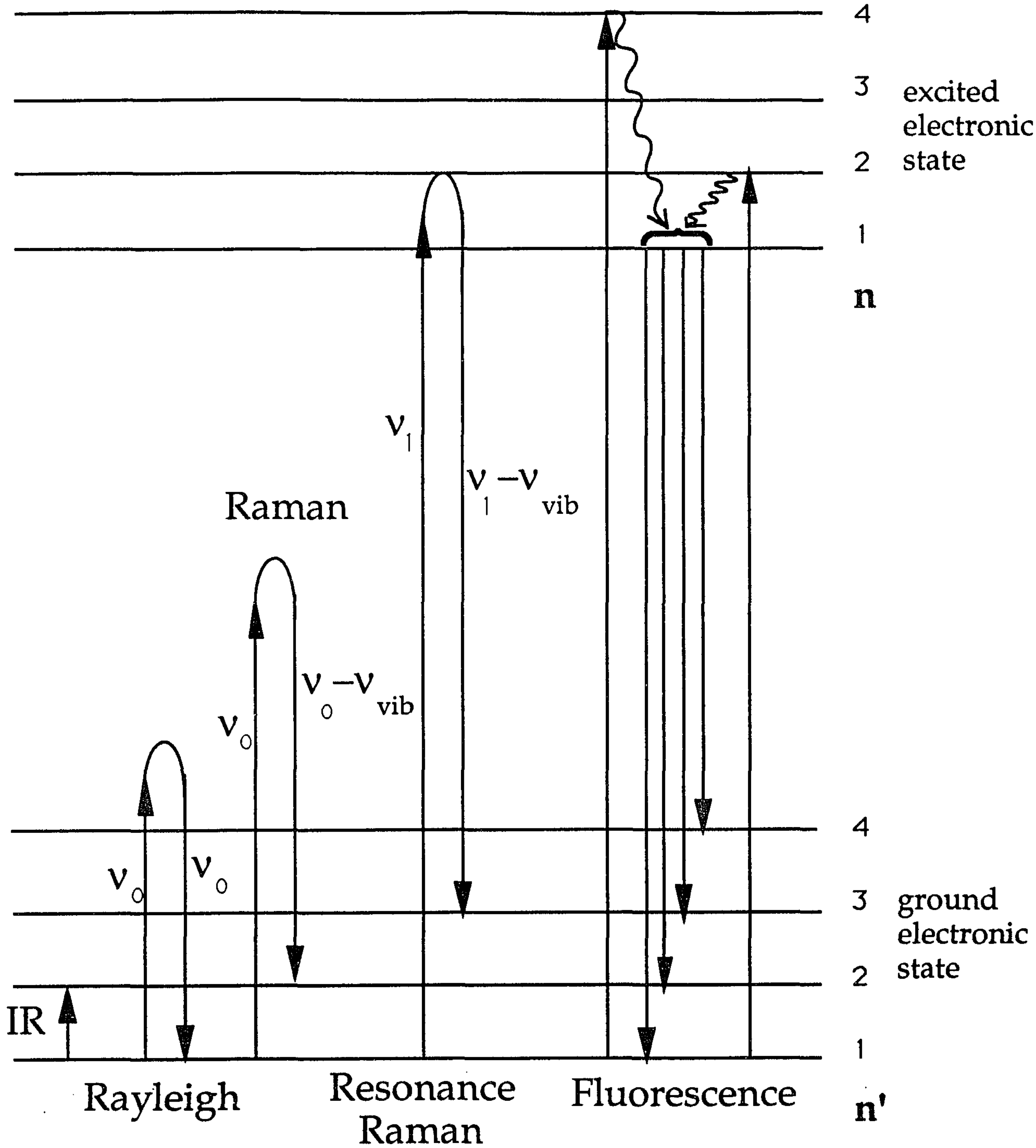

4
3 excited
electronic
2 state
1
n
ν_1
$\nu_1 - \nu_{vib}$
Raman
$\nu_0 - \nu_{vib}$
ν_0
ν_0
ν_0
4
3 ground
electronic
2 state
1
IR
Rayleigh
Resonance
Raman
Fluorescence
n'

Figure 2.1

Figure 2.2: The amide I (a) and amide III (b) group vibrations.

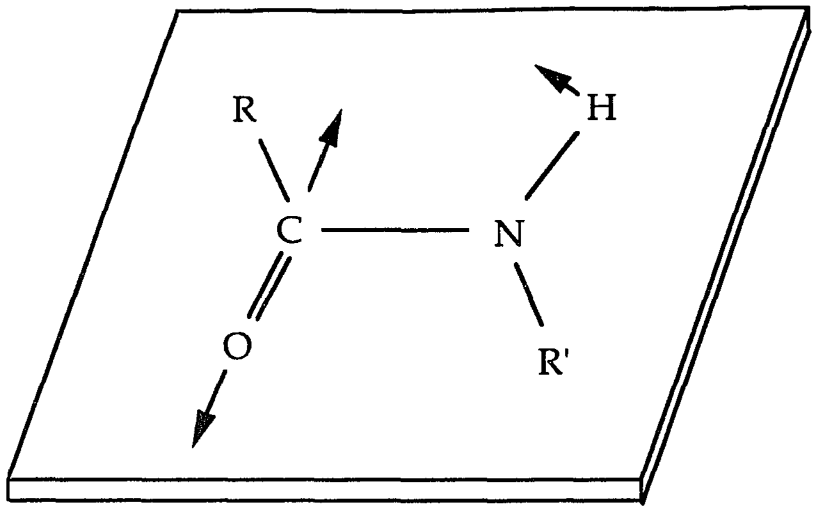

Amide I

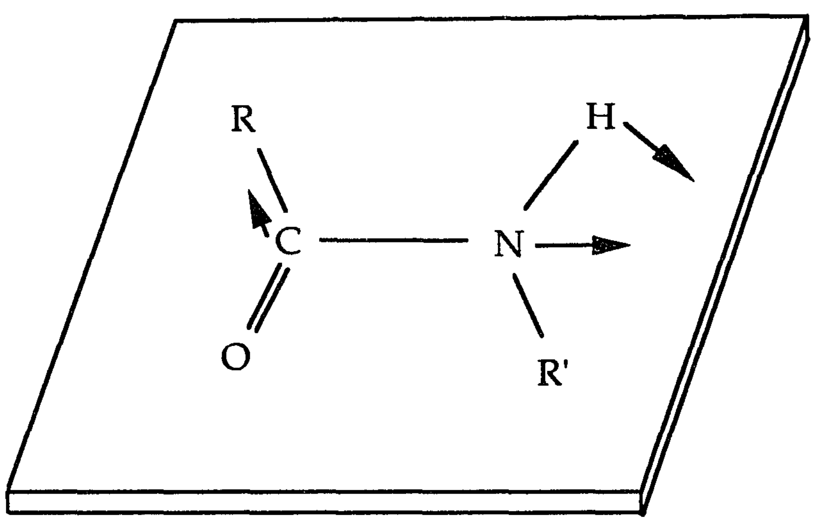

Amide III

Figure 2.2

Figure 2.3: A schematic drawing of the instrumental set up for Raman measurement. The monochromatic light emitted from a laser source is introduced through the sample. The scattered light is focused on the entrance slid of a triplemate monochrometer. The spectrometer disperses the incident light into a frequency spectrum and focus it on to a detector. The spectrum was converted into electrical signals, either by a multi-channel photo diode array or by a charge coupled device, and transferred to a computer for analysis.

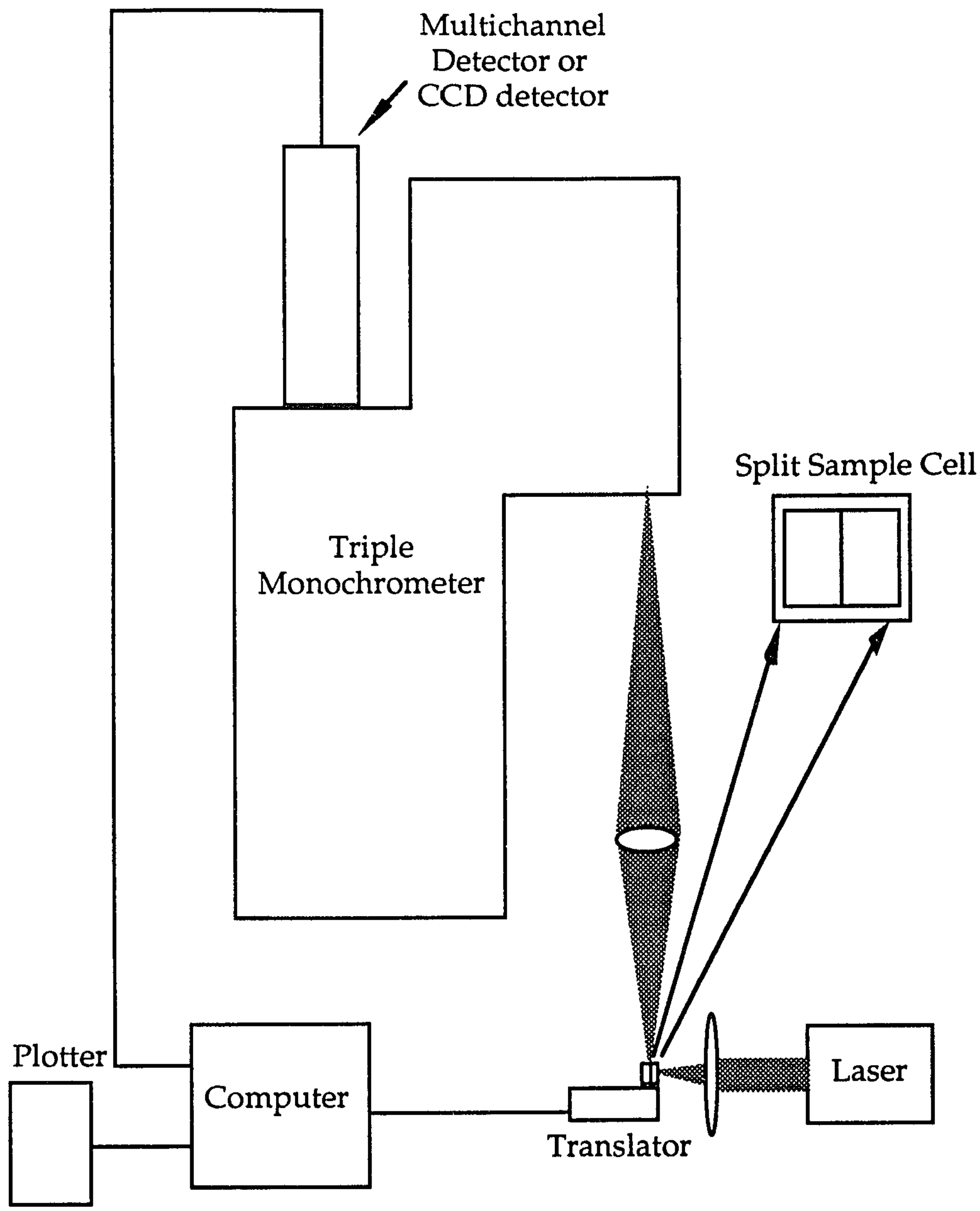
Multichannel
Detector or
CCD detector
Split Sample Cell
Triple
Monochrometer
Plotter
Computer
Laser
Translator

Figure 2.3

Figure 2.4: An example of spectrum "line-up". Spectra p21•GDP_1 (a) and p21•GDP_1 (b) are collected from two separate runs for same sample. Both data sets are collected for about 15 minutes. Without shifting, the difference spectrum (c) shows some derivative-like features. The intensity of the phenylanaline peak is as large as 20% of amid I intensity in this case. The amount of 0.65 cm^{-1} shift is necessary to subtract out phenylanaline peak at 1003 cm^{-1} according to Equation (5). The differences spectrum formed with p21•GDP_2 right shifted 0.63 cm^{-1} (d) shows, not only phenylanaline peak, but all the other small derivative-like features, are subtracted out, left only the short noise. The intensity of the spectrum in (d) is magnified 4 times.

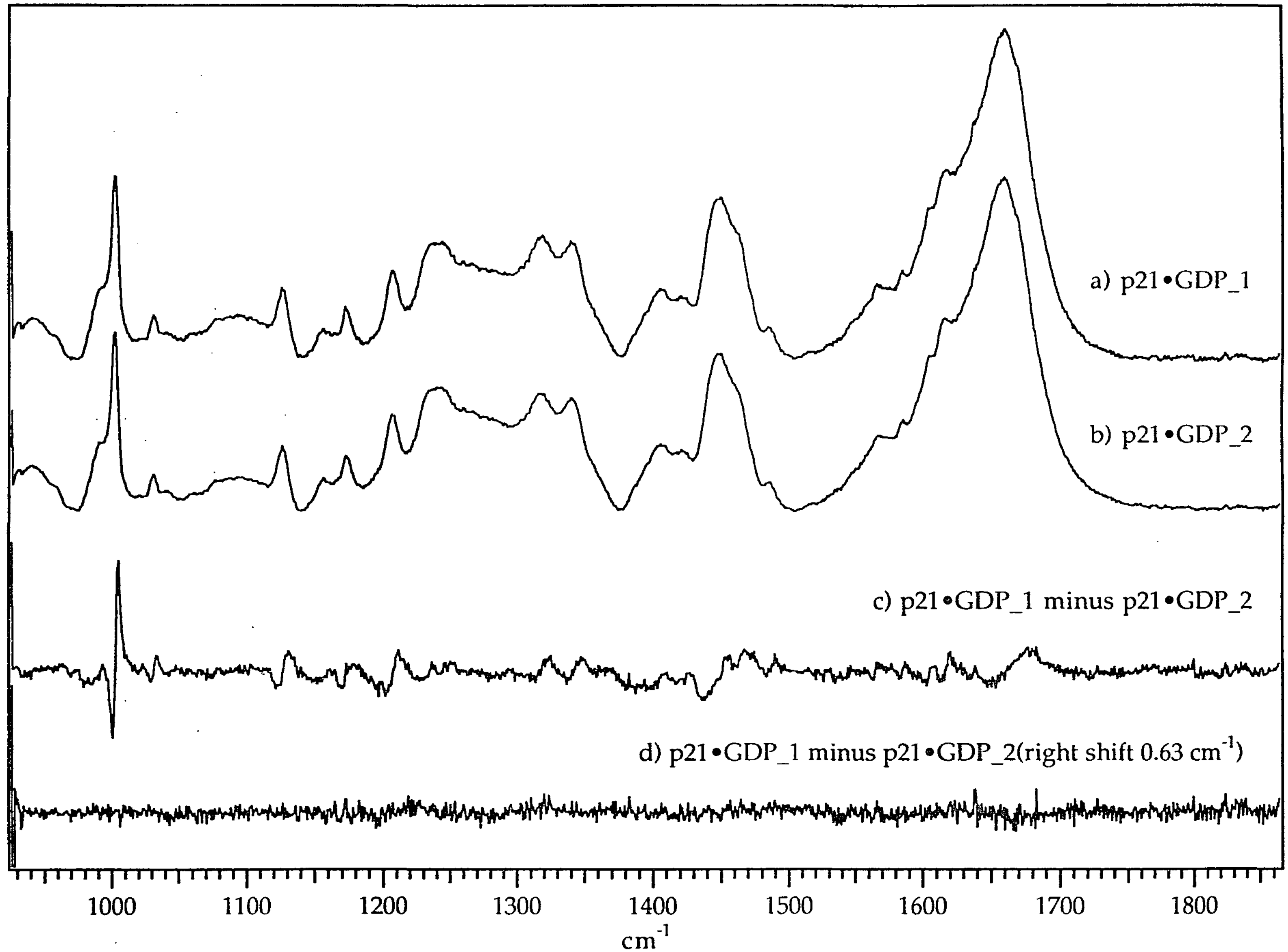
a) p21•GDP_1
b) p21•GDP_2
c) p21•GDP_1 minus p21•GDP_2
d) p21•GDP_1 minus p21•GDP_2(right shift 0.63 cm-1)
1000
1100
1200
1300
1400
1500
1600
1700
1800
cm-1

Figure 2.4

Figure 2.5: The effect of spectrum shift to the difference spectrum. Without shifting, the difference spectrum (a) shows an intense derivative-like peak from phenylanaline residue at around 1000 cm^{-1}. The intensity of this peak is about 5% of the amide I intensity. The amount of 0.061 cm^{-1} shift is necessary to avoid this artifact according to Equation (5). The differences spectrum formed with the EF-Tu•6-^{18}O-GDP spectrum left shifted 0.06 cm^{-1} (b) is free from phenylanaline peak, and the intensities, positions and line shapes of all the major peaks remain almost unchanged upon shifting.

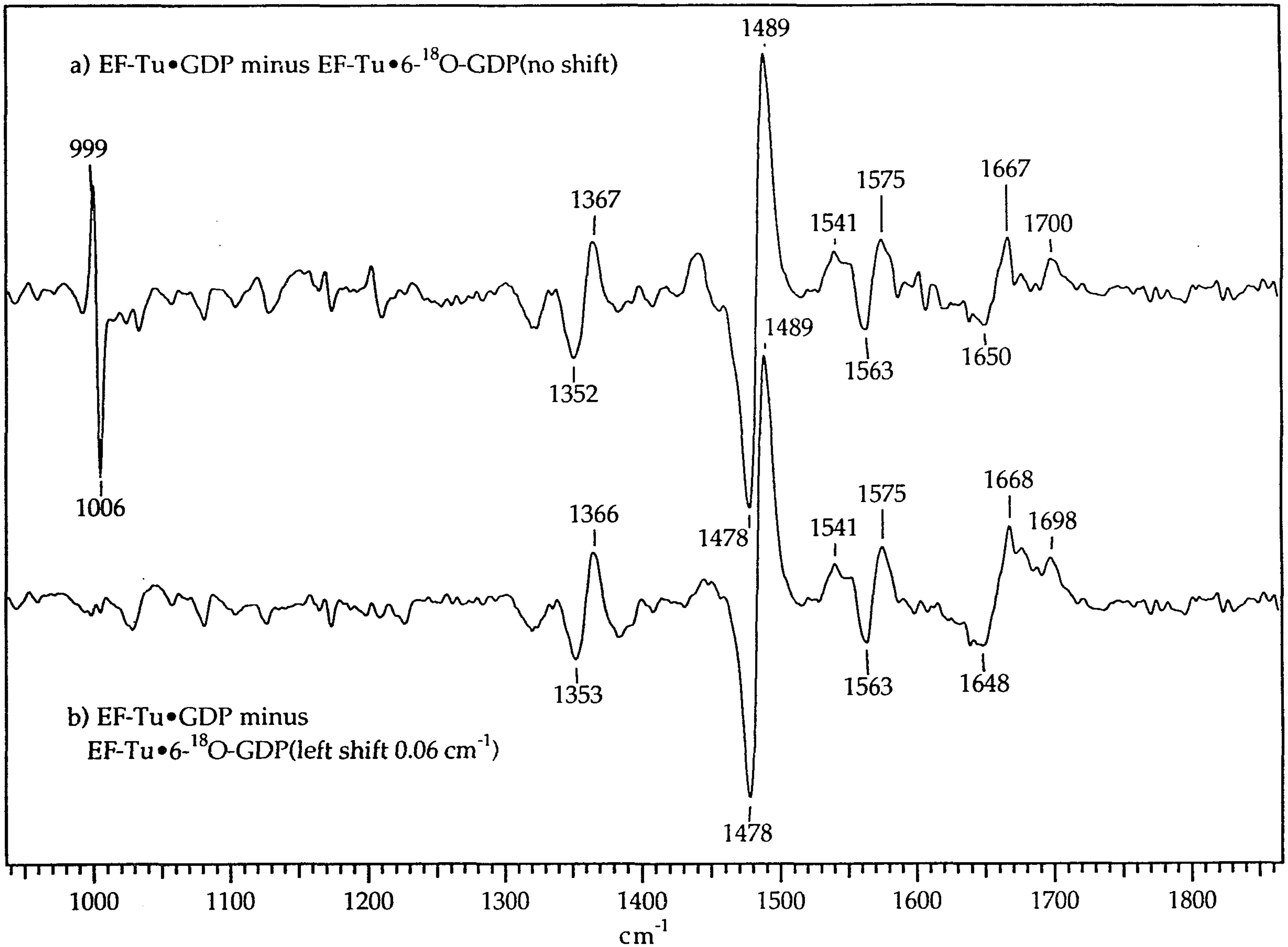
a) EF-Tu•GDP minus EF-Tu•6-18O-GDP(no shift)
b) EF-Tu•GDP minus EF-Tu•6-18O-GDP(left shift 0.06 cm-1)
999
1006
1367
1352
1489
1478
1541
1575
1563
1667
1700
1650
1366
1353
1489
1478
1541
1575
1563
1668
1698
1648
1000
1100
1200
1300
1400
1500
1600
1700
1800
cm-1

Figure 2.5

CHAPTER III

SAMPLE PREPARATION AND CHARACTERIZATION

A. Nucleotides

GDP, IDP, GMP-PCP, GDPβS 6-thioguanosine, ITP and IDP were purchased from Sigma or Boerhinger Mannheim. All other chemicals were from the highest purity available. ^{3}H-GDP (12 Ci/mmole) was from Amersham.

6-thio-GDP was synthesized from 6-thioguanosine by Z-J Chen (Chemistry Department, City College of CUNY) according to ([33]) and ([34]). 2-Amino purine riboside and 6-^{18}O-GDP were sythesized by C-X Chen (Chemistry Department, City College of CUNY)([35], and thesis of C-X Chen).

B. Protein Purification:

Purification of EF-Tu: EF-Tu was prepared from E. *coli* MRE 600 (Grain Processing Corp., Muscatine, IW) as described by Leberman ([37]). Frozen *E. coli* cell paste 200g was suspended in 500 ml buffer A1 (64.4 mM Tris-HCl, pH 7.6, 10 mM $MgCl_2$, 0.5 mM DTT, 10 μM PMSF, and 1 mM NaN_3.) contain 1 mM EDTA and 100 mg lysozyme. After 5 min, 10 ml 4% sodium deoxycholate and 5 mg DNase I was added. The suspension was well stirred and left at room temperature for a further 20 min. The suspension was then centrifuged at 8,000 rpm with GSA rotor for 60 min. to remove cell debris. The supernatant was applied to a column (5x30 cm) of DEAE-Sepharose CL-6B (from Pharmacia) equilibrated with buffer A1. The column then was washed with 500 ml buffer A1, and developed with a 3000-ml linear gradient of 0-0.3 M NaCl in a flow rate of 220 ml/h. The effluent of 22-ml fractions were collected and assayed for EF-Tu activities (Appendix A). The active fractions were pooled and brought to 60% saturation of ammonium sulfate. After stirred at 4°C for 30 min., the protein suspension was centrifuged and the pellet was redesolved and clarified by centrifugation. The total volume of the protein solution should be controlled under 20 ml which was less than 2% of the column volume of the gel filtration system. This sample was then filtered through a series of AcA 44 (from LKB) columns equilibrated with Buffer C1 (Buffer A contains 0.1 mM GDP). This gel filtration system consists of two columns (2.5x120 cm each) in serial connection. The columns were developed with buffer C1 in a flow rate of 20 ml/h. Fractions of 7 ml were collected and assayed for EF-Tu activities. The peak fractions are pooled and EF-Tu was precipitated by adding ammonium sulfate to 70% saturation. The precipitate was collected and stored at -70°C. The EF-Tu obtained this way still contained traces of fluorescence impurity, further purification was carried out according to a procedure obtained from Frances Jurnak's laboratory (Department of Biochemistry, University of California at Riverside, Riverside, CA 92521). EF-Tu pellets from five chromatographic preparations were pooled and extracted in Buffer Tu-E (25 mM Tris-SO_4, pH7.8, 10 mM $MgSO_4$, 0.1 mM L-Arginine HCl, 0.02% NaN_3, 10 mM β-mercaptalethenol, 5×10^{-5} M GDP and 0.1 mM PMSF) with ammonium sulfate (AS). Back extraction was started at 50% AS and ended at 25% AS in 5% decrease of AS each step. Most contaminants came out at 50, 45, and 40% AS. The back extraction at each level must be repeated until the total OD_{280} (absorption at 280 nm) fails to decrease. The protein concentration should be around 1.1 OD_{280}/ml for the best results. The concentration of AS of the supernatants from extraction's of 40% to 25% were increased by 5%, and allowed to set at 4°C until crystals were visible. The crystals were then centrifuged and dialyzed. The purity of the protein was checked by SDS-PAGE electrophoresis. A single band with molecular weight around 43,000 dalton was observed.

Purification of ras-p21: The c-Ha-*Ras* genes was expressed in *E. coli.* strain RRIDM15 under the control of the *tac* promoter ([38]). The cloned *E.coli* strain was a generous gift of Prof. A. Wittinghofer (Heidelberg, FRG). The gene was checked to its plasmid DNA content according to a procedure described in Appendix B. The coloned *E. coli* cells were grown in a high density fermentor (Appendix C). Purification procedure and activity assay are similar to those of EF-Tu. About 110 g of frozen cells were suspended in 500 ml of buff A (64.4 mM Tris-HCl, pH7.6, 1, 0.5 mM DTT, and 0.1 mM NaN_3.). PMSF to 0.01 mM, benzamidine to 0.01 mM, 1 ml 0.5 M EDTA pH 7.6, 200 mg lysozome and 20 mg of DNase I were added and the suspension were homogenized. After 30 min at 4°C, 5 ml of 1 M $MgCl_2$ and 2.5 ml of 4% sodium deoxycholate were added. After a further 60 min. of stirring at 4°C the suspension was centrifuged at 9,000 r.p.m. for 60 min. in a Sorvall GSA rotor at 4°C. The supernatant was applied to a column of DEAE-Sepharose CL-6B (same as the one used in EF-Tu purification) equilibrated with buffer B (buffer A with 10 mM $MgCl_2$). The column was washed with 500 ml of buffer B and then developed with a 5,000 ml linear gradient of 0-0.3 M NaCl in buffer B. The flow rate was 3.6 ml/min and 22-ml fractions were collected. The elution was assayed by GDP exchange assay and by SDS-PAGE. The fractions contain p21 were pooled and brought to 60% saturation with ammonium sulfate. After stirring for 30 min., the precipitation was recovered by centrifugation, dissolved in 15 ml of buffer C (buffer B contain 0.1 mM GDP and 200 mM NaCl), clarified by centrifugation and applied to a system of two columns (one AcA54, 2.5x100 cm and one AcA44, 2.5x100 cm). The columns were developed with buffer C at a flow-rate of 1.2 ml/min and 9 ml-fractions were collected. The peak of GDP exchange activity was located and the fractions free of impurities (as detected by SDS gel electrophoresis) were pooled and brought to 70% saturation with ammonium sulfate. The precipitation was collected by centrifugation and stored under -70°C.

The elusions of the sizing columns usually contains two GDP exchange peaks, which appeared on SDS-PAGE to be two very close bands. The exact differences of these two bands are not clear. It is also found that the purification started right after cell harvest gave very low protein yield. The process of freezing cells to -70°C for storage seems to have helped in cell breaking.

As checked by HPLC, both EF-Tu and ras-p21 prepared according to the above procedures contained a significant nucleotide other than GDP, probably dGDP ([39]) in their active sites. Such samples can not be used directly in certain difference spectroscopic measurement. The protein•GDP complexes need to be prepared in a process similar to the preparing of other complexes to insure that nearly 100% of bound nucleotide are replaced by GDP.

Prior to Raman experiment, proteins were concentrated to 2~4 mM in buffer R (10 mM $MgCl_2$, 20 mM sodium phosphate, pH 7.6) using a Centricon centrifugal concentrator (model 30 for EF-Tu, model 10 for p21, Amicon Corp. Mass). For the experiments measuring phosphate vibrations, 20 mM tris-HCl was used instead of sodium phosphate to reduce the interference of phosphate band from the buffer. Proteins remained fully active during and after the Raman experiment, as determined by the ^{3}H-GDP binding assay ([40]). Protein concentrations were determined spectroscopically using molar extinction coefficients (280 nm) of 40,000 $M^{-1}cm^{-1}$ for EF-Tu and 18,450 $M^{-1}cm^{-1}$ for p21 ([40],[38]), or by the Lowry method ([41]).

C. The Characterization of Nucleotides and their Binding to G-proteins

To study the binding pocket of the G-proteins, we need to incorporate different nucleotides or nucleotide derivatives into the proteins. The binding affinities of these nucleotides were investigated by radioactive binding assays, in which radioactively labeled GDP and different concentrations of the nucleotide derivatives were incubated with protein and the binding competition of the two were measured. The reaction scheme is shown as follow:

$$\begin{array}{ccc} G\bullet GDP + L & \overset{K_{eq}}{\rightleftharpoons} & G\bullet L + GDP \\ + & & \\ GDP^{*} & & \\ \upharpoonleft\downharpoonright & & \\ G\bullet GDP^{*} & & \\ + & & \\ GDP & & \end{array}$$

where G represent the protein; L represent the ligand that competes with radioactive GDP, (i.e. GDP*) for protein binding .

The dissociation constants of the protein for GDP and ligand L, represented by K_D and K_L respectively, are defined as:

$$K_D = \frac{[GDP][G]}{[G\bullet GDP]} \qquad K_L = \frac{[L][G]}{[G\bullet L]}$$

$$K_{eq} = \frac{[G\bullet L][GDP]}{[G\bullet GDP][L]} = \frac{[G\bullet L]}{[G\bullet GDP^{*}][L]} \times \frac{[G]}{[G]} = \frac{K_D}{K_L}$$

where Keq is the equilibrium constant, $[L] = [L]_0 - [G\bullet L]$, $[G]_0 = [G\bullet GDP] + [G\bullet L]$, $[L]_0$ and $[G]_0$ are the total concentration of the ligand and protein respectively;

[GDP*] is the concentration of radioactive labeled [^{3}H]GDP. With the radioactivity assay, we can measure [G•GDP*] v.s $[L]_0$. The value of K_D/K_L can be obtained from the relative concentrations (of nucleotide analogs to GDP) required to displace 50% of GDP* bound to the protein.

We have measured binding affinities of several nucleotides and nucleotide derivatives to EF-Tu and p21. The chemical structures of these compounds are presented in Figure 3.1 and 3.2. The concentrations of the nucleotides and proteins were determined from their UV spectra, using the extinction coefficients listed in Table 3.1.

Since the important quantity to us is the binding affinity of the nucleotide analogs relative to that of GDP, we plot our assay results as the relative concentration of [G•GDP*] against the molar excess of the ligand over GDP (Figure 3.3 to 3.5). Relative concentrations of nucleotide analogs required to displace 50% bound GDP* are listed in Table 3.2.

D. Preparation of Protein-Nucleotide Complexes

Protein Complexed with Isotopically Labeled GDP : Isotopically labeled GDPs are chemically same as GDP. To incorporate these nucleotides into G-proteins, we can incubate G•GDP complexes with excess of labeled nucleotide, which will replace unlabeled GDP that bound to the protein under certain conditions.

Studies show that SO_4^{-2} ion can increase the dissociation rate of GDP from EF-Tu and p21 dramatically ([42, 43]). Removal of Mg^{++} ion by addition of EDTA may increase the dissociation constant of GDP to p21 by a factor of 10, while not effecting the dissociation to EF-Tu ([43]). Based on this knowledge, proteins complexed with 8D-GDP or β-$^{18}O_4$-GDP were prepared in the following way: Protein samples (300μl, ca. 1mM) were incubated with 10-fold molar excess of 8D-GDP (or β-$^{18}O_4$-GDP) in buffer I (200mM tris pH 7.6, 200 mM $(NH_4)_2SO_4$, 0.5 mM DTT, 0.1 mM NaN_3) for 30 minutes, at 37°C. For p21 the incubation mixture included 0.6 mM EDTA, and the exchange carried out at room temperature. The samples were then diluted with 2 mL buffer I including 2mM $MgCl_2$ and concentrated to 100 μl. The incubation with labeled nucleotide was repeated once more. The sample was then washed with buffer R three times or more to remove free nucleotide, and concentrated to yield ~ 60 μl, at 2-4 mM, for the Raman experiment. This procedure ensured > 98% replacement of the unlabeled GDP with less than 0.01 mM nucleotide remaining free in solution.

GMP-PCP and GDPβS Complexes: Complex of G•GMP-PCP can be obtained from following reaction ([44]):

$$\text{G•GDP} + \text{GMP-PCP} \xrightarrow{\text{alkaline phosphotase}} \text{G•GMP-PCP} + \text{Guanosine} + 2\text{ Pi}$$

Alkaline phosphatase is an enzyme that catalysis cleavage of terminal phosphate group of phosphorylated molecules at pH 8-11. It requires Mg^{++} and Zn^{++} ions for its activity and the optimal pH for its activity is pH 9.8.

To save the work of separating the enzyme from G-proteins, water insoluble alkaline phosphatase was used in the preparation, which can be easily removed by centrifugation or by filtration after the reaction is completed.

Since Mg^{++} may affect the dissociation of nucleotides from *ras*-p21, and Zn^{++} may precipitate the highly concentrated G-protein complexes, the commercial product of alkaline phosphatase, which is stored in Mg^{++} and Zn^{++} containing buffer, was washed twice with water and twice with incubation buffer before usage. This step will only remove free ions in solution but not enzyme bound ions because of their high affinities to the protein. But ions must be added back to the enzyme for storage. The enzyme was used repeatedly to lower the cost.

The high pH of 9.8 is not suitable for G-proteins, the buffer condition of pH 8 to 8.2 is chosen. For EF-Tu or p21, the activities of the proteins do not change significantly at pH 6-9.5 ([43]). Lowering the pH not only reduces the activity of alkaline phosphatase, but also activates phosphate diesterase which is another enzyme that cleaves phosphate dieasterate bonds and appears as a contamination in alkaline phosphatase preparation (from the product label of Boerhinger Mannheim). Although this contamination is minor (usually < 0.05%), as a catalyst, it can reduce the concentration of GMP-PCP considerably at neutral pH.

The nucleotide content of the reaction mixture was checked by reverse phase HPLC with a C18 column under ion-pairing conditions ([44, 45]). The elution buffer was 50-100 mM potassium phosphate (depending on the exact character of the column and the experimental conditions), pH 6.5, 10 mM tetrabutylammonium bromide, 0.2 mM NaN_3, and 3-8% acetonitrile (also depending on column and experimental conditions). Raising the concentration of potassium phosphate elutes nucleotides faster, thereby reducing the resolution of the system. Increasing the concentration of acetonitrile increases the retention time of faster eluting nucleotides by small amount, while reducing the retention time of slower eluting nucleotides dramatically.

The enzyme reaction and incubation were carried out at 30°C - 37°C. Except these steps, all operations of preparation of G•GMP-PCP complexes were performed at 4°C. Protein solution ~ 1 mL was passed through a Sephadex PD-10

G-25 column and eluted with buffer I. The first UV absorption peak at 280 nm was collected. This step removes the excess Mg^{++} in the solution. To make EF-Tu•GMP-PCP, this step is unnecessary, instead we washed the protein once or twice with a centricon to change buffer to buffer I and to wash out the free GDP in the storage solution. At room temperature, 2 times molar excess of GMP-PCP was added into protein solution. The GDP/GMP-PCP ratio was monitored by HPLC. Water insoluble alkaline phosphatase (Sigma, ca. 4 units/mg protein) was then added to the solution. As the concentration of GDP gradually decreased, the protein will bind GMP-PCP. Since alkaline phosphatase can only react with free GDP in solution, choosing the conditions that may reduce the binding affinity of GDP to protein can speed up the reaction considerably. GMP-PCP may also be break down considerably by phosphate diesterase contamination during the process. More GMP-PCP should be added if it is necessary. Typically after 1 hour for *ras*-p21, and after 2 hours for EF-Tu, more than 95% of the GDP complexes were replaced by GMP-PCP complexes. Since the relative binding of GMP-PCP compare to GDP is much weaker for EF-Tu than for p21 (table 2), it took longer to complete the reaction for EF-Tu. Alkaline phosphatase was then removed by filtering the mixture though a low protein affinity filter (Millpore HVLP 013). Because G•GMP-PCP was relatively unstable, prolonged reaction may cause protein precipitation. G•GMP-PCP complexes prepared this way has a purity greater than 98%. The compound can be incubated with excess of other nucleotides or nucleotide analogs to get other nucleotide complexes. HPLC spectra of a typical enzyme reaction is shown in Figure 3.6.

GDPβS complex was prepare in the same way as protein•GMP-PCP complexes, because alkaline phosphatase does not recognize the modified phosphate group with one oxygen replaced by sulfur. Usually, GDPβS commercial product is considerably contaminated by GDP because of high desulfanation rate of this compound, but this would not effect making G•GDPβS complexes because alkaline phosphates may cleave all the GDP molecules in solution.

IDP, 6-thioGDP, 6-hydroGDP and GMP-PNP Complexes: For both EF-Tu and *ras*-p21, the binding affinities to these nucleotides are about two orders of magnitude lower than to GDP. It is not efficient to replace bound GDP by these nucleotides using incubation method. To get expected complexes, G•GMP-PCP complexes were made first, and then incubated with excess of corresponding nucleotide analogs. The conditions of the incubation are listed in Table 3.3. These conditions were determined by the results of radio active binding assays (Table 2).

D. The electronic absorption spectra of nucleotides and Protein-Nucleotide Complexes

The electronic absorption spectroscopy (UV absorption) is used frequently to determine the concentrations of nucleotides and proteins, as well as to measure ligand binding. This method is characterized by its effectiveness and simplicity. In our G-protein studies, however, it is not an accurate way to determine the content of bound nucleotide by measuring UV absorption of the protein complexes, since most of the GDP and GTP analogs have similar UV absorption character and the absorption bands overlap with those of proteins. The nucleotide content of G-protein complexes was usually determined by HPLC.

The UV spectrum of free GDP and GDP complexes are shown in Figure 3.7a. GDP absorbs at 253 nm with an extinction coefficient of 13.7×10^{3} M^{-1} cm^{-1}. The A_{280}/A_{260} ratio is ca. 0.67. UV spectrum of G•GDP complexes are dominated by protein absorption peak at 276 nm. The nucleotide band shows up as a little bump at 258 nm in the G•GDP complex. This bump disappears in nucleotide free protein ([44]). The A_{280}/A_{260} ratio of the protein complex is ca. 1.1.

The UV absorption of GDP above 230 nm originates from the conjugated guanine ring. Guanine nucleotides with modified phosphate motif have same UV spectra as GDP; therefore, it is not a surprise to observe that the UV spectroscopic features of GMP-PNP, GMP-PCP and GDPβS complexes are the same as that of G•GDP complex (Figure 3.8a).

Hypoxthine ring absorbs at 248 nm (Figure 3.7b) with a extinction coefficient of 12.4×10^{3} $M^{-1}cm^{-1}$. The absorption of the Hypoxthine ring shows up as two small bump at 251 nm and 258 nm when IDP binds to protein. The two bumps have absorption wavelength somewhat longer than that of free nucleotide, as in the case of G•GDP complexes.

Replacement of oxygen of carbonyl group by a sulfur atom reduces the polarity and bond strength of the this group ([46]), which some how reduces the energy gap between ground state and first excited state of the purine ring, resulting in the longer absorption maximum at 340 nm for 6-thioGDP at pH 7.4. Upon binding to the protein, the absorption maximum is red shifted further to 342 nm (Figure 3.8b). A more sophisticate study on the interaction of EF-Tu with 6-thio nucleotides showed that the red shift is 4 nm with a decreased extinction coefficient ([47]).

The electronic spectra of guanosine and thioguanosine derives from at least two transitions, a π-π^* charge-transfer transition and a n-π^* transition of weaker intensity. The factors that may affect the spectrum of the nucleotide include polarizability of the environment, conformation of the glycosidic bond of the nucleotide, specific interactions between the nucleotide and amino acid residues of the protein, and other tautomeric structures of the purine ring which could be stabilized within the protein-nucleotide complex. The red shifts of the absorption of 6-thio-GDP when upon binding to proteins (EF-Tu and myosin) were interpreted by Eccleston ([47]) as the influence of the hydrophobic environment inside the protein.

Table 3.1: The extinction coefficients of proteins and nucleotides, at pH 7.0.

COMPOUNDS	λ (nm)	ε ($\times 10^3$, M^{-1},cm^{-1})
EF-Tu	280	40
ras-p21	280	18.5
GDP, GDPβS, GTP, GMP-PNP, GMP-PCP	253	13.7
IDP, ITP	242	12.4
6-thio-GDP	340	2.48
6-hydroGDP	302	~6.0

Table 3.2: Relative concentrations (to GDP) required to displace 50% of protein bound [^{3}H]GDP

	EF-Tu	Ras-p21
GDP	1.0	1.0
GTP	~100[a]	0.52[a]
GMP-PCP	723.3	3.4
GMP-PNP	83.5	2.9
GDPβS	25.3	4.05
6-thio-GDP	334.1	>2000
6-hydroGDP	>2000	44.8
IDP	84.8	123.2

[a]From [48].

Table 3.3: Experimental conditions of making protein•nucleotide derivative complexes by incubating excess of nucleotide derivatives with protein•GMP-PCP complexes.

Parameters:

L/G: molar excess of nucleotide derivative (L) over protein (G)

T (°C): incubation temperature

t (min): incubation time

n: incubation repeats

starting protein	EF-Tu•GMP-PCP				*ras*-p21•GMP-PCP			
Parameters	L/G	T (°C)	t (min)	n	L/G	T (°C)	t (min)	n
IDP	10	37	15	1	30	25	40	3
6-thio-GDP	10	25	30	2				
GMP-PNP	10	25	30	2	10	25	40	2

Figure 3.1: Chemical structures of GDP and some of GDP analogs

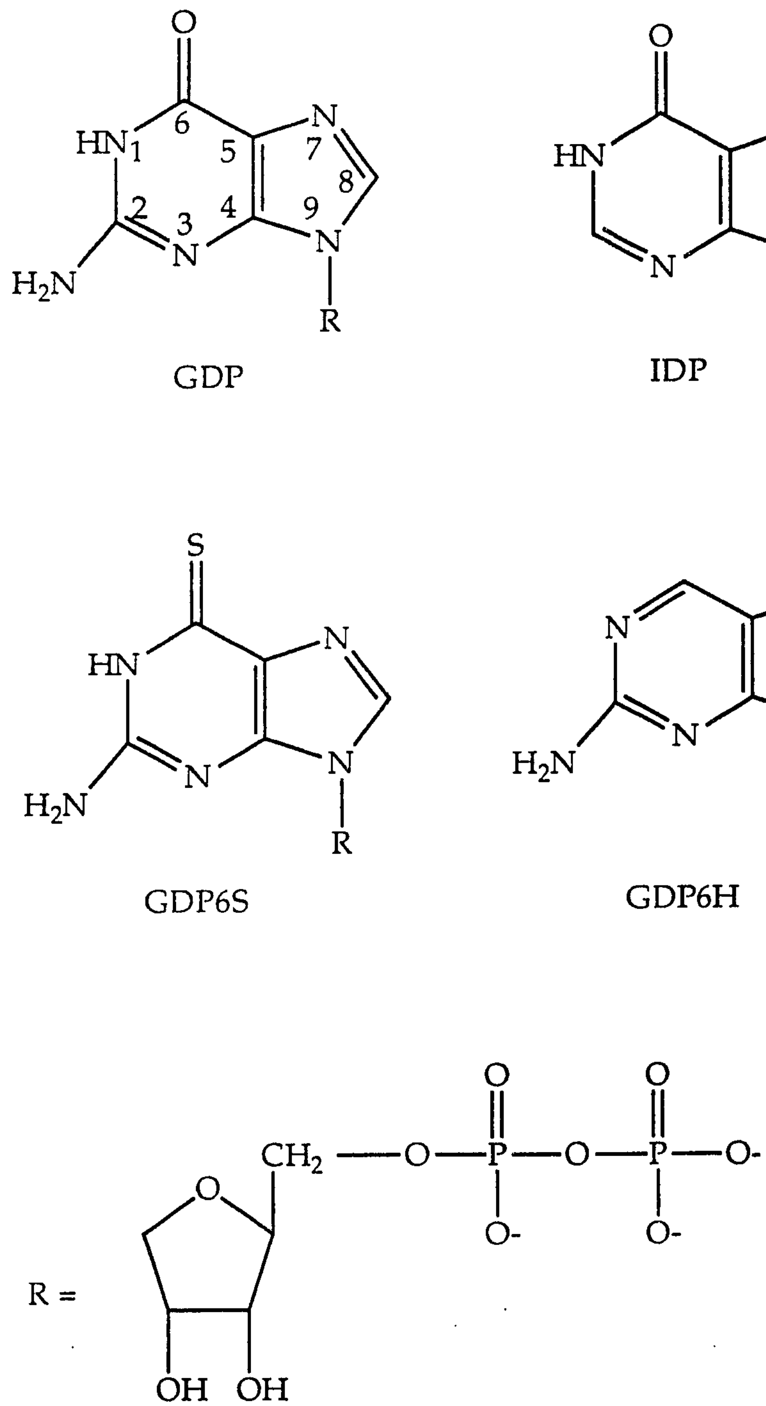

Figure 3.1

Figure 3.2: Chemical structure of GTP and some of GTP analogs

Base =

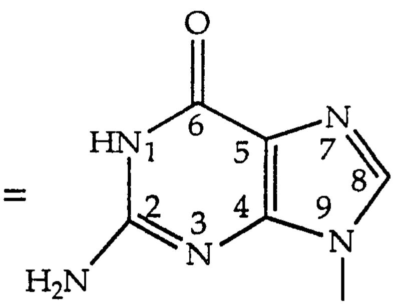

GTP:

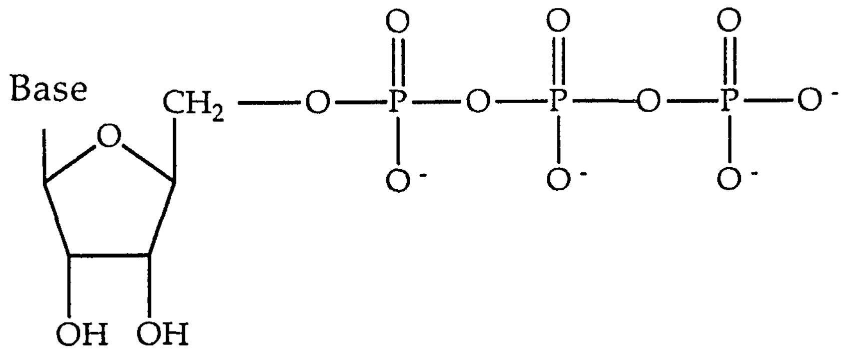

GMP-PNP:

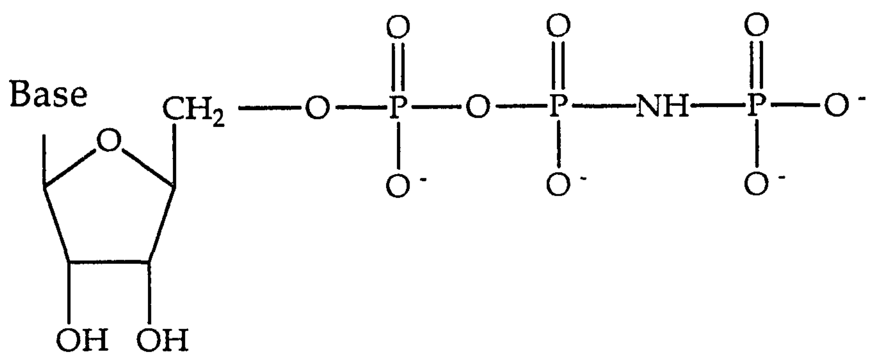

GMP-PCP:

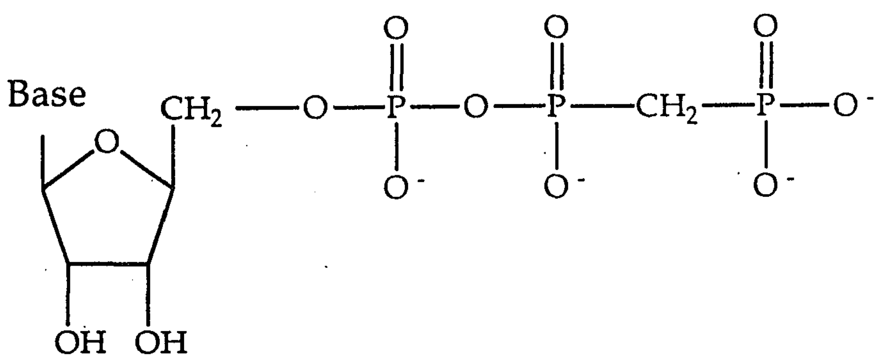

Figure 3.2

Figure 3.3: GTP and GTP analogs over a range of concentrations were allowed to compete with ~ 2 μM [^{3}H]GDP in the presence of ~ 0.5 μM p21. [GTP derivative]$_0$ is the total concentration of the competing GTP derivative; [p21•GDP+GDP*]$_0$ is the sum of the concentration of radio active GDP added in the solution and the unlabeled GDP originally bound to the protein; [p21•GDP*]$_0$ is the concentration of p21•GDP* complex in the mixture in the absence of other nucleotide; [p21•GDP*] is the concentration of p21•GDP* complex in the presence of certain concentration of competing nucleotide.

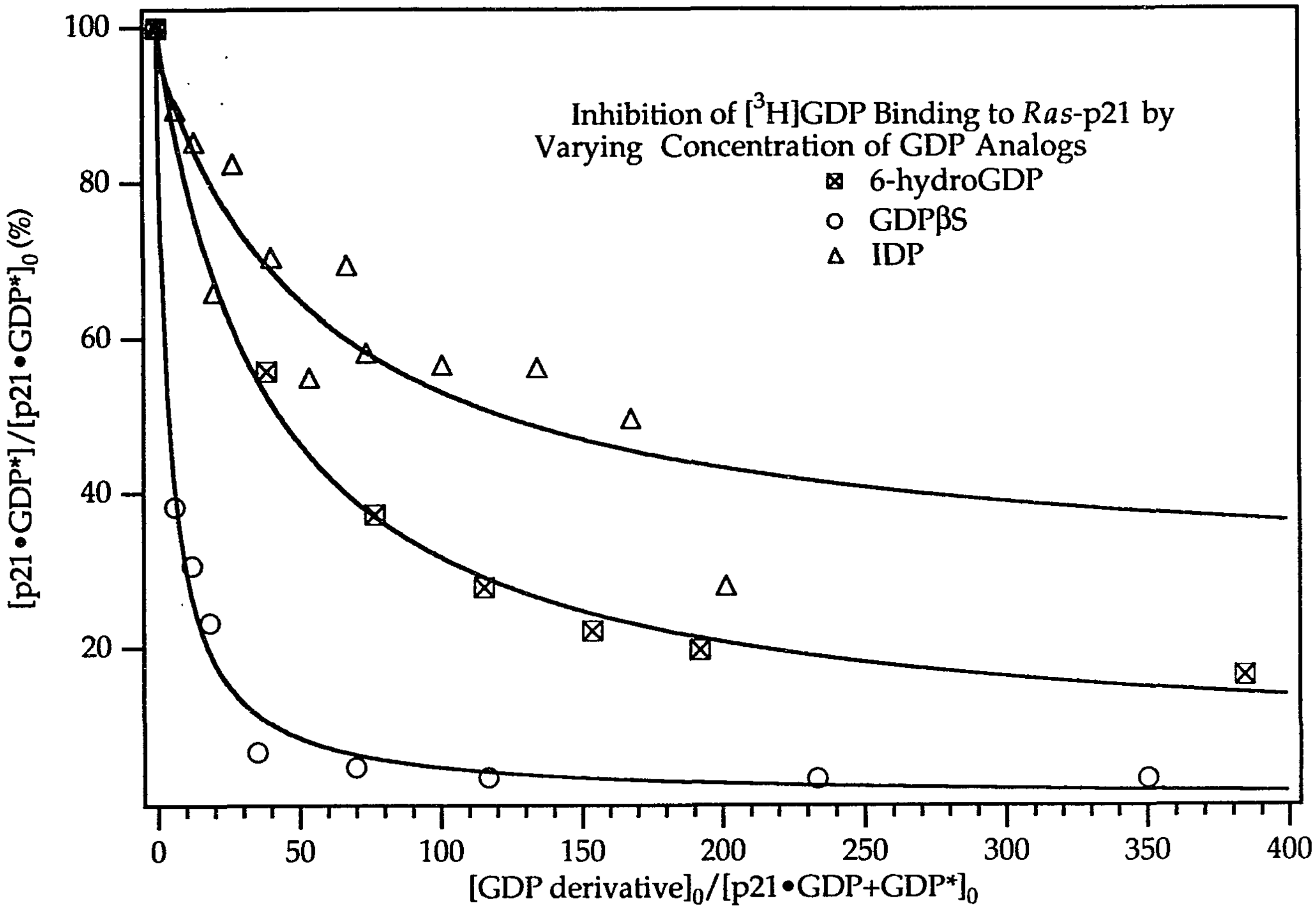

Inhibition of [³H]GDP Binding to *Ras*-p21 by
Varying Concentration of GDP Analogs
6-hydroGDP
GDPβS
IDP
100
80
60
40
20
0
50
100
150
200
250
300
350
400
[p21•GDP*]/[p21•GDP*]$_0$ (%)
[GDP derivative]$_0$/[p21•GDP+GDP*]$_0$

Figure 3.3

Figure 3.4: GDP analogs over a range of concentrations were allowed to compete with ~ 2 μM [^{3}H]GDP in the presence of ~ 0.5 μM p21. $[\text{GDP derivative}]_0$ is the total concentration of the competing GDP derivative; $[\text{GDP+GDP*}]_0$ is the sum of the concentration of radio active GDP added in the solution and the unlabeled GDP originally bound to the protein; $[\text{p21}\bullet\text{GDP*}]_0$ is the concentration of p21•GDP* complex in the mixture in the absence of other nucleotide; [p21•GDP*] is the concentration of p21•GDP* complex in the presence of certain concentration of competing nucleotide.

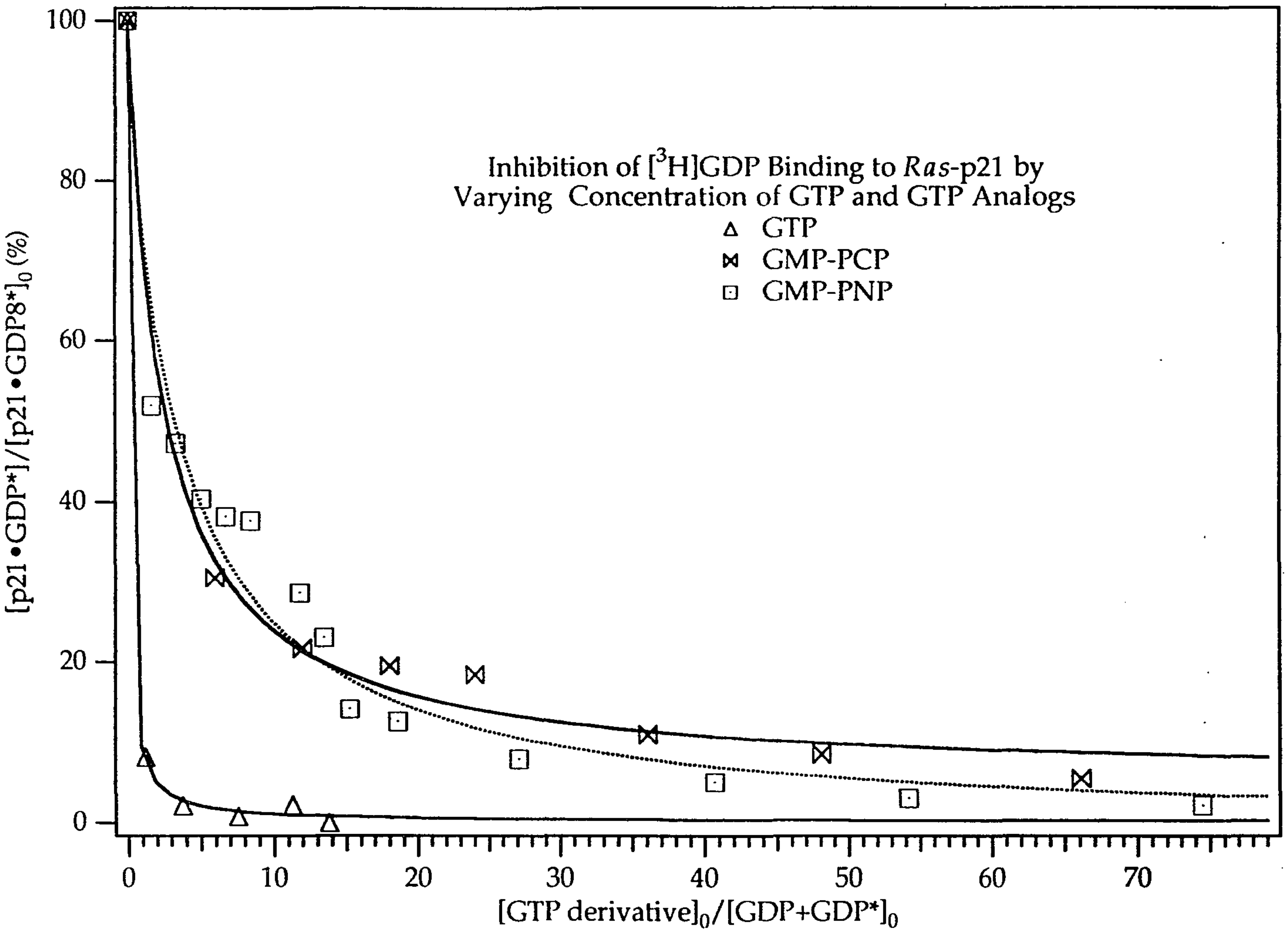
Inhibition of [3H]GDP Binding to Ras-p21 by
Varying Concentration of GTP and GTP Analogs
GTP
GMP-PCP
GMP-PNP
[p21•GDP*]/[p21•GDP8*]0 (%)
[GTP derivative]0/[GDP+GDP*]0
0
20
40
60
80
100
0
10
20
30
40
50
60
70

Figure 3.4

Figure 3.5: GDP analogs over a range of concentrations were allowed to compete with ~ 2 μM [^{3}H]GDP in the presence of ~ 0.5 μM EF-Tu. [GDP derivative]$_0$ is the total concentration of the competing GDP derivative; [GDP+GDP*]$_0$ is the sum of the concentration of radio active GDP added in the solution and the unlabeled GDP originally bound to the protein; [EF-Tu•GDP*]$_0$ is the concentration of EF-Tu•GDP* complex in the mixture in the absence of other nucleotide; [EF-Tu•GDP*] is the concentration of EF-Tu•GDP* complex in the presence of certain concentration of competing nucleotide.

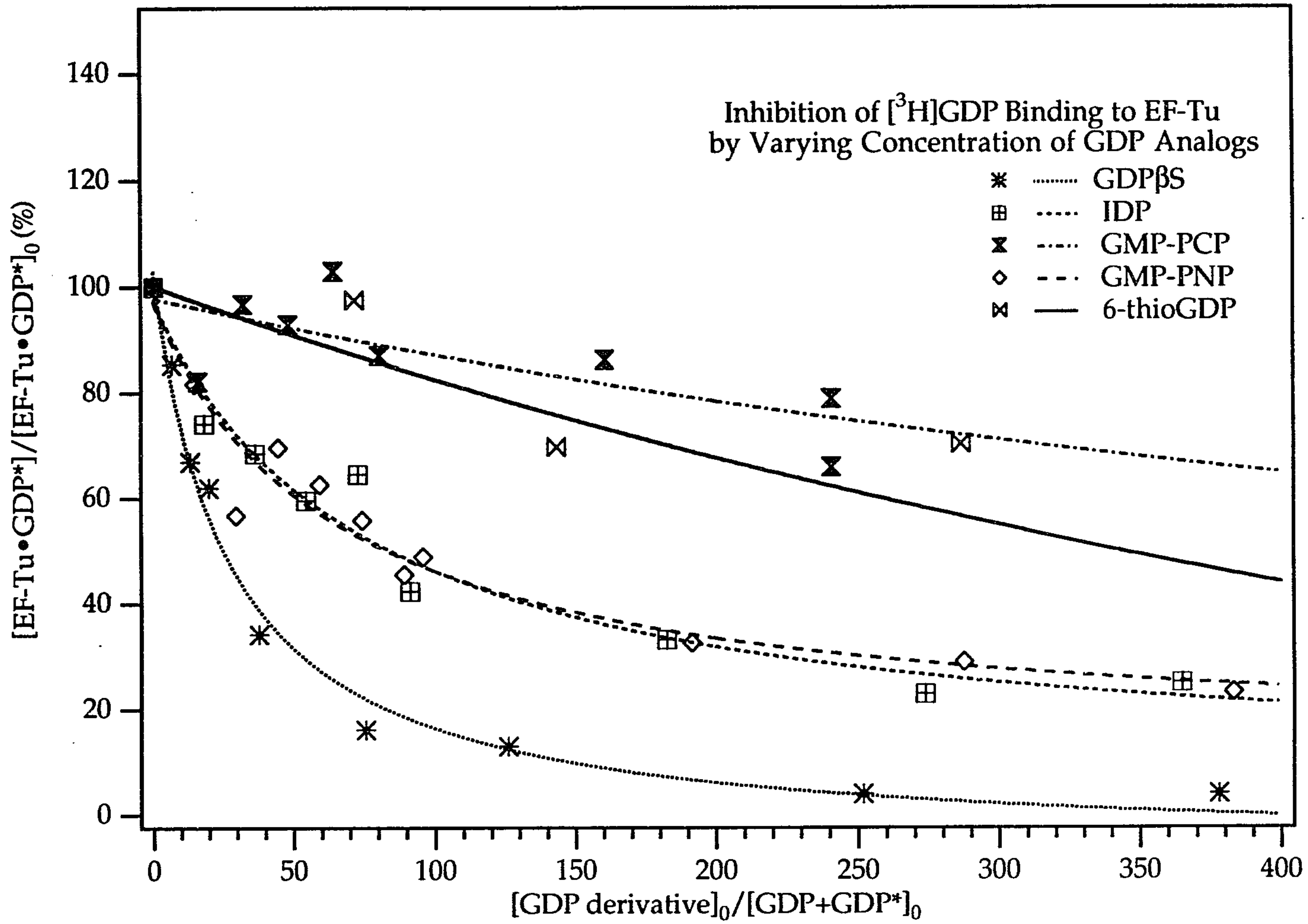
Inhibition of [3H]GDP Binding to EF-Tu
by Varying Concentration of GDP Analogs
GDPβS
IDP
GMP-PCP
GMP-PNP
6-thioGDP
[EF-Tu•GDP*]/[EF-Tu•GDP*]0 (%)
0
20
40
60
80
100
120
140
0
50
100
150
200
250
300
350
400
[GDP derivative]0/[GDP+GDP*]0

Figure 3.5

Figure 3.6: HPLC chromatography of making p21•GMP-PCP complex. The nucleotides are detected at 253 nm. (a): GDP solution; (b): GMP-PCP solution; (c): p21•GDP, the second peak is, probabily, from dGDP that bound to the protein; (d): p21•GDP plus about two molar excess of GMP-PCP; (e): alkaline phosphotase add to p21•GDP/GMP-PCP solution at t=0; (f): t=15 min; (g): t=30 min; (h): t=45 min. Spectra (e)-(h) show that GDP and the dGDP are cleaved by alkaline phosphotase as indicated by the appearance of guanosine peak and diminishing of GDP and dGDP peaks.

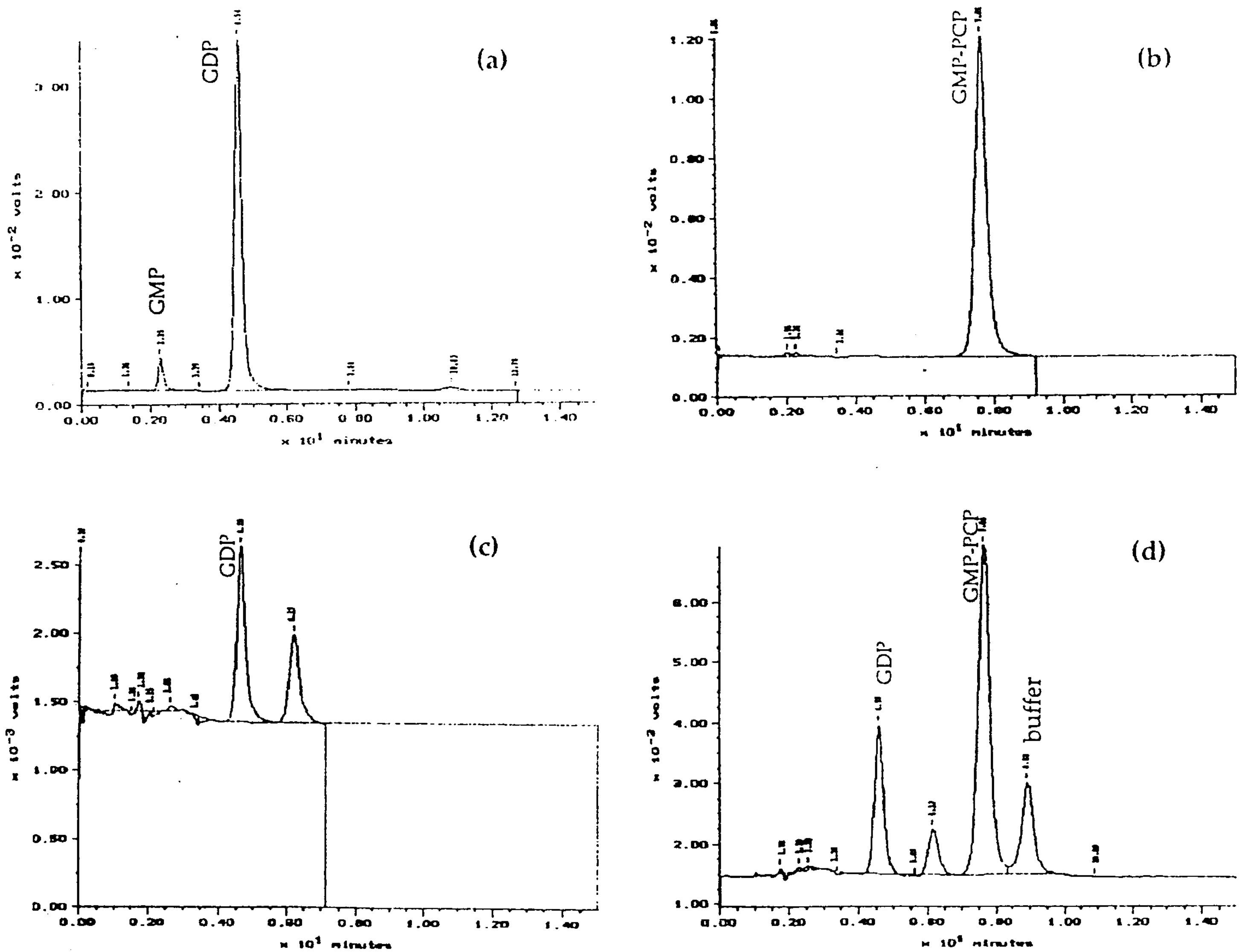
(a)
GMP
GDP
x 10^{-2} volts
x 10^{1} minutes
(b)
GMP-PCP
x 10^{-2} volts
x 10^{1} minutes
(c)
GDP
x 10^{-3} volts
x 10^{1} minutes
(d)
GDP
GMP-PCP
buffer
x 10^{-2} volts
x 10^{1} minutes

Figure 3.6

Figure 3.6

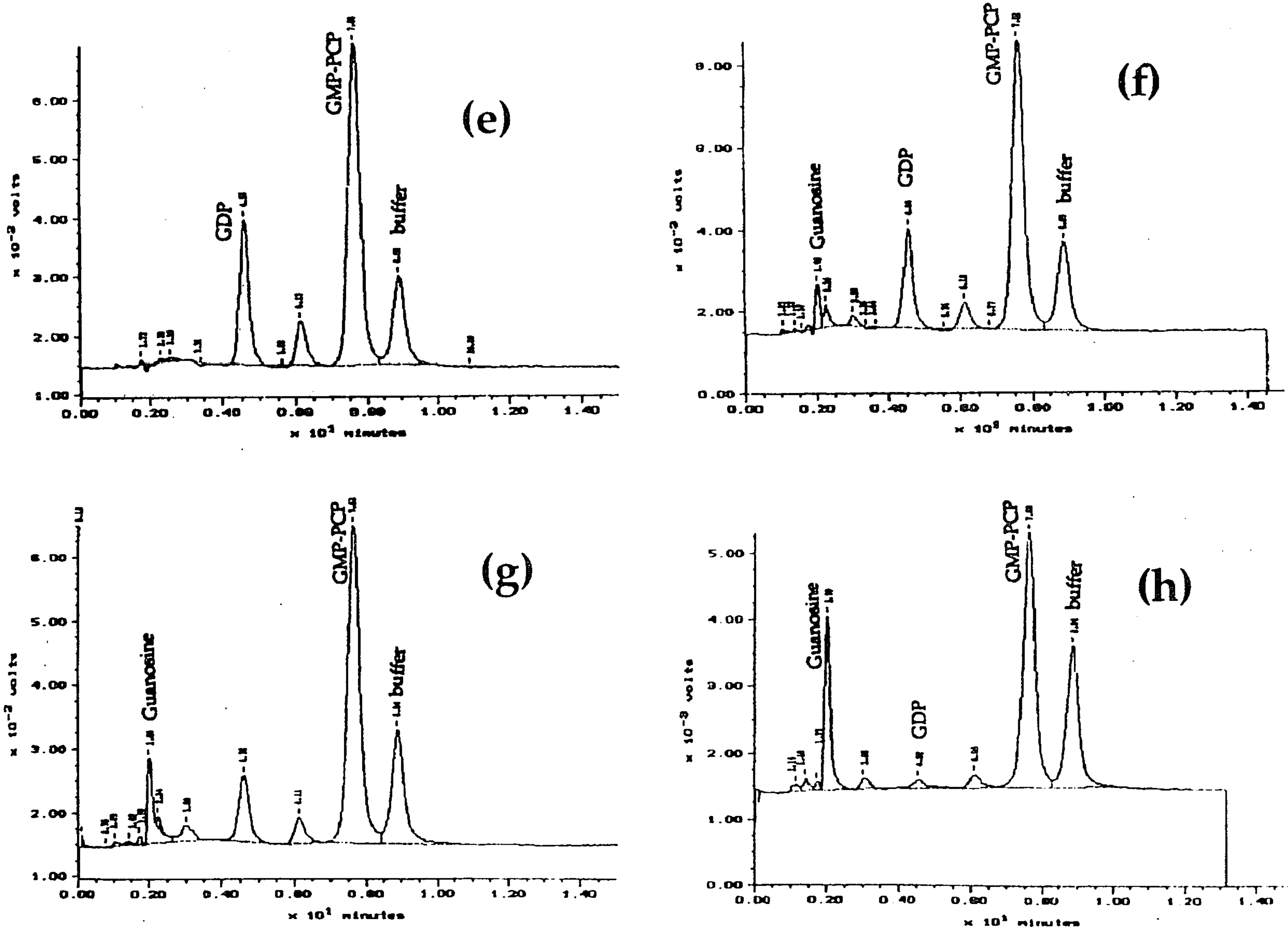
(e)
GDP
GMP-PCP
buffer
(f)
Guanosine
GDP
GMP-PCP
buffer
(g)
Guanosine
GMP-PCP
buffer
(h)
Guanosine
GDP
GMP-PCP
buffer
x 10^-2 volts
x 10^-3 volts
x 10^1 minutes

Figure 3.7: UV spectra of GDP, IDP and EF-Tu•GDP, EF-Tu•IDP, p21•GDP and p21•IDP complexes.

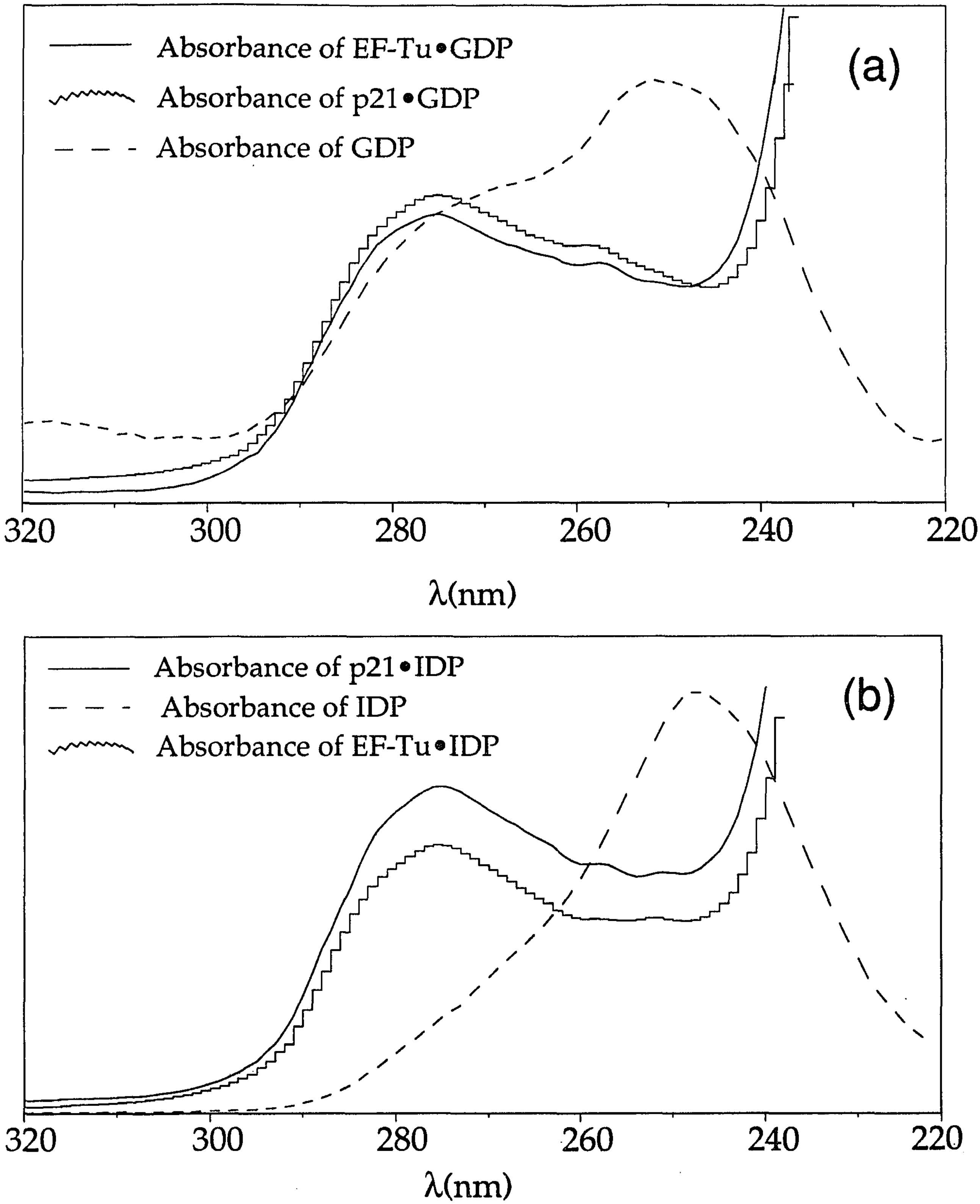

Absorbance of EF-Tu•GDP
Absorbance of p21•GDP
Absorbance of GDP
(a)
320
300
280
260
240
220
λ(nm)
Absorbance of p21•IDP
Absorbance of IDP
Absorbance of EF-Tu•IDP
(b)
320
300
280
260
240
220
λ(nm)

Figure 3.7

Figure 3.8: UV spectra of EF-Tu•GDP, EF-Tu•GDPβS, EF-Tu•GMP-PNP (a) and 6-thioGDP, EF-Tu•6-thio-GDP (b).

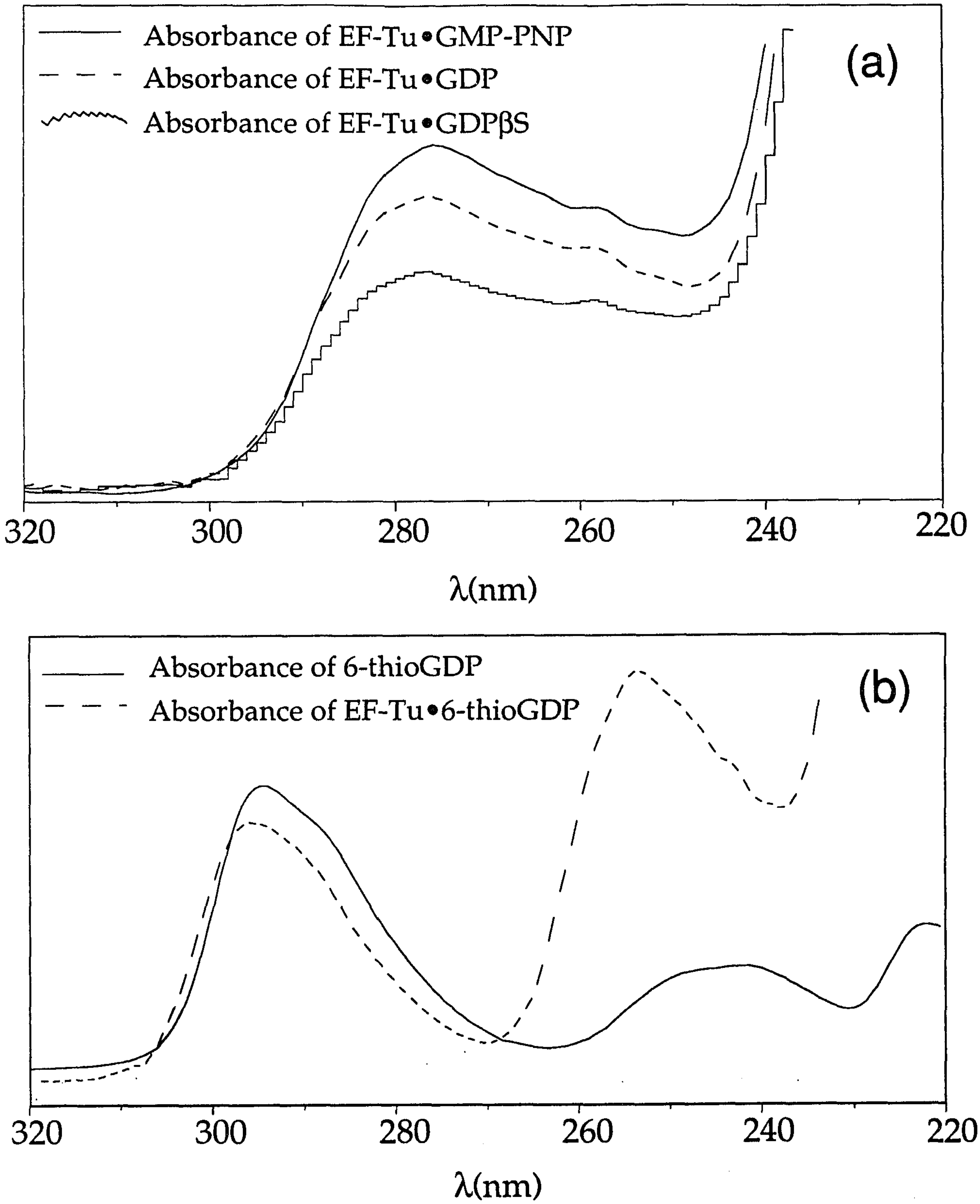

Absorbance of EF-Tu•GMP-PNP
Absorbance of EF-Tu•GDP
Absorbance of EF-Tu•GDPβS
(a)
320
300
280
260
240
220
λ(nm)
Absorbance of 6-thioGDP
Absorbance of EF-Tu•6-thioGDP
(b)
320
300
280
260
240
220
λ(nm)

Figure 3.8

Chapter IV

THE FEASIBILITY OF THE APPLICATION OF RAMAN DIFFERENCE TECHNIQUE TO G-PROTEINS

A. The nucleotide free EF-Tu and p21 protein are unstable

In general, G proteins are very unstable in the absence of bound nucleotides. Figure 4.1 shows the Raman spectra of EF-Tu•GDP (a) and nucleotide free EF-Tu (b). The two samples share few common spectral features. The amide I region of the nucleotide free EF-Tu is about 50% broader than that of the EF-Tu•GDP complex and the amid III band is very different from that of GDP complex. The intensities of the doublet at 853 cm^{-1} and 830 cm^{-1} which are assigned to the vibrations of tyrosine residues ([31]), as well as 850/830-cm^{-1} ratio of the nucleotide free protein increased dramatically. In addition, the absorption band resembling that of the protein was found in the filtrate when the nucleotide free protein was concentrated by centricon-30. These observations indicate that major structural changes have taken place, the secondary structure may have collapsed after nucleotide release. Clearly, efforts at getting nucleotide bands from the difference spectrum formed between EF-Tu•GDP and nucleotide free EF-Tu failed.

Nucleotide free ras-p21 can be made according to following reaction ([44]):

$$\text{p21•GMP-PCP} \xrightarrow{\text{phosphadiesterase}} \text{p21•Gunosine}$$

Since there was no insoluble phosphodieasterase available, this enzyme had to be separated from the reaction mixture by chromatography after the reaction was completed. The p21 lost almost all the ability to re-bind GDP after the over night gel filtration .

The limited stabilities of these nucleotide free G-proteins forced us to take an alternative way to investigate binding properties of nucleotides to the proteins by difference Raman spectroscopy (see detailed description in Chapter III.C).

B. The difference spectra of GDP minus 8D-GDP in EF-Tu and p21

The feasibility of the alternative approach described in Chapter III.C was proved first in the Raman studies on G•GDP and G•8D-GDP complexes.

Nucleotide spectroscopy: Raman spectrum of the nucleotides in solution are shown in Figure 4.2a (GDP) and 4.2b (8D-GDP). There have been a number of previous Raman studies of nucleotides and isotopically substituted derivatives ([49-51]). The spectrum of GDP is dominated by bands which are associated with the guanine ring. The substitution of the hydrogen atom at the C8 position of guanine moiety by a deuterium affects the frequencies of a number of bands. The strongest band at 1487 cm^{-1}, which has been assigned to C7=C8 ring stretch and 8-CH deformation, shifts down nearly 20 cm^{-1} to 1464 cm^{-1} in the 8D-GDP data. This band shifts substantially to lower frequency upon complexion with heavy ions or hydrogen bonding to guanine's N7 ([52]).

Tsuboi and his colleagues ([52]) have determined the Raman spectra of a number of guanosine (and cytidine) salts and have compared their Raman spectra with the guanosine conformations determined by X-ray diffraction analysis.

Their studies showed that the Raman bands in 1300-1400 cm^{-1} region, which arise from ring motions and contain also substantial motions from the bonded ribose group, as well as the bands in the 600-700 cm^{-1} region are quite sensitive to the torsional angle about the glycosidic bond and the pucker state of the ribose ring (see Appendix D). In GDP solution spectrum (Figure 4.1a), the patterns of the bands in the above two regions most closely follow crystal spectrum where the guanosine conformation is C2' *endo-anti*, although the position of the 666 cm^{-1} band of Figure 4.1a is slightly low for this conformation, about 10 cm^{-1}. It has been proposed that the peak at 1178 cm^{-1} is sensitive to hydrogen bonding to guanine's $-NH_2$ group. This mode is believed to be composed of guanine ring plus C-N (amino) stretch. Thus, variations in hydrogen bonding to the amino group, which would be expected to influence the C-N stretch, may be reflected in this mode's frequency. Peticolas and his coworkers interpreted a 5 cm^{-1} downward shift in this band upon warming poly(G) from 25°C to 90°C as the breaking of hydrogen bonds to this group ([53]). The band at 1085 cm^{-1} arises principally from motions on the phosphate (P-O stretch) part of GDP. Underneath this band is a small peak which has been assigned to motions of the ribose group.

As discussed above (Chapter III.C.), our procedure for measuring the Raman spectrum of the bound nucleotide involved isotopically 'editing' the *in situ* nucleotide and forming the Raman difference spectrum between the labelled and unlabeled protein-ligand complex. Figure 4.2c shows the difference spectrum between Raman spectra of GDP (Figure 4.2a) and 8D-GDP (Figure 4.2b). All normal modes which include the C8-H coordinate are affected by deuteration of the 8 position, and these show as positive and negative peaks in the difference spectrum. For example, the strongest band in the GDP spectrum (1485 cm^{-1}), assigned to stretching vibration of the N7=C8 bond and 8-CH deformation, is shifted to 1464 cm^{-1}, giving rise to the derivative-like feature dominating the difference spectrum. Most of the guanine bands found in the GDP spectrum are affected by the substitution of deuterium at C8, and this results in a complex and rich difference spectrum.

The zero crossings are of importance in a difference spectrum. Assuming that a particular band can be described by a Lorentzian intensity profile centered at ν_u (for unlabeled) and that the band shifts by $\Delta\nu$ to ν_l (for labelled) upon labelling without change in intensity or band width, then the intensity profile for the the unlabeled band is

$$I_u = \frac{A}{(\nu - \nu_u)^2 + \frac{1}{4}\Gamma^2}$$

while the profile for the labelled band is:

$$I_l = \frac{A}{(\nu - \nu_l)^2 + \frac{1}{4}\Gamma^2}$$

where Γ is the bandwidth and A is an intensity scaling constant. It can be easily calculated[2] that the difference between I_u and I_l goes to zero at the average frequency position, $(\nu_u + \nu_l)/2$, regardless of the band width and frequency shift. Thus, for example, the 1178 cm^{-1} band in the GDP spectrum shifts to 1185 cm^{-1} in the 8D-GDP spectrum. The positive and negative 'couple' that this yields in the difference spectrum is found at 1172 and 1190 cm^{-1}, respectively. The average of 1178 and 1185 cm^{-1} at 1181.5 cm^{-1} corresponds well to the 1181.0 cm^{-1} zero crossing in the difference spectrum. This relation will be used below to find the average 'position' of a band for the bound GDP data.

On the other hand, it is clear that some information is lost in forming a difference spectrum. Of course, bands not associated with the substitution, like the 1085 cm^{-1} phosphate band, subtract out and are not observed. Additionally, it is sometimes difficult, without knowing the answer, to make a clear cut association between a positive and negative 'pair' in the difference spectrum and a band in the GDP spectrum and its associated shifted band in the 8D-GDP spectrum. For example, the 666 cm^{-1} GDP band shifts to 663 cm^{-1} in 8D-GDP. However, there are other nearby bands which shift differently. The result is a negative band at 660 cm^{-1} in the difference spectrum without a clearly identifiable corresponding positive peak.

Protein spectroscopy: The classical Raman spectra of the GDP-bound proteins are shown in Figures 4.3a (EF-Tu) and 4.3c (p21). A few initial notes are worth mentioning on the quality of the data. We have found that the non-resonance Raman signals of the most intense guanine bands to be on the order of 3% of the 1449 cm^{-1} protein band of proteins having a molecular weight of ca. 40000, like EF-Tu. This is a convenient marker band because it arises from a CH_2 scissoring mode which is fairly insensitive to environment. A requirement for an adequate measurement of bound guanine by difference spectroscopy is that the measured protein signals achieve a signal to noise ratio of much better than 30 to 1. We have found EF-Tu to be one of the more suitable proteins for Raman studies. The purification procedures for this protein work very well with regard to fluorescing impurities (we expect no fluorescence from the protein because the visible excitation used to stimulate the Raman light is far from any protein absorption band). EF-Tu yields virtually no background fluorescence. Moreover, it is easy to prepare in high concentrations (~2 mM) with no aggregation. We are unable to determine the signal to noise in the EF-Tu data because the channel resolution along the frequency axis is not sufficiently fine. However, the signal to noise of the data in Figure 4.3a exceeds 1000 to 1. On the other hand, p21 does show some background fluorescence levels, and the signal to noise ratio for the data of Figure 4.3c is somewhat less, near 300 to 1. This results in a somewhat more noisy difference spectrum for p21 than for EF-Tu (see below). In addition, we observed a non-reversible change of the Raman spectrum, which looks similar to that of nucleotide free protein, when EF-Tu and p21 were highly concentrated (>6 mM).

Protein Structure. Because the Raman spectra of proteins were shown to represent the spectral sum of its constituent amino acids ([54]), most Raman peaks in Figures 4.3a and 4.3c can be assigned to their corresponding residues as is shown in Table 4.1. Except for minor position changes, all amino acids that are present in both proteins show similar frequency and intensity patterns.

GDP Bound to EF-Tu and p21: Figure 4.4a shows the difference spectrum of EF-Tu•GDP (Figure 4.3a) with that of EF-Tu•8D-GDP (Figure 4.3b). The corresponding difference spectrum for the c-Harvey *ras*-p21 protein is shown in Figure 4.4b, and the solution difference spectrum, given in Figure 4.2c, is reproduced in Figure 4.4c for comparison. All peaks which are larger than our inherent signal to noise in these measurements and which have been observed in several independent measurements are labelled in the figure. Qualitatively, the three difference spectra are very similar. In general, the protein spectra are sharper than the solution spectrum, and the p21 spectrum is somewhat sharper than the EF-Tu spectrum. However the peak positions are not much affected by binding.

The bound data of Figure 4.4 clearly reflect part of interactions between the guanine moiety and its protein pocket. The peak at 1178 cm^{-1}, believed to be sensitive to hydrogen bonding to guanine's $-NH_2$ group (see above), shifts to lower frequency when GDP binds to EF-Tu and p21. This is seen from the data of Figure 4.4 by calculating the zero intensity position of this band in the various difference spectra. In solution, the positive and negative peaks in the difference spectrum are found at 1172 and 1190 cm^{-1}, respectively. We take the zero position as the average of the positive and negative values (see above), which is 1181 cm^{-1} here. Using the same criterion, we find a zero crossing for this band at 1178 cm^{-1} from the EF-Tu data and 1174 cm^{-1} from the p21 spectrum. The band has downshifted -3 cm^{-1} for GDP in EF-Tu and -7 cm^{-1} in p21. Thus the data suggest that guanine's amino group interacts differently to both proteins than in solution. This is consistent with binding studies ([55]) and the available X-ray diffraction studies ([8, 21-26]) which suggest that the guanine base is anchored by two major interactions: an aspartic acid residue (Asp119 in p21 and Asp138 in EF-Tu) which is hydrogen bonded with the amino substituent in position 2 and an interaction between the 6-keto group and a main chain amine of Ala146 in p21 and the side chain amine of Asn135 in EF-Tu. It should be pointed out that the correlation found previously for the 1178 cm^{-1} band suggests that a decrease in frequency to be indicative of a stronger hydrogen bond. However, the mode is a fairly complicated one, and it is unclear just how it will respond to particular hydrogen bonding groups (which is unknown in the previous work as opposed to a carboxylate here) and their positioning. These parameters may well affect the exact response of a particular mode ([56]) and the sign of a shift for a complicated mode. This needs to be probed more fully with direct isotopic labelling of the amino group.

The data clearly indicates that the guanine ring *in situ* does not interact with the protein in both p21 and EF-Tu through the N7 position differently than it interacts with water in solution. This is seen from the general similarity of the bound difference data to that of the solution data. In particular, the 1487 cm^{-1} band, which is shifted by the C8 deuterium substitution to 1464 cm^{-1}, is not affected at all by binding. As discussed above, this band has been shown to be a marker band for hydrogen bonding to N7. This conclusion is supported by the fact that modification of the 8 position with bulky groups as in 8-Br-GDP has almost no influence on the binding affinity to either EF-Tu or p21 ([57, 58]).

The general correspondence in the conformational sensitive 600-700 cm^{-1} and 1300-1400 cm^{-1} regions between the solution spectrum and the protein spectra suggests that binding does not affect the conformation of the nucleotide. As discussed above, the solution spectrum suggests an *anti* conformation about the glycosidic ring and a C2'-*endo* sugar pucker. Thus, the data strongly suggest that the conformation of the nucleotides to EF-Tu and p21 is also C2'*endo* -anti. This is in agreement with X-ray diffraction studies on these bound complexes which show a C2'-*endo* sugar pucker and a torsional angle of χ = -125° for GDP bound to EF-Tu and χ = -113° for p21 in the crystalline state ([8, 21-26]). It is also consistent with the crystallographic observations that the ribose moiety of the nucleotide has only weak interactions with the protein and a large portion of it (the 2' and 3' hydroxyls) is exposed to the solvent. The additional sharpness of the bands in the bound data suggest that there is less conformational accessibility for GDP bound to the proteins than when in solution. We suspect that the difference band at 661 cm^{-1} is somewhat sharper for GDP in p21 than in EF-Tu because the range of angles from an equilibrium C2'-*endo* ribose pucker angle is somewhat larger in EF-Tu than in p21. This conjecture, as well as the extra sharpness of the p21 spectrum compared to the EF-Tu spectrum generally, is in agreement with the somewhat greater binding affinity of p21 for GDP ($K_d = 2x10^{-11}$ M, [44]) than that of EF-Tu ($K_d = 2x10^{-9}$ M, [59]).

The experimental results above provide a proof that the essential idea given Chapter III.C works very well. We have measured the difference Raman spectrum of protein bound nucleotides. Some structural information has been infered from this study.

Table 4.1: Raman peak frequencies and mode assignments for the GDP-bound forms of EF-Tu (left) and p21 (parentheses) proteins. Taken from the spectra shown in Figure 1. str.-stretching, def.- deformation, sc.- scissoring. Assignments are based on ([60-62]) and references cited therein.

Raman frequency (cm^{-1})	**Assignment**
643 (---)	Tyr
825 (830)	Tyr (buried)
850 (850)	Tyr (exposed)
936 (938)	Val, CH_3 sym. rock
950 (951)	C-C str.
1001 (1002)	Phe
1030 (1030)	Phe
--- (1059)	C-N str
1124 (1124)	C-N str
1172 (1174)	Phe, Tyr, Val, Leu CH_3 asym. rock
1207 (1207)	Phe, Tyr
1200 - 1300	Amide III
1317 (1320)	C-H def.
1338 (1339)	C-H def.
1400 (1407)	COO^- str, Asp, Glu
1449 (1450)	CH_2 sc.
1571 (1570)	?
1605 (----)	Phe, Tyr
1618 (1618)	Phe, Tyr, Trp
1667 (1663)	Amide I

Figure 4.1: Raman spectra of EF-Tu•GDP (a); EF-Tu (b). All the proteins were at 2 mM in buffer R and was excited with 150 mW of 488 nm argon laser light. Temperature of sample holder was set to 4°C.

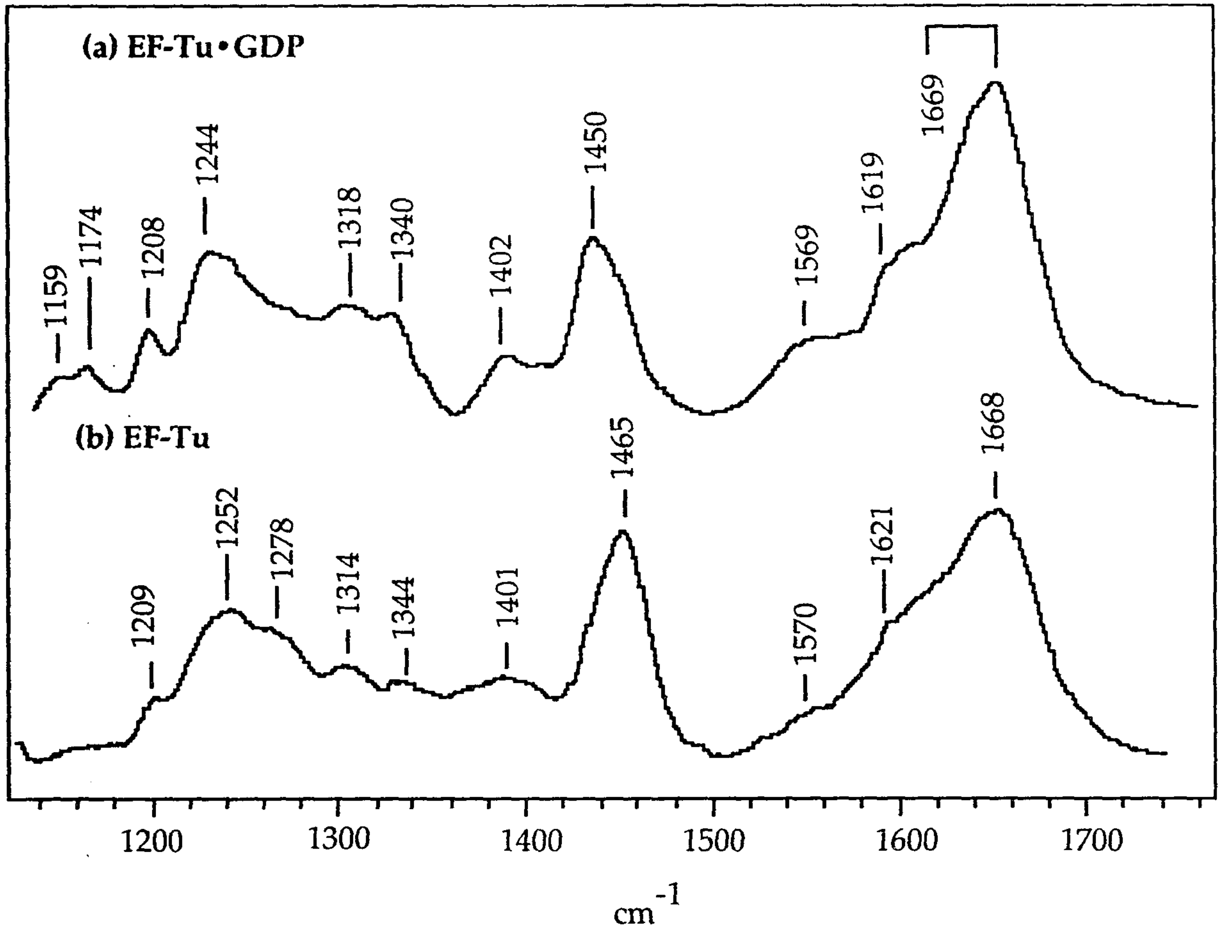
(a) EF-Tu•GDP
1159
1174
1208
1244
1318
1340
1402
1450
1569
1619
1669
(b) EF-Tu
1209
1252
1278
1314
1344
1401
1465
1570
1621
1668
1200
1300
1400
1500
1600
1700
cm-1

Figure 4.1

Figure 4.2: Raman spectra of (a) GDP, (b) 8D-GDP and (c) the calculated difference spectrum. Both samples are at 50 mM in H_2O, pH 7.5. Excitation is with 100 mW of 488 nm argon laser light.

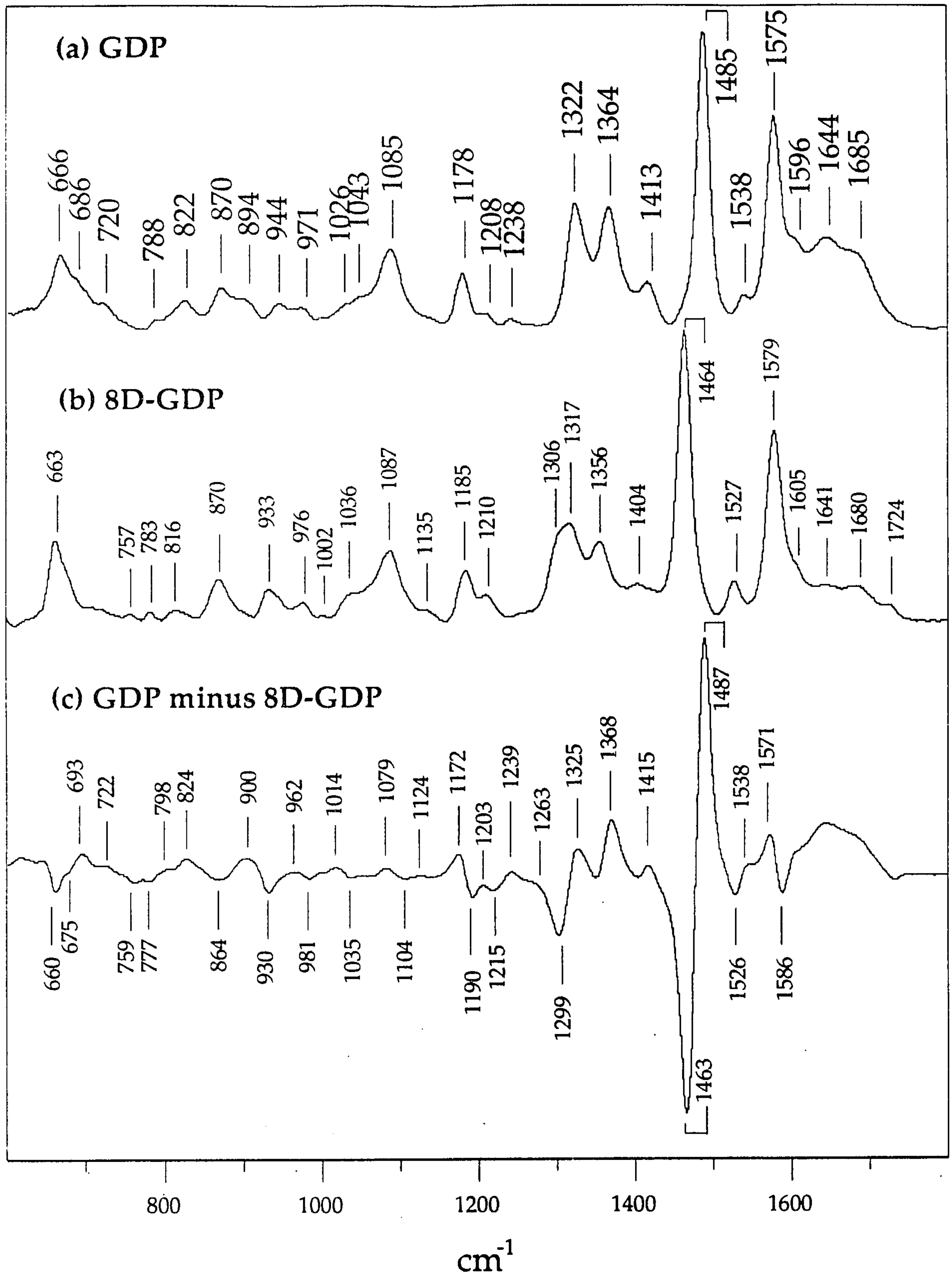

(a) GDP
666
686
720
788
822
870
894
944
971
1026
1043
1085
1178
1208
1238
1322
1364
1413
1485
1538
1575
1596
1644
1685
(b) 8D-GDP
663
757
783
816
870
933
976
1002
1036
1087
1135
1185
1210
1306
1317
1356
1404
1464
1527
1579
1605
1641
1680
1724
(c) GDP minus 8D-GDP
660
675
693
722
759
777
798
824
864
900
930
962
981
1014
1035
1079
1104
1124
1172
1190
1203
1215
1239
1263
1299
1325
1368
1415
1463
1487
1526
1538
1571
1586
800
1000
1200
1400
1600
cm-1

Figure 4.2

Figure 4.3: Raman spectra of (a) EF-Tu•GDP, (b) EF-Tu•8D-GDP and (c) p21•GDP. EF-Tu•GDP is at 2 mM in buffer R and is excited with 180 mW of 488 nm argon laser light. p21•GDP is at 3.6 mM in buffer R and is excited with 150 mW of 530.2 nm krypton laser light.

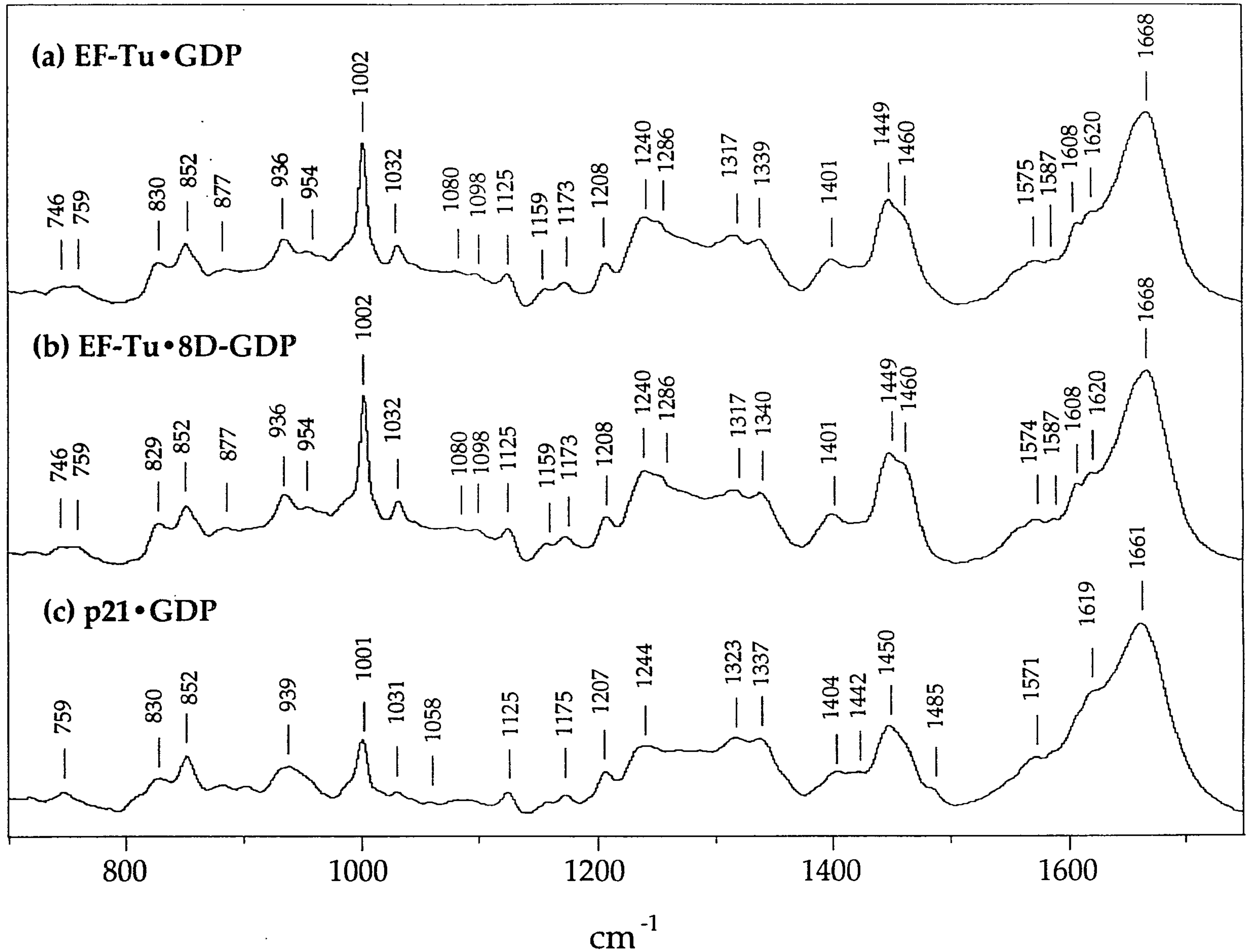
(a) EF-Tu•GDP
746
759
830
852
877
936
954
1002
1032
1080
1098
1125
1159
1173
1208
1240
1286
1317
1339
1401
1449
1460
1575
1587
1608
1620
1668
(b) EF-Tu•8D-GDP
746
759
829
852
877
936
954
1002
1032
1080
1098
1125
1159
1173
1208
1240
1286
1317
1340
1401
1449
1460
1574
1587
1608
1620
1668
(c) p21•GDP
759
830
852
939
1001
1031
1058
1125
1175
1207
1244
1323
1337
1404
1442
1450
1485
1571
1619
1661
800
1000
1200
1400
1600
cm-1

Figure 4.3

Figure 4.4 Difference spectra between the GDP and 8D-GDP complexes in (a) EF-Tu and (b) p21. Spectrum (c) is the solution difference spectrum (same as Figure 2(c)).

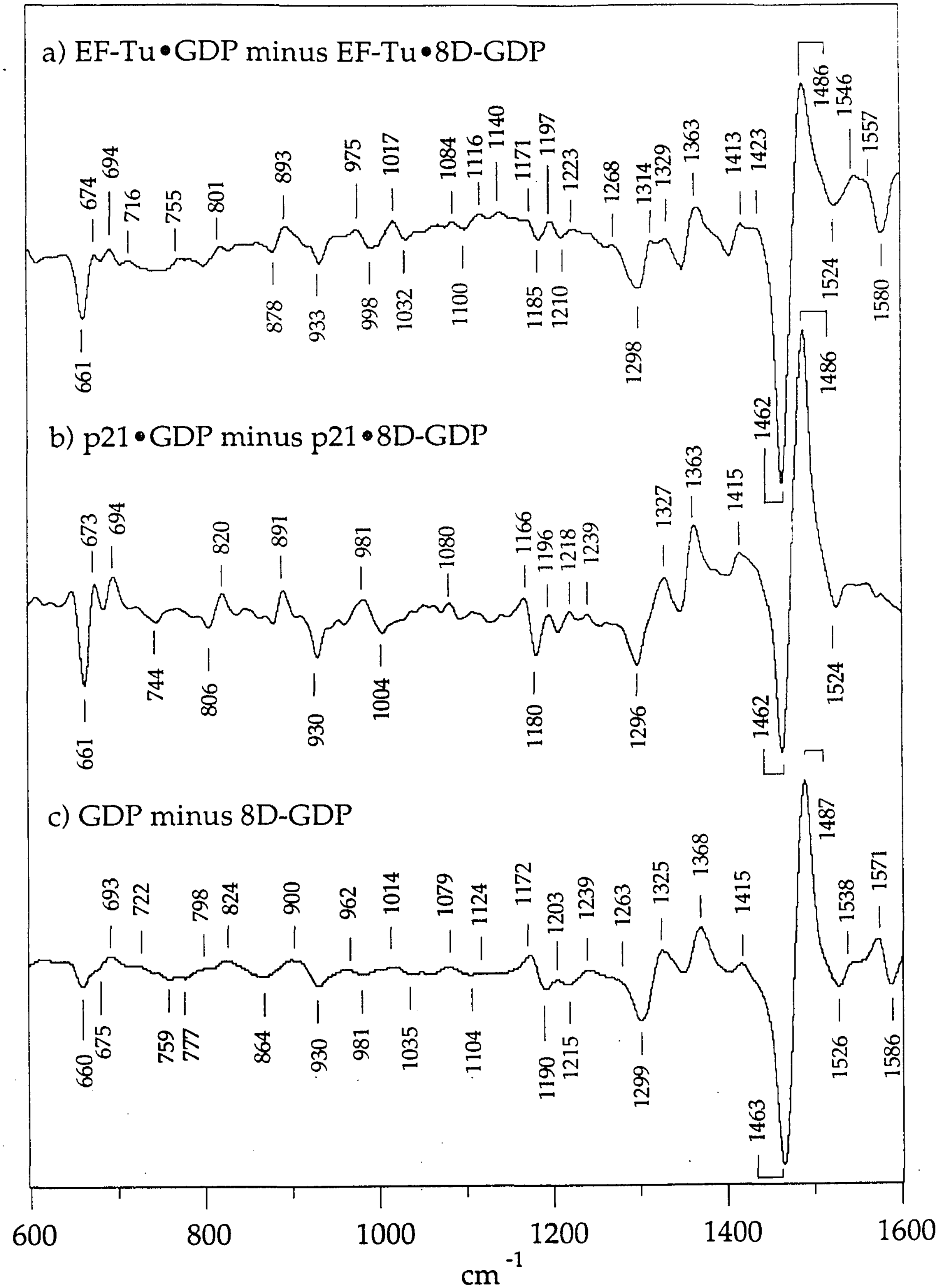

a) EF-Tu•GDP minus EF-Tu•8D-GDP
661
674
694
716
755
801
878
893
933
975
998
1017
1032
1084
1100
1116
1140
1171
1185
1197
1210
1223
1268
1298
1314
1329
1363
1413
1423
1462
1486
1524
1546
1557
1580
b) p21•GDP minus p21•8D-GDP
661
673
694
744
806
820
891
930
981
1004
1080
1166
1180
1196
1218
1239
1296
1327
1363
1415
1462
1486
1524
c) GDP minus 8D-GDP
660
675
693
722
759
777
798
824
864
900
930
962
981
1014
1035
1079
1104
1124
1172
1190
1203
1215
1239
1263
1299
1325
1368
1415
1463
1487
1526
1538
1571
1586
600
800
1000
1200
1400
1600
cm -1

Chapter V

THE INTERACTIONS OF NUCLEOTIDES WITH G-PROTEINS I: HYDROGEN BONDING WITH THE GUANINE RING MOIETY OF THE NUCLEOTIDES

X-ray structures of EF-Tu and *ras*-p21 show that the two binding 'handles' between the protein and the nucleotide, namely, the carbonyl at position 6 and the 2-amino group, both on the guanine ring, are crucial for the *in situ* anchoring and specificity of GDP to the binding site via hydrogen bonding to protein residues. Here, we investigate these interactions utilizing nucleotide analogues *chemically* modified at selected positions, suitable for instances where isotopic labeling is either more complicate or more expensive from a synthetic point of view. Accordingly, two nucleotide analogues were chosen: IDP which lacks the 2-amino group, and 6-thio-GDP which contains a sulfur atom replacing the 6-oxygen. The chemical structures of these nucleotides are shown in Figure 3.1. To confirm the results that we got from the chemically modified nucleotide, and to get the interaction of the carbonyl group of GDP with *ras*-p21, isotopically labeled 6-^{18}O-GDP was also synthesized.

A. Nucleotide spectroscopy of GDP, IDP and 6-thio-GDP

Solution data of GDP, IDP and 6-thio-GDP are shown in Figure 5.1. The vibrational spectra of guanine and hypoxanthine as well as their respective nucleosides and nucleotides have been published and discussed previously (e.g. [51, 63-67]). We follow the previous spectral assignments in our discussion below. As the spectra of both GDP and IDP are dominated by bands which are associated with the purine base moiety of the molecule (guanine and hypoxanthine, respectively), the major negative and positive peaks in difference spectrum formed between GDP and IDP (figure 5.2a) arise from this part of the molecule. Since the only chemical difference between the two molecules is the presence of the 2-amino group in GDP, this difference spectrum exemplifies the different types of effects a single substitution has on the vibrations of a ring system. For example, GDP delocalized purine breathing motions, which show the strongest Raman intensities, the GDP bands at 1577 cm^{-1}, assigned primarily to the C4=C5 of the ring and at 1487 cm^{-1}, assigned primarily to N7=C8 stretch, are shifted to 1554 and 1473 cm^{-1}, respectively, in IDP. Localized motions that are directly associated with the 'extra' amine group present in GDP are also clearly affected. These are, in general, much weaker as seen in the external C-N stretching mode observed at 1178 cm^{-1} and the $-NH_2$ scissoring mode at 1646 cm^{-1} in the GDP spectrum ([52, 68]), both of which are absent from the IDP spectrum. Importantly for this study, the some what weak and broad carbonyl (C=O) stretching mode located at 1685 cm^{-1} in GDP, shifts and because stronger and sharper at 1692 cm^{-1} in the IDP spectrum (Figure 5.1b). In the difference spectrum of 5.2a, IDP's carbonyl peak clearly shows up as a negative peak at 1695 cm^{-1}. On the other hand, GDP's weaker and broader carbonyl peak is essentially unobserved in the solution difference spectrum.

The solution spectrum of 6-thioGDP is shown in Figure 5.1c. The replacement of GDP's keto oxygen by sulfur affects a number of GDP's bands. C=S group in 6-thio-GDP is less polar than the carbonyl linkage, and the vibration does not give rise to as characteristic a band as the C=O due to the complication of correlation's. However, the high polarizability of the sulfur atom leads to strong Raman spectrum from all bonds connected to it. Due to the greater mass of sulfur the C=S vibration is expected to occur at considerably lower frequencies than C=O vibration. Calculations and model compound studies indicate that the C=S frequency would be found in the 1050-1200 cm^{-1} region ([69],[46]). The most important spectroscopic feature of 6-thioGDP for our protein study is that this spectrum contain no bands in 1620-1750 cm^{-1} region. Consequently, its difference spectra with GDP (Figure 5.3a) and with IDP (Figure 5.3c) show clearly GDP's and IDP's C=O stretches and GDP's -NH_2 scissoring mode.

B. Difference spectroscopy of GDP, IDP and 6-thio-GDP in EF-Tu and *ras*-p21

Figure 5.2 shows the difference spectrum formed between the GDP and IDP when bound to EF-Tu (5.2ba) and p21 (5.2c). The solution difference spectrum is given in Figure 5.2a. A comparison between the difference spectra of bound nucleotides and their corresponding solution spectra shows that the overall shape of the spectra are not much affected by binding, a similar result as the "isotope editing" experiment (Chapter IV.B), however the bound difference spectra are somewhat sharper than that of free nucleotides (especially in p21).

Protein difference spectra formed between protein•nucleotide and protein•nucleotide analogue contain nucleotide bands which shift in frequency or are absent in the spectrum of the analogue. In addition, it is possible, and even expected, that the difference spectra will also contain bands which arise from protein vibrations that are perturbed differently in their interaction with the nucleotide compared with the nucleotide analogue. We may safely assign the largest of the bands in the protein difference spectra as arising from the bound nucleotide. The non-resonance Raman cross sections of the aromatic purine rings and analogues are quite large compared to the vast majority of apo-protein vibrations and their expected changes [20]. For example, the intensity of the 1487

cm^{-1} band in the GDP spectrum is about 3% of that of the 1449 cm^{-1} protein band of EF-Tu and about 6% of the corresponding protein band in the p21 spectrum [70]. From our previous studies, which determined difference spectra between EF-Tu and p21 containing isotopically labeled and unlabeled nucleotides (and therefore the difference spectra could not include any apo-protein bands), this band's position and intensity are unaffected by binding to these two proteins. In the protein GDP-IDP difference spectra of Figure 5.2b and 5.2c, an intense band is also observed at 1487 cm^{-1}, at the solution position (Figure 5.2a), and its intensity relative to apo-protein bands is preserved. Thus, it is certain that this band arises from the bound nucleotide. On the same grounds, we can assign other major bands in the protein difference spectra to nucleotide bands which preserve their relative intensity from the solution difference spectrum and which show either no or only small shifts upon binding. Those bands of special interest for this study which meet these criteria, their internal mode assignment, and shifts upon binding are tabulated in Table 5.1.

Figure 5.2a shows the difference spectrum formed between GDP and IDP. The positions of a few vibrational modes change upon protein binding. A major purine peak appears at 1487 cm^{-1} for GDP and at 1473 cm^{-1} for IDP (see Figure 5.1). This band was assigned to the ring N7=C8 stretching motion coupled with 8-CH deformation ([51). When bound to both EF-Tu and p21, the position of this band remains unchanged from its solution value, indicating no interactions between the 7 and 8 positions of the nucleotide and the binding site. Lack of interactions at this position is supported also by previous Raman and chemical modification studies (see Chapter IV.B and Wittinghofer, 1977 #351]). The stretching vibration of the C4=C5 atoms in the purine ring contribute most of the intensity to the peaks observed at 1577 cm^{-1} and 1555 cm^{-1} in the Raman spectra of GDP and IDP, respectively ([51, 67, 71]). This results in negative and positive peaks at these locations in the difference spectrum (Figure 5.2a). These bands shift down when the nucleotide bind to proteins.

The presence of the 2-amino group ($-NH_2$) of GDP is observed as contributions to two Raman intensities: an external C-N stretching mode at 1178 cm^{-1}, and an amine scissoring motion at 1646 cm^{-1}, resulting in positive peaks at 1179 cm^{-1} and 1644 cm^{-1} (see above and Figure 5.2a) in the difference spectrum. Upon binding, the scissoring mode shifts to 1652 cm^{-1} and 1660 cm^{-1} in EF-Tu and p21, respectively. The external C-N stretching mode shifts down to 1176 cm^{-1} in EF-Tu and to 1174 cm^{-1} in p21. This assignment of the two bands in the 1600-1700 cm^{-1} range in the protein difference spectra to the nucleotide C=O stretch mode and the $-NH_2$ scissors mode is reinforced by observation of these bands in more than one difference spectrum. For example, the $-NH_2$ scissors mode is observed clearly at the same position and relative intensity in EF-Tu in the difference spectrum formed between GDP and IDP as well as that formed between GDP and 6-thio-GDP. Moreover, no negative peaks are observed in the GDP minus 6-thioGDP and IDP minus 6-thio-GDP protein difference spectra as is observed when apo-protein peaks are affected upon ligand binding ([20]).

Figure 5.3 shows the difference spectrum formed between GDP and 6-thioGDP in solution (5.3a) and in EF-Tu (5.3b), and the difference spectrum formed between IDP and 6-thio-GDP in solution (5.3c) and in EF-Tu (5.3d).

The C=S stretch is much more susceptible to coupling effects ([46]). It is expected that the C=S stretch, in which the carbon atom moves much more than sulfur, the influence of angle effects and of the effects of compression of the adjacent C-N, C-C bonds will be considerably more pronounced than in the carbonyl vibration. In spectra 5.3b, 5.3d, the vibration pattern of bound 6-thio-GDP changed dramatically due to protein-nucleotide interactions. The hydrogen bonding with C=S motif may change ring coupling, therefor effecting the vibration mode that are coupled with C=S stretch.

C. Difference spectroscopy of GDP and 6-^{18}O-GDP in EF-Tu and *ras*-p21

One disadvantage of forming difference spectrum between protein-ligand complex and protein with chemically modified ligand is that the effect of protein changes induced by the modification is hard to estimate, especially when the interesting vibrational band overlaps with a strong protein band. For this reason, GDP with ^{18}O labeled at 6 position was synthesized.

As expected, the major spectroscopic effect of replacing the oxygen at 6-position by ^{18}O is the down shift of the C=O stretch (Figure 5.4, 5.5). However, the amount of 10 cm^{-1} down shift is far less than the 33 cm^{-1} down shift predicted for the isolated C=O stretch by the simple mass law, *ie.* ν is proportional to $\sqrt{(m_1/m_2)}$, where m_1 and m_2 are reduce masses. The ring stretch peak at 1487 cm^{-1} is also down shifted 3 cm^{-1} upon isotopic labeling. This indicates an interaction of C=O stretch with other vibrations of the conjugated guanine ring. The difference spectrum formed between GDP and 6-^{18}O-GDP has a positive peak at 1695 cm^{-1} and a negative peak at 1659 cm^{-1} (Figure 5.6a). The zero crossing of this derivative-like peak is at 1673 cm^{-1}.

Figure 5.6 also shows the difference spectra of GDP minus 6-^{18}O-GDP in EF-Tu (Figure 5.6b) and in p21 (Figure 5.6c). The overall features of these two difference spectra are very similar to that of the free nucleotides. The ring stretch at 1478 cm^{-1} is not affected by binding in both proteins, which confirms the results obtain with chemical modification of the nucleotide. The C=O stretch is affected by protein binding to a different extent in the two proteins. In EF-Tu, the zero crossing of the derivative-like carbonyl stretches shifts down from 1673 to 1658 cm^{-1}, while in ras-p21, it shifts down to 1663 cm^{-1}.

By using isotopically labeled nucleotide, the first order effect of protein changes can be ruled out. The relative intensities and positions of C=O stretches observed in this study are consistent with the observations of using chemically modified nucleotides, thus, confirms our previous result (Chapter V.B).

D. Discussion

The frequencies of the bands observed in vibrational spectroscopy are determined by the masses of the atoms and bond force constants of the internal coordinates that make up the observed normal mode. The force constants are functions of the distribution of the electrons in the internal coordinates. Thus, the observed band frequencies report on several structural attributes of the interacting atoms. For small molecular systems in particular, the geometry of the atoms may be surmised in some cases. In our previous work on the binding of GDP to EF-Tu and p21 (Chapter IV), we showed that the purine ring-ribose glycosidic bond adopted an anti conformation while the pucker of the sugar is C2' *endo*-anti, in agreement with crystallographic studies ([8, 25, 72]). Virtually all Raman bands in the difference spectra of the protein-bound nucleotides are sharper then those observed in solution, the effect being more pronounced with p21 then with EF-Tu. We interpret this qualitative difference to arise from a more constrained conformation of the nucleotide when bound to the protein.

Consistently, the binding constant of GDP to p21 ($K_d = 2 \times 10^{11}$ M; John et al., 1990) is significantly higher than to EF-Tu ($K_d = 2 \times 10^{9}$ M; [59]).

The major interest in this section centers on the interactions that exist between the bound nucleotide's purine ring with EF-Tu and p21. For both proteins, high resolution x-ray crystallographic structures have been determined and a set of interactions between the guanine moiety of GDP and an array of conserved residues was implied ([8, 25, 72]). Utilizing the conventional crystallographic criteria for hydrogen bonding (i.e. donor to acceptor distance ≤3.4 Å), the guanine base is anchored in the binding site with 7 hydrogen bonds in EF-Tu and 5 hydrogen bonds in p21. However, it is not possible to asses the magnitude of these interactions with crystallographic data because of the limited accuracy of such studies, even for a 1.3 Å resolution study now available for p21 ([11, 72]). The reason for this is that the shift in distance between atoms associated with even a strong hydrogen bond is a fraction of a tenth of an angstrom. On the other hand, the electrons associated with the moiety forming the hydrogen bond respond quite strongly, and this leads to easily measurable changes in vibrational force constants and the associated frequencies of the observed bands. For example, the frequency of an isolated ketone C=O stretch is quantitatively related to the hydrogen bond interaction energy formed with nearby hydrogen bond donors to a good approximation. Every 2 cm^{-1} shift in the C=O stretch implies one kcal/mol in interaction enthalpy. At the same time, a 2 cm^{-1} shift implies a distance change of the ketone bond of less than 0.01 Å ([73, 74]). Thus, changes in frequency of bands associated with bonds undergoing hydrogen bonding (or lack thereof) when the nucleotide binds have implications for our understanding of the binding parameters.

The intense purine peak which appears at 1487 cm^{-1} for GDP and at 1473 cm^{-1} for IDP in solution (see Figure 5.1) is assigned to the ring N7=C8 stretching motion coupled with 8-CH deformation ([51, 63]), and the position of this band is sensitive to the magnitude of hydrogen bonding to N7 ([52]). When bound to both EF-Tu and p21, the position of this band remains unchanged from its solution value (Table 1), indicating no change in interaction between N7 of the nucleotide and the binding site relative to its interaction with water. Lack of a change in interaction at this position is supported also by previous Raman and chemical modification studies ([57, 70]). These results do not imply that there are no interactions between N7 and its environment. There is presumably some hydrogen bonding with water for GDP in solution, and the X-ray show N7 to be close enough to Asn116 in p21 (3.2 Å) and Asn135 in EF-Tu (3.0 Å) for effective hydrogen bonding.

A pronounced spectral shift is observed in the ring mode assigned to the C4=C5 stretching motion. This band, observed at 1577 cm^{-1} in GDP and at 1555 cm^{-1} in IDP, shifts down by 7 cm^{-1} upon binding to EF-Tu, and by 10 cm^{-1} when bound to p21 (see Table 5.1). In solution this band is virtually unchanged for ^{15}N labels at 7-N and 9-N positions ([75]) and for all the deuterium labeled derivatives. ^{15}N labels at 1-N, 2-N and 3-N positions down shifted this band about 7 cm^{-1} ([75]). The nearest nitrogen atom to C4=C5 double bond among the three is 3-N, it seems reasonable to assume the down shift of C4=C5 stretch is mainly caused by mass increase of 3-N. Despite the insensitivity to deuteration on position 1-N, 2-N or 8-C, this vibration band is very sensitive to environmental changes. This mode has shown to be sensitive to ^{15}N labeling on the 6 membered ring ([75]) and to solvent polarity: its frequency is down shifted by 12 cm^{-1} when guanosine is dissolved in DMSO and increases gradually with incremental additions of water.

The data therefore suggests that the protein-induced down shifts of this mode arise primarily from the different polarity of the environment of the nucleotide when in water *vs.* when bound to the protein. The x-ray studies have showed the different roles of a conserved Lysine residue around Guanine ring in EF-Tu than in p21 ([26, 29]). These difference in interactions may functioned via nitrogen atom at 3 position.

A major effect of binding is seen on the vibrational modes associated with positions 2 and 6 of the guanine base. In general, the formation of a stronger hydrogen bond will increase the frequency of a donor deformation vibration like $-NH_2$ scissoring while decreasing the frequency of an acceptor stretching vibration like the C=O stretch ([18, 76,77]). This is because the H-N-H scissoring motion will be 'stiffened' by the hydrogen bond. On the other hand, electrons are drawn from the C=O bond by attractive electrostatic interactions which lower its bond order and hence its frequency. The amine deformation mode of GDP, observed at 1646 cm^{-1} in solution, is shifted up by 8 and 16 cm^{-1} upon nucleotide binding to EF-Tu and p21, respectively. The carbonyl stretching frequency of IDP is shifted down by 15 cm^{-1} and 20 cm^{-1} when bound to EF-Tu and p21, respectively, while the carbonyl stretch of GDP down shifts by 15 cm^{-1} and 10 cm^{-1} when it binds to EF-Tu and p21 (Table 5.1). This indicates stronger hydrogen binding (ΔH) of the 6-keto and 2-amino moieties of the nucleotides to EF-Tu and p21 than with water. Interactions with these positions are conserved in EF-Tu and p21 as well as among other members of the GTPase super family, as part of the NKXD motif (e.g. [78]). The 2-amino group is known to be only 3Å or less away from an invariant Asp residue (Asp138 in EF-Tu and Asp119 in p21), while the 6-keto group is hydrogen bonded to the main chain NH of a conserved Alanine residue (Ala146 in p21 and Ala174 in EF-Tu). In principle, it is possible to determine the magnitude of the hydrogen bond from the shifts in frequency of the C=O stretch and $-NH_2$ scissors modes since, in general, fairly accurate correlations are found between bond frequencies and the interaction enthalpy between donor and acceptor (Badger-Bauer relationships; see e.g. [73]). However, quantitative relationships require calibrating model solution studies between the purine ring of GDP or IDP, in this case, and a series of proton donors in the case of the C=O moiety and proton acceptors for $-NH_2$. This has not yet been performed. From our previous work (see e.g. [79]), the shifts observed for the $-NH_2$ scissors mode upon binding suggest relatively small interaction enthalpies. On the other hand, the shifts in the C=O stretch suggest reasonably strong hydrogen bonding between this group and protein, on the order of a few kcal/mol.

Hydrogen-bond-induced shifts observed in the present study are such that, in the interaction with GDP, the strength of the hydrogen bond with NH_2 group is greater in p21 than in EF-Tu, while the hydrogen bond with C=O group is weaker in p21 than in EF-Tu (see Table I). This is consistent with the available x-ray crystallographic data ([72, 80]). The 6-oxygen is seen to be interacting with three hydrogen bond acceptors in EF-Tu (3Å from Ala174, 2.7Å from Asn145, and 3.2Å from Ser173), while it is interacting with only one acceptor on p21 (2.9Å from Ala146). But, a somewhat conflicting situation is seen in the vibrational modes involving the 2-amino group. The exocyclic amine's distance of closest approach to its hydrogen bonding Asp in EF-Tu is identical to that in p21 (2.9Å), where the interaction is expected to be slightly weaker, since the carboxylate's electronegativity in p21 is also shared by a nearby (2.8Å) structural water molecule. On the other hand, the spectral shifts of both the $-NH_2$ deformation (1647 cm^{-1} in solution), and the external C-N stretching (1178 cm^{-1} in solution) are roughly twice as pronounced for the nucleotide in p21 then in EF-Tu.

Hydrophobic interactions and hydrogen bondings are the two major interactions that anchor the nucleotide in the proteins. In EF-Tu and ras-p21, these interactions contribute to a different extend on nucleotide binding. The radioactive binding assay showed that the replacement of the 6-oxygen by a hydrogen atom abolishes the affinity of the nucleotide to EF-Tu, while the affinity of the nucleotide to p21 is only reduced by 25 fold. This result indicate that the hydrogen bonding at 6 position is more important in nucleotide binding in EF-Tu than in p21, which is consistent with the result of Raman measurement that the hydrogen bonding at this position is stronger in EF-Tu. Binding assays showed that the elimination of $-NH_2$ group on the guanine ring reduces the affinity of the nucleotide to EF-Tu by a factor of 85, while, in p21, the reduction is a factor of 123. This result is consistant with the Raman study that the hydrogen bonding at $-NH_2$ position contributes more in the binding in p21 than in EF-Tu. When IDP binds to p21, the reduced affinity due to the absence of hydrogen bonding at 2-position seems, partly, to be compensated by the increase in the hydrogen bond strength at 6-position, since the observed frequency shift for IDP's C=O stretch is clearly greater in p21 then in EF-Tu (-15 cm^{-1} vs. -20 cm^{-1}, respectively), which is the opposite case of C=O stretch of GDP (table 5.1). The mechanism of such a rearrangement of interactions is currently unclear. Overall, p21 binds GDP ([57, 81]) some 100-fold more strongly than does EF-Tu. Hydrophobic interactions may play an important role in p21 binding to the nucleotide. The substitute guanine ring of the 6-thioGDP is more hydrophilic than that of GDP. Decreasing the hydrophobicity of the nucleotide by replacing 6-oxygen with a sulfur completely abolish the binding affinity of p21 to the nucleotide while the elimination of the carbonyl group only reduce the affinity by 25 fold.

We take the above mentioned data to indicate that although the hydrogen bond with 6-oxygen is weaker in p21 than in EF-Tu, the overall interactions of the guanine moiety of the nucleotide are tighter in p21 then in EF-Tu. The hydrogen bonding with NH_2 group and the hydrophobic interactions are important in the interactions with p21, thus contributing majorly to the reduced dissociation constant observed in p21. The binding affinity of the two proteins to different nucleotides (6-thioGDP and 6-hydroGDP) support this notion. Both proteins bind IDP, suggesting that the hydrogen bonding of the 2-amino group, while definitely contributing, is not an absolute requirement. Accordingly, GDP analogues substituted at this position with bulky groups such as tolyl-, butyl-, or phenyl- bind with similar or even greater affinity to p21 ([48]). On the other hand, while p21 binds 6-hydroGDP with greater affinity than IDP, EF-Tu does not show any significant binding of this analogue when measured in a filter exchange assay. The situation is reversed with respect to 6-thioGDP (Table 3.2). The binding of 6-thioGDP to EF-Tu was shown to be accompanied by a decrease in the pK of the thiol group of 0.7 units ([47]).

Table 5.1: Frequencies (in cm^{-1}) of selected nucleotide vibrations in solution and their frequency shifts when complexed to p21 and Elongation Factor Tu.

MODE	ν (solution)	Δν (EF-Tu)	Δν (p21)
	GDP vibrations		
N7=C8 stretch	1487	$0^{a,b}$	$0^{a,b}$
C4=C5 stretch	1577	-7^{b}	-10^{b}
C2-NH_2 stretch	1179	-2^{b}	-5^{b}
-NH_2 scissor	1646	$+8^{b,c}$	$+16^{b}$
C=O stretch	1685	$-15^{c,e}$	-10^{e}
	IDP vibrations		
C4=C5 stretch	1555	-5^{b}	-10^{b}
C=O stretch	1691	-15^{d}	-20^{d}

(a) shift in frequency obtained from [70]; (b) difference spectrum formed between GDP and IDP, which may have some error because of overlapping bands in C=O stretch region; (c) difference spectrum formed between GDP and 6-thio-GDP; (d) difference spectrum formed between IDP and 6-thio-GDP; (e) difference spectrum formed between GDP and 6-^{18}O-GDP, (see Figure 5.6a and 5.6c).

Figure 5.1: Solution Raman spectra of (a) GDP, (b) IDP, and (c) 6-thio-GDP. Samples are at 0.1 M in H_2O, pH 7.5. Excitation is with 150 mW of the 488 nm Ar^+ laser line for (a) and (b), and 150 mW of 568.2 nm line from a Kr^+ ion laser for (c).

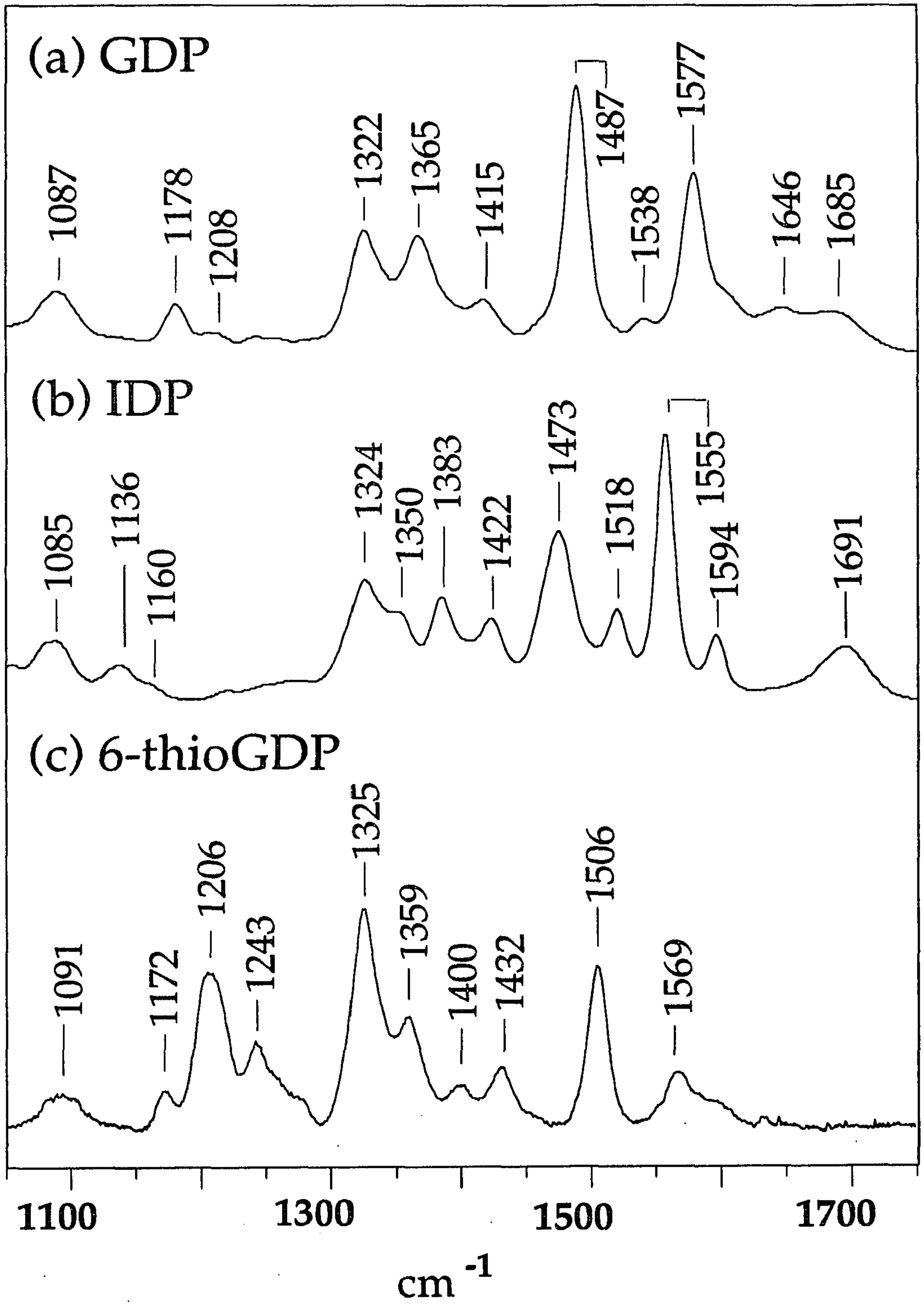

(a) GDP
1087
1178
1208
1322
1365
1415
1487
1538
1577
1646
1685
(b) IDP
1085
1136
1160
1324
1350
1383
1422
1473
1518
1555
1594
1691
(c) 6-thioGDP
1091
1172
1206
1243
1325
1359
1400
1432
1506
1569
1100
1300
1500
1700
cm -1

Figure 5.1

Figure 5.2. Raman difference spectra formed between GDP and IDP. (a) in solution, (b) complexed with EF-Tu and (c) complexed with c-H-*ras* p21. Panel (a): the difference spectrum obtained from the data in Figures 5.1a and 5.1b. Panel (b): EF-Tu is at ca. 2.5 mM in buffer R and excitation is with the 530 nm line from a Kr^+ ion laser. Panel (c): p21 is at ca. 3.5 mM in buffer R and is excited with the 568.2 nm line from a Kr^+ ion laser.

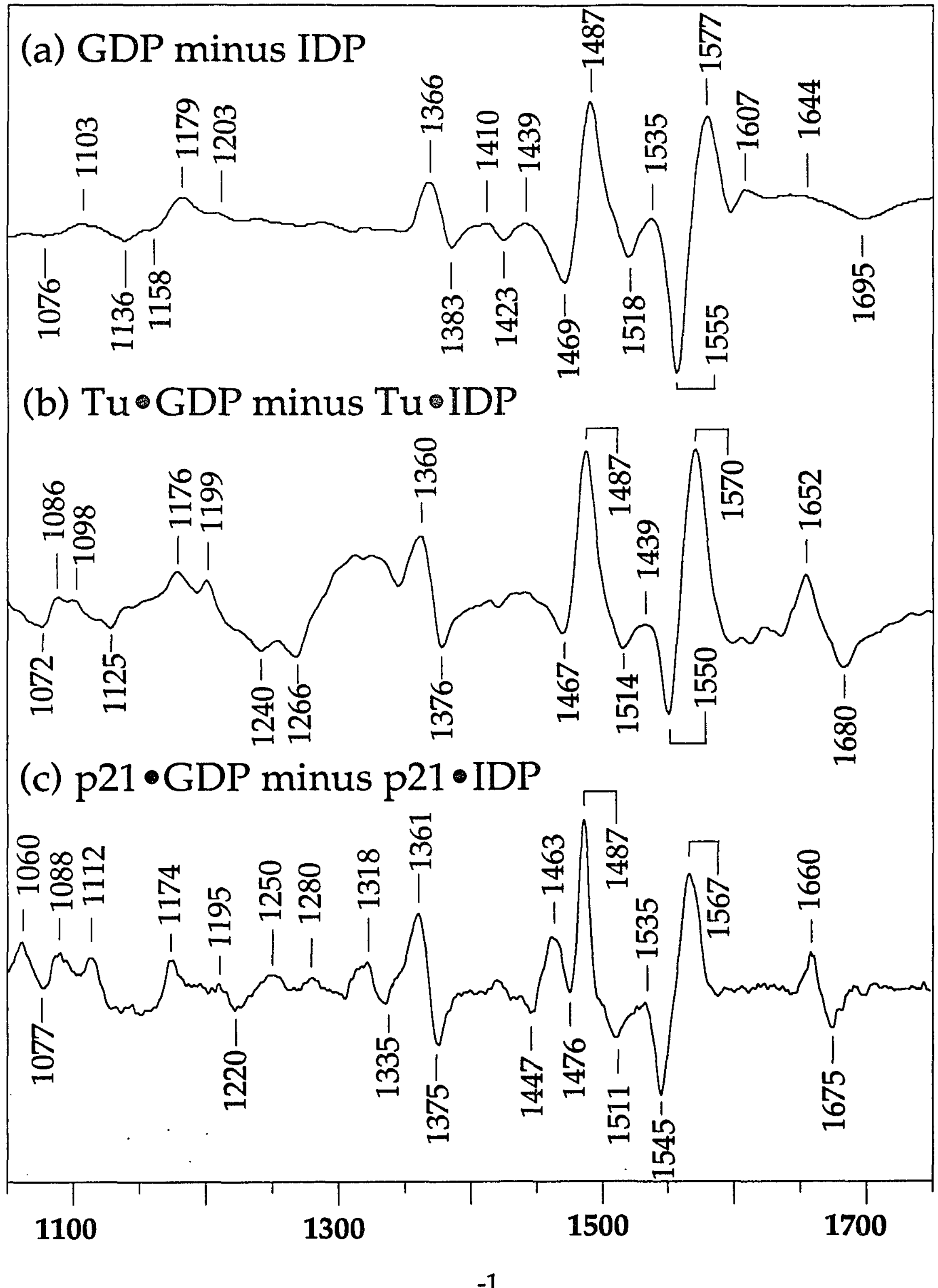
(a) GDP minus IDP
1076
1103
1136
1158
1179
1203
1366
1383
1410
1423
1439
1469
1487
1518
1535
1555
1577
1607
1644
1695
(b) Tu•GDP minus Tu•IDP
1072
1086
1098
1125
1176
1199
1240
1266
1360
1376
1467
1487
1514
1439
1550
1570
1652
1680
(c) p21•GDP minus p21•IDP
1060
1077
1088
1112
1174
1195
1220
1250
1280
1318
1335
1361
1375
1447
1463
1476
1487
1511
1535
1545
1567
1660
1675
1100
1300
1500
1700
cm-1

Figure 5.2

Figure 5.3: Raman difference spectra of GDP minus 6-thio-GDP in solution (a) and in EF-Tu (b), and the difference spectra of IDP minus 6-thio-GDP in solution (c) and in EF-Tu (d). Solution spectra (a, c) were obtained with 180 mW of the 568.2 nm line from a Kr^+ ion laser, the nucleotide concentrations are at ca. 0.1 M, pH 7.4. EF-Tu is at ca. 2.5 mM in buffer R and excitation is with the 530 nm line from a Kr^+ ion laser. P21 is at ca. 3.5 mM in buffer R and is excited with the 568.2 nm line from a Kr^+ ion laser. Right Panel shows the expanded view of the high frequency region for the corresponding difference Raman spectra at left panel.

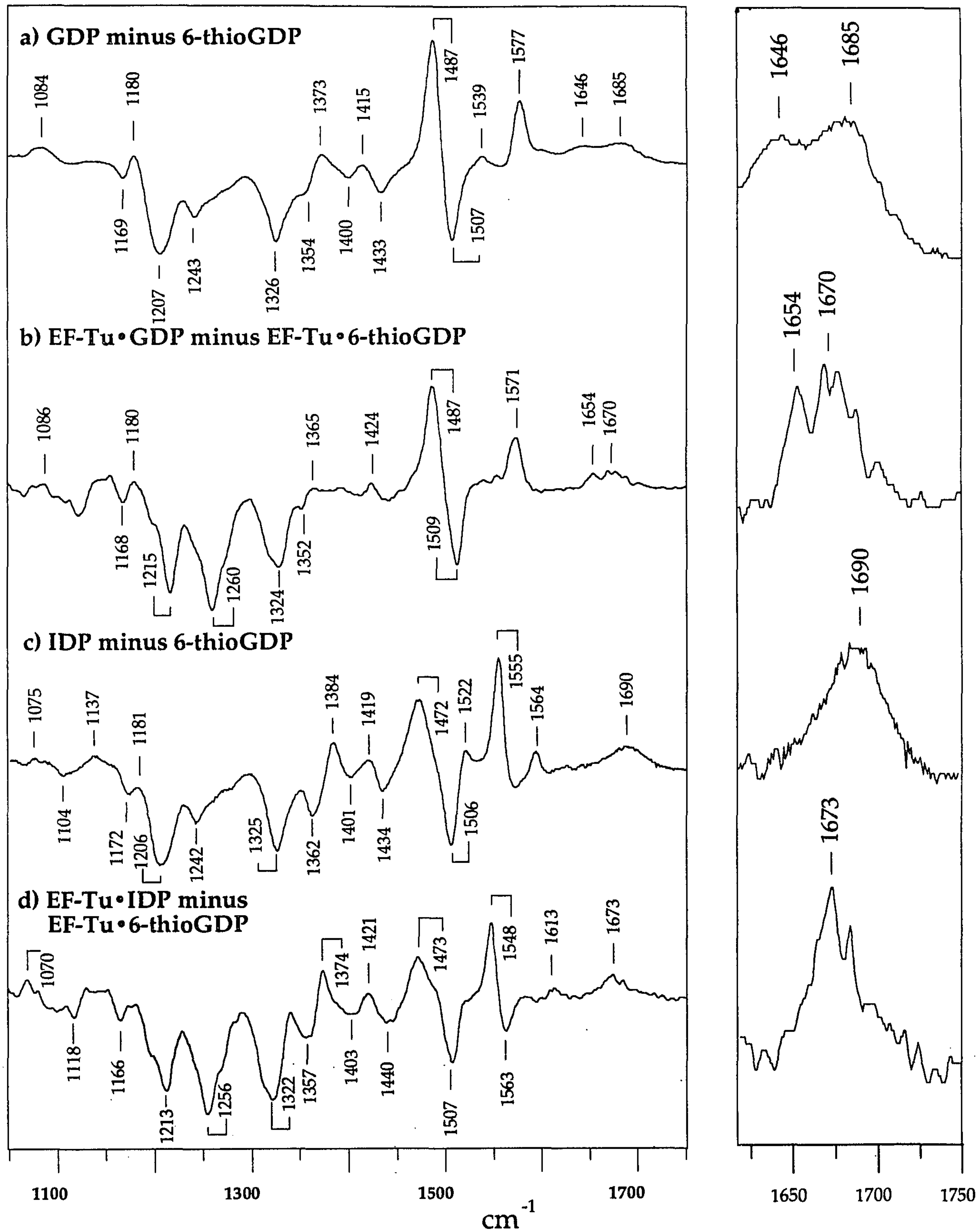
a) GDP minus 6-thioGDP
b) EF-Tu•GDP minus EF-Tu•6-thioGDP
c) IDP minus 6-thioGDP
d) EF-Tu•IDP minus EF-Tu•6-thioGDP
1100
1300
1500
1700
1650
1700
1750
cm-1

Figure 5.3

Figure 5.4: Raman spectra of GDP (a) and 6-^{18}O-GDP (b) in solution. The spectra were obtained with 180 mW of the 568.2 nm line from a Kr^{+} ion laser, the nucleotide concentrations are at ca. 0.1 M, pH 7.4.

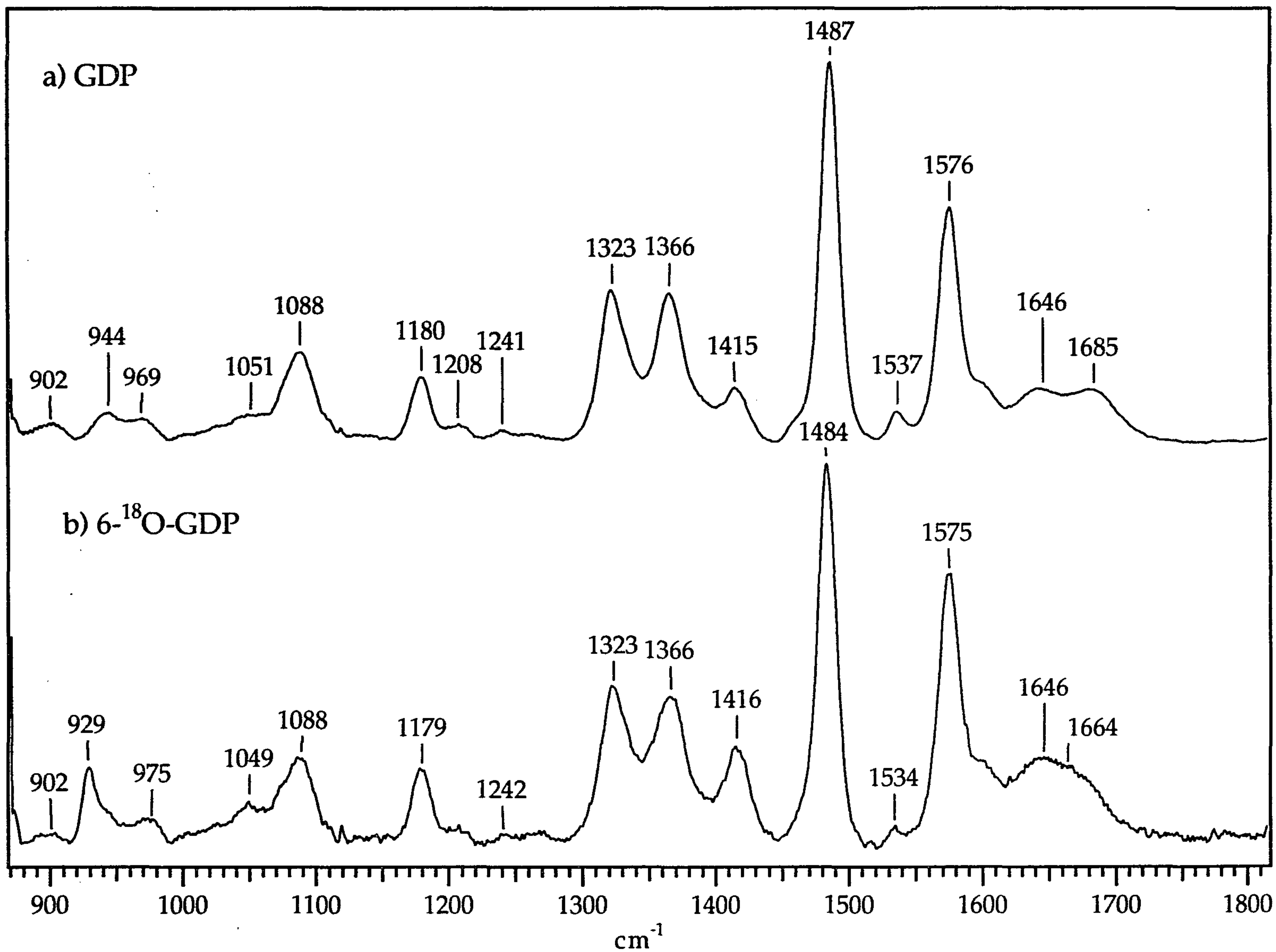
a) GDP
902
944
969
1051
1088
1180
1208
1241
1323
1366
1415
1487
1537
1576
1646
1685
b) 6-18O-GDP
902
929
975
1049
1088
1179
1242
1323
1366
1416
1484
1534
1575
1646
1664
900
1000
1100
1200
1300
1400
1500
1600
1700
1800
cm-1

Figure 5.4

Figure 5.5: A blow-up view of the C=O stretch regions of the Raman spectra of GDP (a) and 6-^{18}O-GDP (b) in solution. The two spectra are normalized to the intensity of the peak at 1577 cm^{-1}. The $-NH_2$ bending and C=O stretch modes of GDP are fitted to two Lorenzian peaks. In the spectrum of 6-^{18}O-GDP, the Lorenzian peak at 1641, which is obtained from the fitting of the GDP spectrum (a), was subtracted out from the overlaped C=O stretch and $-NH_2$ bending modes. This operation leaves the C=^{18}O stretch at 1675 cm^{-1}. The C=O stretch shifts down 10 cm^{-1} upon the isotopic labeling.

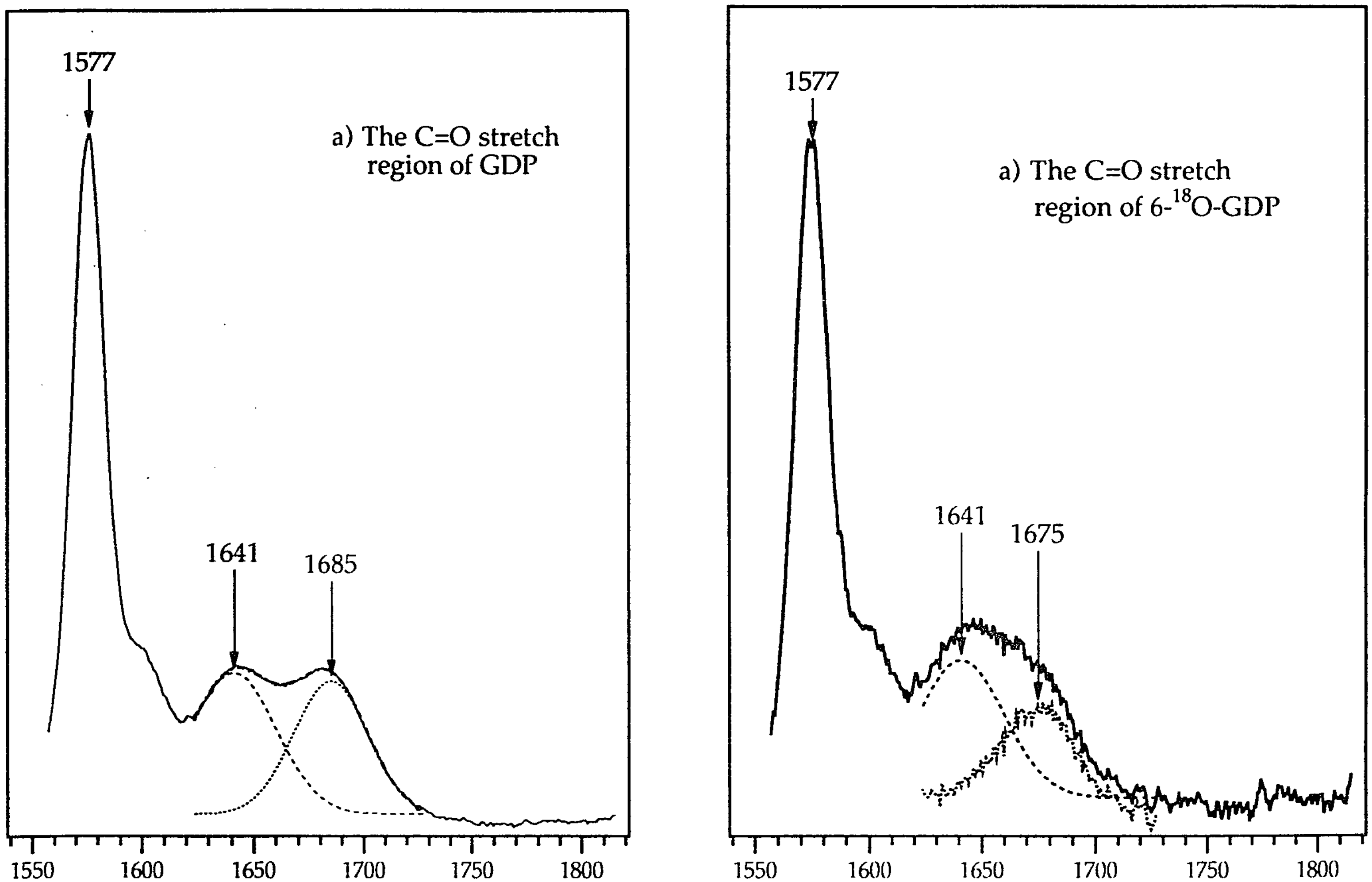
1577
a) The C=O stretch
region of GDP
1641
1685
1550
1600
1650
1700
1750
1800
1577
a) The C=O stretch
region of 6-^{18}O-GDP
1641
1675
1550
1600
1650
1700
1750
1800

Figure 5.5

Figure 5.6: Raman difference spectra of GDP minus 6-^{18}O-GDP in solution (a), in EF-Tu (b) and in p21 (c). The "zero crossing" ponts of the spectra are labeled with arrow lines. Solution spectra (a) was obtained with 180 mW of the 568.2 nm line from a Kr^+ ion laser, the nucleotide concentrations are at ca. 0.1 M, pH 7.4. EF-Tu is at ca. 2.5 mM in buffer R and excitation is with the 568.2 nm line from a Kr^+ ion laser. P21 is at ca. 3.5 mM in buffer R and is excited with the 568.2 nm line from a Kr^+ ion laser.

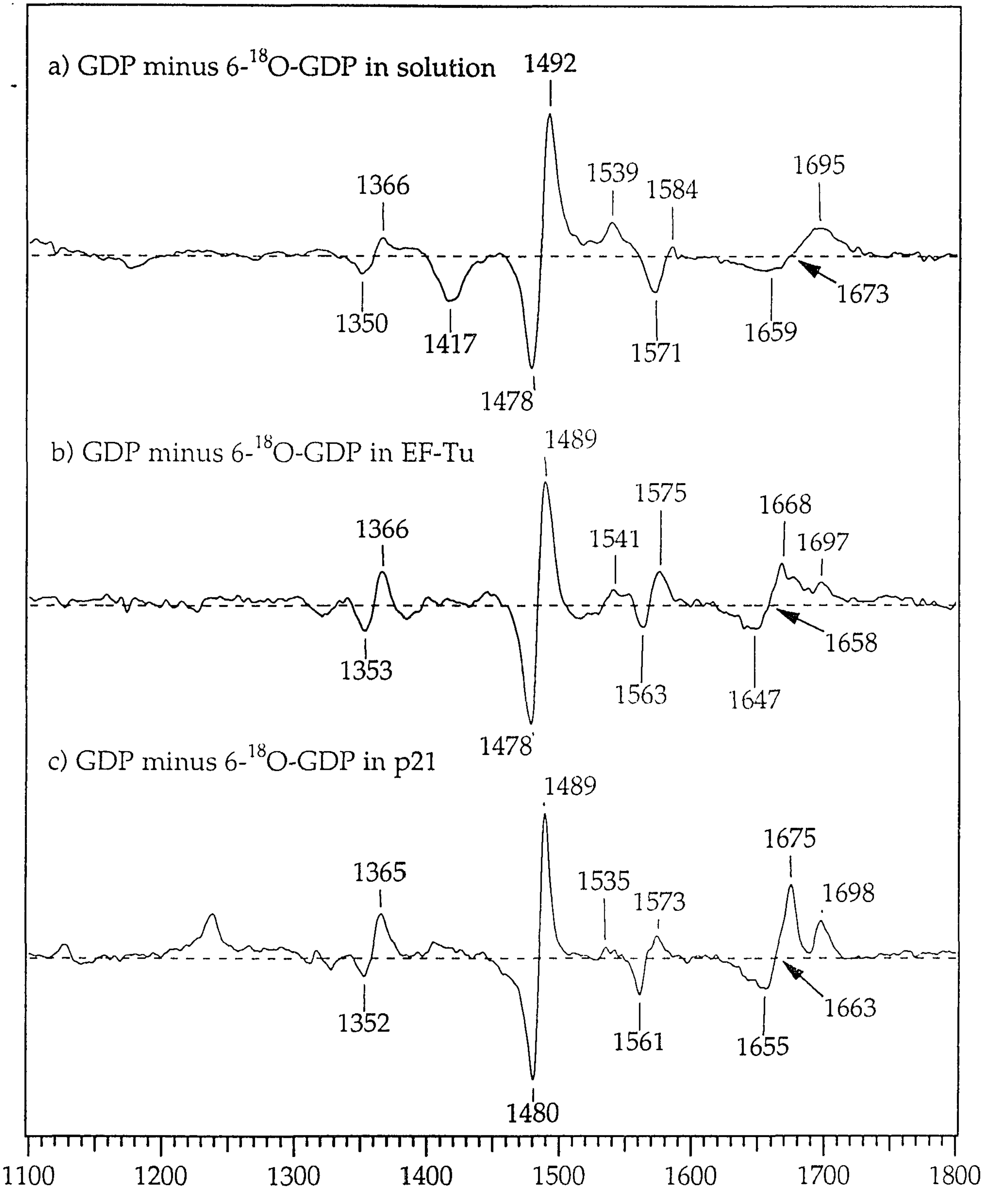
a) GDP minus 6-18O-GDP in solution
1492
1366
1539
1584
1695
1350
1417
1478
1571
1659
1673
b) GDP minus 6-18O-GDP in EF-Tu
1489
1575
1366
1541
1668
1697
1353
1563
1647
1658
1478
c) GDP minus 6-18O-GDP in p21
1489
1675
1365
1535
1573
1698
1352
1561
1655
1663
1480
1100
1200
1300
1400
1500
1600
1700
1800

Figure5.6

Chapter VI

THE INTERACTIONS OF NUCLEOTIDES WITH G-PROTEINS II: INTERACTION WITH THE PHOSPHATE MOIETY OF GUANINE NUCLEOTIDES

The phosphate motif of nucleotide is very important for binding. Removal of the β-phosphate from GDP reduces its affinity to the *ras*-p21 by a factor of more than 10^6 ([44]). Phosphate groups on GDP and GTP are negatively charged under physiological pH. As is generally the case for nucleotide-binding proteins ([82]), the phosphate binding of EF-Tu and *ras*-p21 are stabilized by a positive dipole moment of the phosphate binding loop. In x-ray studies of EF-Tu, the four main-chain nitrogen atoms in the loop Asp21 to Lys24 encircle the β-phosphate group within a distance of approximately 3.5 Å. In *ras*-p21, the phosphate binding site is also characterized by a number of interactions. Thus, attempts were taken to address the specific interactions on the phosphate group.

A. Difference Spectrum of EF-Tu•GDP and EF-Tu•GDPβS

GDPβS is a commercially available compound where one of the oxygens on β-phosphate is replaced by a sulfur atom. Measurements were carried out with EF-Tu that contains a GDPβS in its active site. The difference spectrum of GDP minus GDPβS is shown in Figure 6.1a. A number of Raman bands of GDP are affected by the sulfur substitution. When one of the β-phosphate oxygen is changed to sulfur, the symmetry of the β-phosphate is broken as well. On unsubstituted β-phosphate, the two negative charges are distributed equally on all the three oxygen atoms which lead to a tetrahedral bond conformation for β-phosphate. The symmetric stretch of β-PO_3^{2-} group appears around 1090 cm^{-1}

which overlaps with the symmetric stretch of α-PO_2^- group at 1087 cm^{-1}. Since sulfur is less electro-negative than oxygen, the P=S bond on substitute β-phosphate contain more double bond character. Sulfur substitution breaks the symmetry of the β-phosphate group and effects bond strength and bond order of the other two P-O^- bonds, which, in turn, affects the vibrations of the phosphate group extensively. The negative peak at 612 cm^{-1} in Figure 6.1a is assigned to P=S stretch ([69]), while the positive peaks around 1090 cm^{-1} can be assigned to the symmetric stretch of the β-PO_3^{2-} group. The symmetric vibration of α-PO^- is at 1087 cm^{-1} in the GDP solution spectrum. This vibration is unlikely to be effected by a sulfur substitution on β-phosphate, therefore is subtracted out when forming the difference spectrum, leaving the β-PO_3^{2-} stretch in the 1050 cm^{-1} to 1150 cm^{-1} region. The peak at 1107 cm^{-1} may due to asymmetric vibration of α-PO_2^- which is also affected by the substitution ([83]). The peak at 942 cm^{-1} of the solution difference spectrum of Figure 6.1 can be signed to the P-O stretch of the phosphate backbone ([83]). This mode is strongly affected by sulfur substitution, for which the corresponding vibration in the substituted phosphate is hard to assign.

The protein complex difference spectra in Figure 6.1b has a small magnitude compared to the ring vibration modes of the nucleotides, the largest peak in the solution difference spectrum being only 18% of the guanine ring vibration at 1360 cm^{-1}. This indicates that the signal being detected in the protein difference spectrum is about 0.5% of the strongest protein peak.

The protein difference spectrum (Figure 6.1b) shows sharp vibrations in the region above 1200 cm^{-1} where no obvious difference peaks are observed for free nucleotides (Figure 6.1b). Comparing to the differences of free nucleotides, this protein spectrum is dominated by protein changes which obscure the nucleotide bands. Although it seems likely that the bands at 436 cm^{-1} and 459 cm^{-1}, 632

cm^{-1}, 670 cm^{-1}, 715 cm^{-1}, and 932 cm^{-1} of the protein spectrum may correspond to the bands at 445 cm^{-1}, 612 cm^{-1}, 665 cm^{-1}, 724 cm^{-1}, and 941 cm^{-1} of the solution difference receptively, it is very hard to confirm these assignments. The maximum magnitude of the protein changes are about 0.8% of the strongest protein band.

B. Difference Spectrum of EF-Tu•GDP and EF-Tu•β-$^{18}O_4$-GDP

In our previous studies, the protein changes induced by ligand binding were on the order of 1% of the strongest protein Raman peaks. In the studies describe in the Chapter VI.A, the phosphate vibrational modes were obscured by protein changes. The phosphate vibrations are generally very weak, isotopic labeling seems to be the only option to study phosphate vibration mode using Raman difference technique, since all the protein bands should be subtracted out when forming difference spectrum.

To study phosphate binding, β-$^{18}O_4$-GDP was synthesized. At pH. 7.4, the pyrophosphate group on GDP is ionized, which consists a α-PO_2^- and a β-PO_3^{-2}. The vibrations of those P-O bonds are correlated. The symmetric stretching vibration of the α-PO^- appears to be a strong Raman band at 1087 cm^{-1} ([83]). This band is not affected by ^{18}O labeling on β-phosphate. The small positive peak at 1092 cm^{-1} in the solution difference spectra formed between GDP and β-$^{18}O_4$-GDP (Figure 6.2b) may be due to the stretching vibration of the β-PO_3^{2-} group, which shifts down to lower frequency upon isotope labeling. The stretching vibrations of P-O bonds of the pyrophosphate backbone give a vibration of medium intensity at 943 cm^{-1}. This band shifts down to 894 cm^{-1} when β-phosphate is labeled with

^{18}O, an effect of replacing the oxygen atom linking α- and β- phosphate groups by ^{18}O.

The difference spectrum (Figure 6.2a) formed between EF-Tu•GDP and EF-Tu•β-$^{18}O_4$-GDP complexes is considerably simpler than the spectrum of Figure 6.1b. Since the chemical structure of labeled and unlabeled nucleotide are the same, all the protein bands should be canceled out during the subtraction, we assign the differences in Figure 6.2a to the bound nucleotides. The signal to noise ratio of Figure 6.2b is not very high due to the weak vibrations of the phosphate group. The largest peak is about 0.7% of the protein peak at 1003 cm^{-1}. The signals we measured here are just above the sensitivity of the instrument.

The correspondence of the two difference spectra in Figure 6.2 seems very obvious. One striking difference of the two spectra is the solution P-O stretching vibration at 943 cm^{-1} is considerably sharpened and down shifted to 918 cm^{-1} when the nucleotide binds to the protein. There are not enough information for us to address the cause of the down shift, but the shift seems unlikely due to the interactions of the phosphate groups with Mg^{++}, since the difference spectrum formed between GDP and GDP/Mg^{++} (in 1:1 ratio) does not show the effect on 943 cm^{-1} band (data not shown). The symmetric vibration of β-PO_3^{-2} in solution at 1092 cm^{-1} shifts up to 1102 cm^{-1} in protein and which has similar band width in the two environments.

Figure 6.1: Raman difference spectra formed between GDP and GDPβS in (a) solution, concentration of the nucleotides is ca. 0.1 M, pH 7.0, 4°C, and (b) in EF-Tu, the concentration of the complexes is at ca. 2.5 mM in buffer R. Both spectra were excited with 488 nm line from an Argon laser.

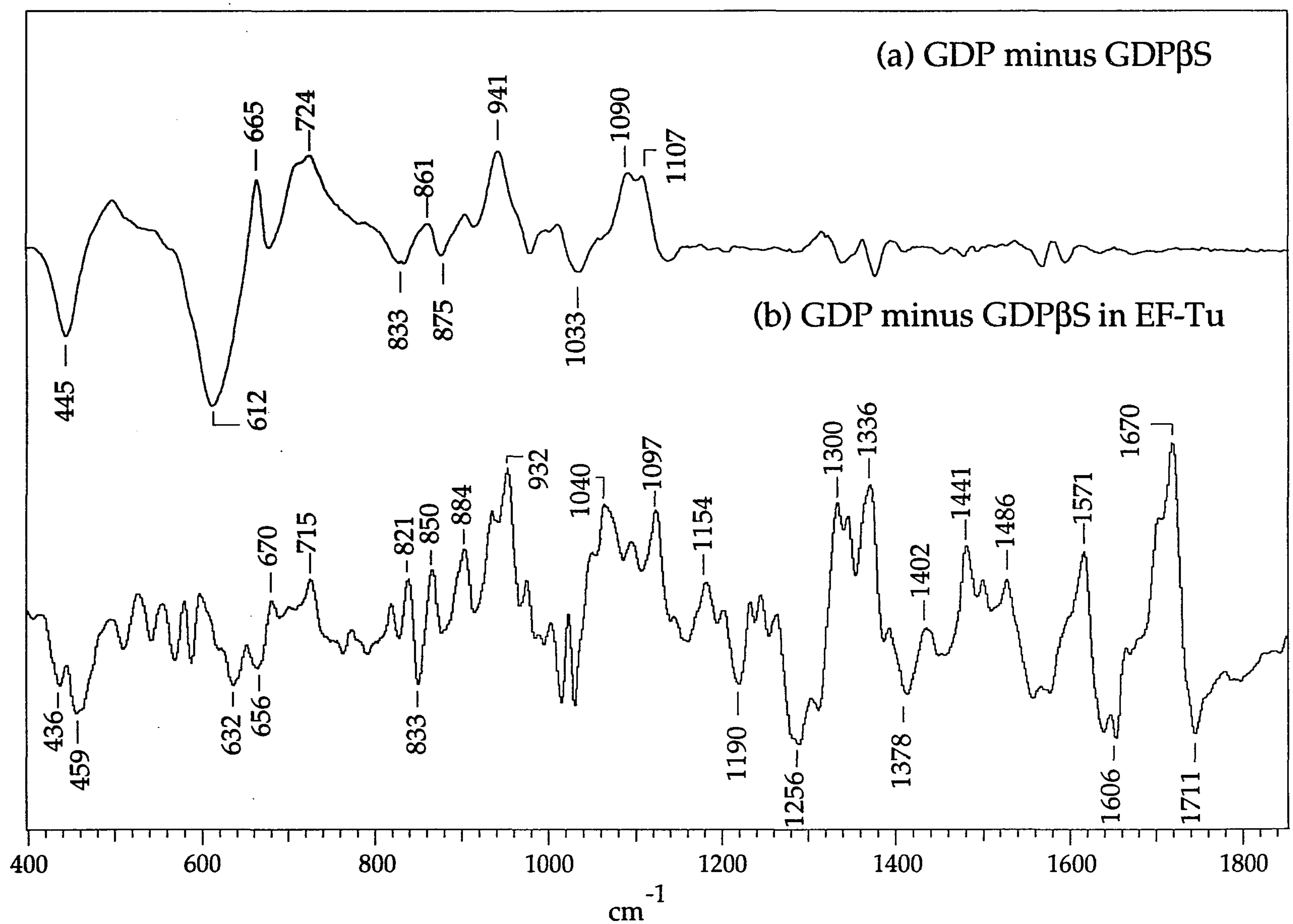
(a) GDP minus GDPβS
(b) GDP minus GDPβS in EF-Tu
445
612
665
724
833
861
875
941
1033
1090
1107
436
459
632
656
670
715
821
833
850
884
932
1040
1097
1154
1190
1256
1300
1336
1378
1402
1441
1486
1571
1606
1670
1711
400
600
800
1000
1200
1400
1600
1800
cm-1

Figure 6.1

Figure 6.2: Raman difference spectra formed between GDP (c) and β-$^{18}O_4$-GDP (d) in solution (a), concentration of the nucleotides is at ca. 0.1 M, pH 7.0, 4°C; (b) in EF-Tu, which is at ca. 2.5 mM in buffer R' (20 mM tris-HCl, pH 7.4, and 10 mM MgCl). Both spectra were excited with 568 nm line from a Kr^+ laser. In GDP (c) and β-$^{18}O_4$-GDP (d) spectra, phosphate modes are labeled with (p).

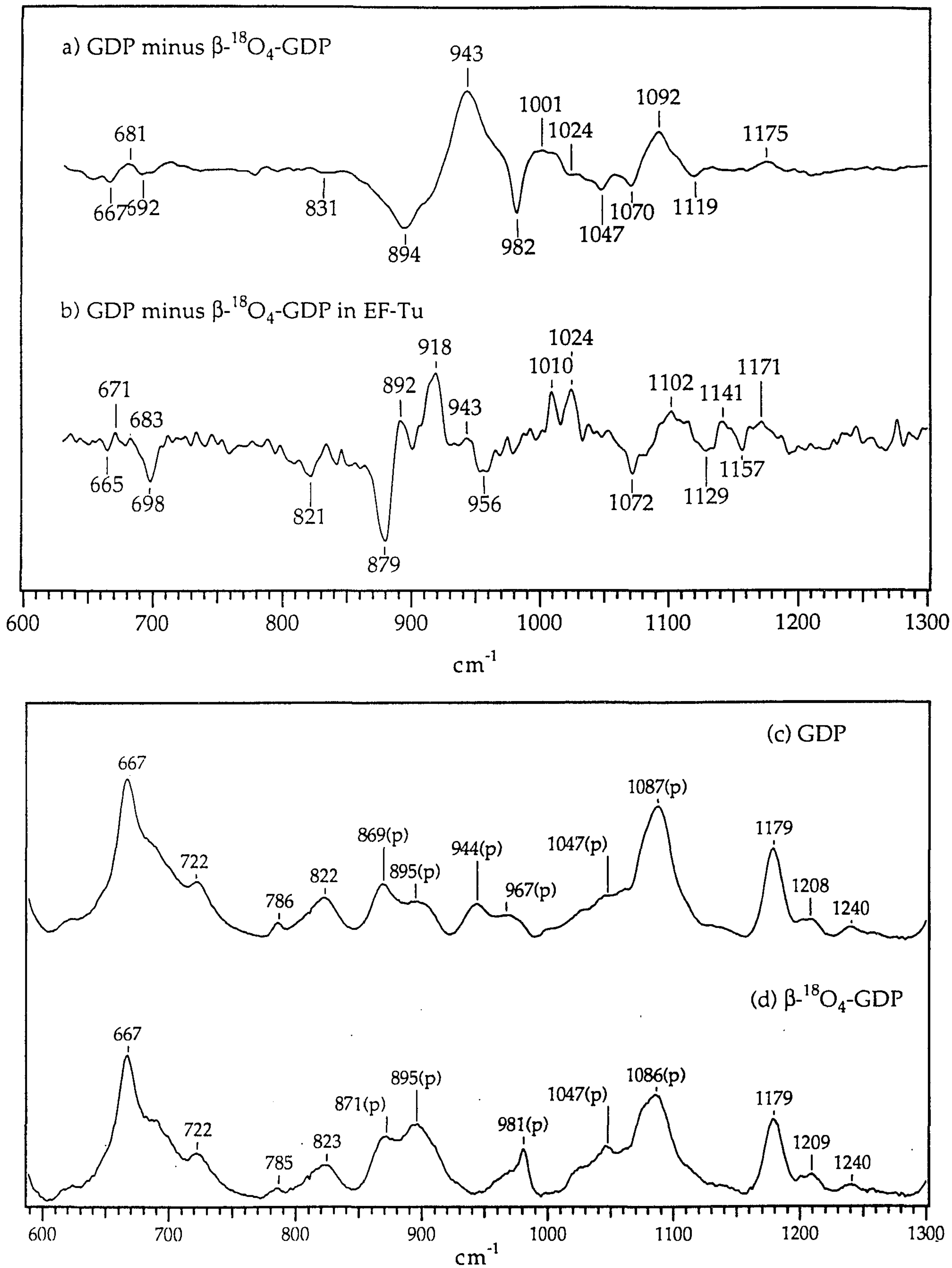
a) GDP minus β-18O4-GDP
943
1001
1024
1092
681
1175
667
692
831
894
982
1047
1070
1119
b) GDP minus β-18O4-GDP in EF-Tu
1024
918
1010
1171
671
892
1102
1141
683
943
665
698
821
956
1072
1129
1157
879
600
700
800
900
1000
1100
1200
1300
cm-1
(c) GDP
667
1087(p)
1179
869(p)
944(p)
1047(p)
722
895(p)
822
967(p)
1208
786
1240
(d) β-18O4-GDP
667
1086(p)
895(p)
1047(p)
1179
871(p)
981(p)
722
823
1209
785
1240
600
700
800
900
1000
1100
1200
1300
cm-1

Figure 6.2

Figure 6.3: Raman spectra of monophosphate (a) and ^{18}O labeled monophosphate (b). Both samples are at pH 7.4, and concentration ca. 0.1M. The four oxygens are all replaced by ^{18}O from ^{18}O labeled phosphate. At pH 7.4, monophosphate solution contains two species, HPO_4^{3-} and $H_2PO_4^{2-}$. The modes at 1077 cm^{-1} and 877 cm^{-1} are assigned to the symmetric stretches of the P-$O^{\delta-}$ and the P-OH groups on $H_2PO_4^{2-}$, while the strongest peak at 991 cm^{-1} comes from the symmetric stretching vibration of three P-$O^{\delta-}$ groups on HPO_4^{3-}. All these three vibrations shift down about 50 cm^{-1} upon isotopic labeling. Both spectra (a) and (b) were excited with 488 nm line from an Argon laser. The difference spectrum formed between unlabeled and labeled phosphates is shown in (c).

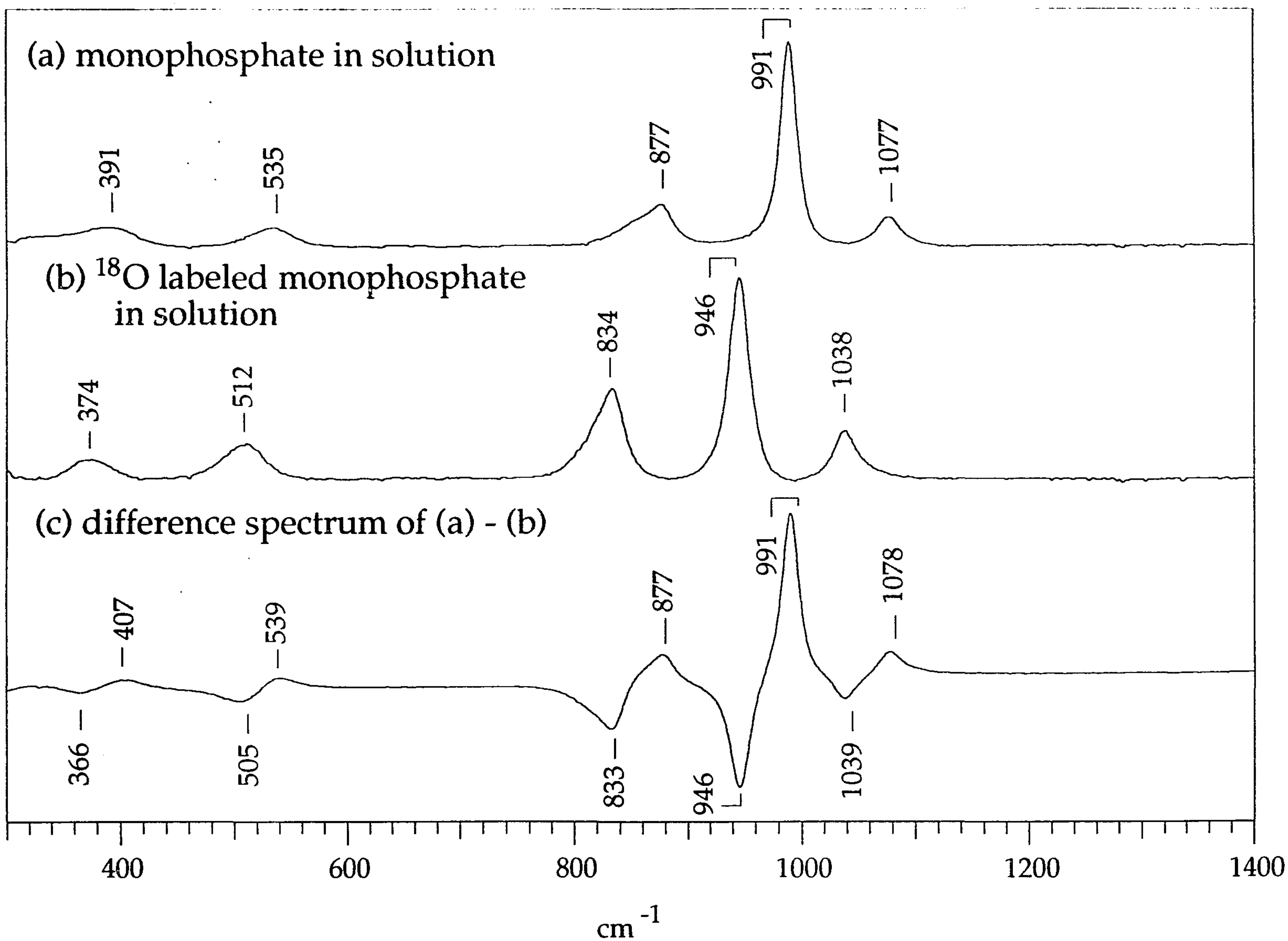
(a) monophosphate in solution
391
535
877
991
1077
(b) ^{18}O labeled monophosphate in solution
374
512
834
946
1038
(c) difference spectrum of (a) - (b)
407
539
877
991
1078
366
505
833
946
1039
400
600
800
1000
1200
1400
cm $^{-1}$

Figure 6.3

Chapter VII

THE CONFORMATIONAL CHANGES OF THE G-PROTEINS DURING THE TRANSITION FROM INACTIVE TO ACTIVE FORM

A. GTPase Activities of EF-Tu and *ras*-p21

For G-protein, the change from an inactive state to an active state, with respect to signal transduction, is induced by GTP binding. All G-proteins have some intrinsic GTPase activity (the ability of hydrolyze GTP). In some well studied cases, the acceleration of GTPase activities is the result of the G-protein binding to another protein, dissociation of a molecular complex as a result of GTP hydrolysis, or catalysis of GDP/GTP exchange by another protein ([30]).

EF-Tu and *ras*-p21 are both monomeric G-proteins. Their intrinsic GTPase activities are considerably lower than those of trimeric G-proteins which are in the ranged of 3-5 min^{-1} ([78]). The hydrolysis rate of bound GTP of EF-Tu is about 0.036 min^{-1} ([6]), while that of *ras*-p21 is 0.02 min^{-1} at 37°C as measured by Eccleston *el. al* ([84]) .

According to Arrhenius law, the chemical reaction rate is 2-4 times slower for every 10°C temperature drop. To check the GTPase activity of p21 under conditions of spectroscopic measurement (in buffer R, with a protein concentration of ~ 2 mM), the hydrolysis rate of GTP was measured (Figure 7.1). According to the simple reaction scheme:

$$p21 \bullet GTP \xrightarrow{k} p21 \bullet GDP + Pi$$

the data should follow first order kinetics:

$$[p21 \bullet GTP]/[p21]_0 = \exp(-kt)$$

where $[p21 \bullet GTP]$ is the concentration of the GTP complex at time t and $[p21]_0$ is the total concentration of the protein. At room temperature, the reaction curve is found to fit to a value of $k = 9.4 \times 10^{-3}$ min^{-1} (Figure 7.1). At 0°C, $k = 2.9 \times 10^{-4}$ min^{-1}, corresponding to a half life time ($t_{1/2}$) of about 40 hours. This hydrolysis rate is low enough to allow Raman measurement on the complex of p21•GTP. The spontaneous hydrolysis of GTP in solution, at room temperature, is less than 2% in a time period of 20 hours. Obviously, the presence of p21 accelerates GTP hydrolysis.

In our Raman spectroscopic studies, we wish to measure Raman spectra of both active and inactive form of the proteins, so that differences in the vibrational properties of these forms can be revealed. To obtain the Raman spectrum of the proteins in their active forms, the lifetime of protein•GTP complexes has to be long enough to allow the sample preparation and data collection, or slowly hydrolyzable GTP analogs have to be incorporated into the protein. In the case of EF-Tu, two GTP analogs: GMP-PCP and GMP-PNP were used. For *ras*-p21, GTP was used directly because of the low intrinsic GTPase activity of this protein. The spectra of these complexes will be discussed in this chapter.

B. Raman Spectra of GTP and GTP analogs

The Raman spectra of GTP, GMP-PNP and GMP-PCP are shown in Figure 7.2b-d. The spectra of GDP (Figure 7.2a) is also shown for comparison. The ring stretching region, from 1200 cm^{-1} to 1600 cm^{-1}, of these spectra are very similar, reflecting the fact that all these nucleotides share the same purine base. The largest differences of these spectra are located at the phosphate mode region (1050 to 1150 cm^{-1}). Peaks in this region are labeled in the figure. All nucleotides show a phosphate band at 1087 cm^{-1}, assigned to the out-of-phase symmetric vibration of the PO_2^- groups ([83]). For GTP and GTP analogs, additional phosphate bands show up at higher frequency, at 1118 cm^{-1} for GTP, at 1109 cm^{-1} for GMP-PNP and at 1106 cm^{-1} for GMP-PCP respectively. This band is associated with the third phosphate group and is assigned to an in-phase stretching mode of the γ-PO_3^{2-} group ([83]). This vibration is correlated with backbone P-O bond stretches to some degree, so that the frequency of this band shifts down slightly when the oxygen linkage of the third diester bond is replaced by atoms of smaller mass.

Usually, G-proteins require Mg^{++} ion for their biological activities. It was shown that Mg^{++} can interact with the phosphate group of guanine nucleotides and change their conformation. Raman studies show the direct evidence of these interaction (Figure 7.3). When Mg^{++} is added to solutions in 1:1 molar ratio with nucleotides, the phosphate band of GDP at 1088 cm^{-1} shifts to 1090 cm^{-1} and the phosphate band of GTP at 1118 cm^{-1} up shifted to 1122 cm^{-1}.

C. Conformational Changes of EF-Tu from Protein "Off" State to "On" state

To study the differences of EF-Tu in its active state, slowly hydrolyzable GTP analog GMP-PNP was incorporated into EF-Tu. The Raman spectra of EF-Tu•GDP and EF-Tu•GMP-PNP were measured.

Difference spectra of the nucleotides: The difference spectrum formed between GDP and GMP-PNP is shown in Figure 7.4a. The strongest difference band in the phosphate region is about 22% of the purine vibration at 1488 cm^{-1}. Considering that the strongest band of purine ring is about 3% of the intensity of the amide I peak of EF-Tu, the difference band at 1118 cm^{-1} (Figure 7.4a) would be less than 1% of the protein Raman amide I intensity.

Difference Spectrum of EF-Tu•GDP and EF-Tu•GMP-PNP: The spectrum formed between EF-Tu•GDP and EF-Tu•GMP-PNP, both in solution, is shown in Figure 7.4b. This spectrum shares no common features with the one obtained in solution (Figure 7.4a). The intensity of the largest feature in the spectrum is about 3% of the most intense protein peak, more than three times larger than the expected intensity for nucleotide differences. Comparing the intensity and overall shape of the spectrum (Figure 7.4b) with that of free nucleotide in solution (Figure 7.4a), we conclude that most of these differences are due to protein changes. This is not an unexpected result, since the protein is known to undergo conformational change from GDP bound form to GTP bound form, to "switch on" protein function.

Amide III band: When protein is dissolved in D_2O buffer, Raman intensities at 1220 cm^{-1} to 1320 cm^{-1} region shift down. Most of Raman bands in this region which are affected by deuteration are called amide III band. These vibrations are mainly involve the N-H bending vibration of polypeptide bonds (Figure 2.2). The biggest intensity of the spectrum 7.4b is located in this region, characterized by a broad negative peak centered at 1255 cm^{-1} and sharper peak at 1301 cm^{-1} and 1337 cm^{-1}. Amide III vibrations are sensitive to protein conformational changes. Hydrogen bonding exerts a great effect on the frequencies of the amide I and III bands. When a peptide-bond N-H or C=O is involved in hydrogen bonding, it decreases the amide I band frequency, whereas it increases the amide III band frequency. The difference in amide III region, in Figure 7.4b, can be invoked by the down shift of amide III band when protein is activated, which implies a weakening of hydrogen bonding formed between backbone N-H group and nearby protein residues.

Amide I band: Differences also show up in amide I region between 1645 cm^{-1} and 1700 cm^{-1}. Bands in this region arise mainly from peptide-bond carbonyl stretching vibrations (Figure 2.2). The positive band at ~1666 cm^{-1} of EF-Tu•GDP and the negative band of EF-Tu•GMP-PNP may be interpreted as an up-shift of backbone carbonyl stretch. If we assume that the intensity of amide I band is proportional to the number of backbone carbonyl groups, the Raman intensity in the difference spectrum, being 0.76% of the area of the total amide I band, corresponds to at least 3 residual C=O stretches. The up-shift of carbonyl stretch indicates a weakening of the hydrogen bonding of this group. It seems that in the GTP bound form, peptide carbonyl groups of several residues are more accessible to water. This conclusion is consistent with the analysis discussed above in relation to the amide III band.

Tyrosine residue changes: It was found that the relative intensities of the Raman bands at 830 cm^{-1} and 850 cm^{-1} in proteins are related to the environment of the tyrosine side chain ([85, 86]). The intensity ratio of 850/830-cm^{-1} is lower when tyrosine is buried and acting as a strong hydrogen-bond donor, while if tyrosine is on the surface of a protein exposed to aqueous solution, this ratio is higher ([31]). In the difference spectrum Figure 7.4b, a positive peak at 822 cm^{-1} and a negative peak at 858 cm^{-1} are observed, indicating that the GTP bound form of the protein has a higher 850/830-cm^{-1} ratio than the GDP form. This indicates that one or more tyrosine residue may involved in the loop that become more exposed to water during protein activation.

Cysteine residue changes: The sulfhydryl group of cysteine is one of the most chemically reactive functional groups in proteins, confirming its nucleophilic nature and the polarity. A common feature of the interaction of cysteinyl S and S-H groups with protein side chains is the requirement of a shift of electron density from the donor hydrogen toward its covalently bonded sulfur, yielding partial charge separation $S^{\delta-}$-$H^{\delta+}$, thereby facilitating favorable interaction at either end of the dipole with an appropriate, oppositely charged group.

Cysteine's specific S-H stretching mode is unique in its isolated appearance in the Raman spectrum (~2500 cm^{-1}). The Raman band at this region could be a sensitive probe of conformations of cysteine residues.

Figure 7.5 shows the Raman spectra of EF-Tu•GDP and EF-Tu•GMP-PNP in the S-H stretch region. The peak maximum of S-H vibration is located at 2565 cm^{-1} and 2569 cm^{-1} for EF-Tu•GDP and EF-Tu•GMP-PNP respectively. The vibrational bands have different shapes for the two complexes. This S-H stretching band is result of the vibrations, of the three cysteine in this protein ([87]. Figure 7.5 shows the analysis of these data. The experimental data were fit to three Gaussian bands, corresponding to the S-H stretching modes of three cysteine residues in EF-Tu. The two lower frequency Gaussian peaks are located at 2549 cm^{-1} and 2563 cm^{-1} in the EF-Tu•GDP complex. These two bands are not effected by the protein activation, since in the EF-Tu•GMP-PNP complex the fitting yields about same results of these two bands at 2547 cm^{-1} and 2563 cm^{-1} respectively. However, the third band at higher frequency is shifted from 2571 cm^{-1} to 2576 cm^{-1} when the protein changed from GDP bound state to GMP-PNP bound state. This result indicates only one cysteine residue out of the three is affected by the switching.

Jonak el al. ([88]) have studied the role of cysteine residue in the biological function of EF-Tu. They found N-Tosy-L-phenylalanyl chloronethane (TPCK), a known sulfhydryl modifying agent, can be used as a specific irreversible inhibitor of EF-Tu from *Escherichia coli* and *Bacillus stearothermophilus*, and this compound destroyed the ability of EF-Tu to bind aminoacyl-tRNA by modifying residue Cys81. High resolution x-ray study ([72]) showed that Cys81 is located at the beginning of the effector loop of Cys81-Pro-Gly-His-Ala85 (Figure 1.2a). This loop corresponds to L4 loop of *ras*-p21 (Figure 1.2b). Cys81 of EF-Tu may have same function as Gly60 or Gln61 of p21. Point mutations at these positions in p21 effect the GTPase activity of the protein by disrupting GAP binding. It seems reasonable to assign the shifted S-H band to Cys81.

The other cysteine of EF-Tu, Cys137, is in the loop Asn135-Lys-Cys-Asp138, which is responsible for the interaction with guanine base. X-ray study ([26]) showed that in the presence of GDP, the loop containing Cys137 is held in a conformation that maintains the cysteine's side chain in a half-buried, half-exposed position. The environment of Cys137 in the three-dimensional structure is similar to that of Cys81 which is also not fully exposed but half buried. Because the position of the S-H stretch of a cysteine residue is influenced by its environment, we assign S-H at 2563 cm^{-1}, which is the band closer to Cys81 band, to Cys137. The third cysteine band at 2547 cm^{-1} is signed to Cys257 which is located at domain II of EF-Tu.

Li and Thomas ([89]) have systematically studied the correlation of the Raman S-H band with hydrogen bonding and intramolecular geometry in model compounds. They found that the most definitive change in Raman S-H stretching band is its shift to lower frequency when S-H acts as a hydrogen bond donor, and the frequency interval in which the Raman S-H stretching vibration occurs is diagnostic of S-H donors which are strongly hydrogen bonded (2525-2560 cm^{-1}), moderately hydrogen bonded (2560-2575 cm^{-1}), or weakly hydrogen bonded (2575-2580 cm^{-1}). According to these model compound studies, the three EF-Tu's cysteine residues are hydrogen bonded to the near by groups to different extent, Cys257 is strongly hydrogen bonded, giving a S-H stretching mode as low as 2547 cm^{-1}, while the other two cysteines are moderately hydrogen bonded. Because of its crucial location, Cys81 was expected to undergo conformational changes, depending on whether GDP or GTP is bound. Our Raman results not only confirm that this change indeed occurs, but also indicate that the hydrogen bonding status of this residue is influenced by the GTP analog binding. When dissolved in water, 1-proanethiol, a compound that has same structure as cysteine's side chain, has a S-H stretching band at 2578 cm^{-1}, this band is at 2577 cm^{-1} when dissolved in a hydrogen bonding donor solvent and shifts to 2582 cm^{-1} when dissolved in the inert solvent carbon tetracloride ([89]). Accordingly, we can interpret the change we observe as the binding of the third phosphate group may pushed away effector loop of residue 80-93, thus reducing the hydrogen bonding of Cys81 with near by protein residue and exposing this residue more to the solvent.

Conclusion: Comparing to GDP binding form of EF-Tu, certain residues of the protein are more exposed to water in the GTP binding form. From our Raman results, the loop that under goes changes may contain one cysteine residue and at least one tyrosine residue. These result are consistent with the result of x-ray studies, which show that Cys81-Pro-Gly-His-Ala-Asp-Tyr-Val-Lys-Asn-Met-Ile-Thr93 compose the effective loop of tRNA binding, which is expected to undergo conformational changes on the protein activation.

D. Conformational Changes of *ras*-p21 During Protein Switching

Ras proteins participate as a molecular switch in the early steps of the signal transduction pathway that is associated with cell growth and differentiation. When the protein is in its GTP complexed form it is active in signal transduction, whereas it is inactive in its GDP complexed form. X-ray studies revealed that the "on" and "off" state of the switch are distinguished by conformational differences that are localized in two regions: residues 30 to 38 (the switch I region) and 60 to 76 (the switch II region) ([22]). Since the lifetime of the complex p21•GTP is long enough for Raman measurement, the possibility to probe protein changes by difference Raman spectroscopy was explored.

The time course of the protein changes during GTP hydrolysis: Raman spectra of p21•GDP and p21•GTP were measured at 4°C. Totally 8 runs were completed during a period of about 12 hours. The GTP content of the GTP complex was monitored by HPLC and found to decrease from 85% to 50% within this period.

Figure 7.7 shows the difference spectra of p21•GDP minus p21•GTP for the first, fourth and eighth runs. These three spectra have same features except that the size of the difference signal is decreasing with time, at t=0 (85% GTP) the maximum difference is 3.7% of the amide I intensity. The maximum difference for t=12 hrs is only about 2.7%. This dynamic change is a result of the internal GTPase activity associated with the protein. The results here show the potential application of difference Raman spectroscopy to track the protein changes during transitions.

Protein changes from GDP binding to GTP binding: Figure 7.8 shows the total difference spectrum of eight runs and the spectrum of GDP minus GTP in p21.

It is not surprising that there are changes in protein amid I and amide III regions since certain protein loops are moved by the third phosphate binding ([22, 23]), but the changes here seems different from those in EF-Tu activation since the difference spectrum in these regions have different shapes.

When p21 is activated, the environment of tyrosine residue(s) seems also changed. The doublet of tyrosine residues at 830 cm^{-1} and 850 cm^{-1} show up as negative peaks in the protein difference. The negative peak at 830 cm^{-1} is more intense than the peak at 850 cm^{-1}. It seems that tyrosine residues move to a more hydrophobic environment when protein is "switched on". The opposite situation was observed in EF-Tu (see above).

COO^- group has a strong vibration around 1400 cm^{-1}. In Figure 7.8b, the changes in 1350 cm^{-1} region to 1430 cm^{-1} may correspond to changes of COO^- group in the two protein forms. There are 7 side chain COO^- are involved in the switch regions.

The phosphate binding in the active form of ras-p21: The vibrations of phosphate group are rather weak compared to those of puring ring's. The maximum peak in the difference spectrum of GDP minus GTP (Figure 7.8a) is 25% of the strongest puring vibration at 1487 cm^{-1}. When incorporated in p21, this difference may compose about 1.3% of the Amide I Raman intensity. One of the advantages of Raman difference measurements on *ras*-p21 is its smaller mass compare to EF-Tu, the same difference signal that can be detected in p21 may fall to half that in EF-Tu.

The major peak in the solution difference of nucleotides complexed with Mg^{++}, is the peak associated with the vibration of the terminal phosphate which appears at 1122 cm^{-1}. Although the protein differences are much more complicated compared to those in solution, both the intensity and the position of the negative peak at 1122 cm^{-1} of the protein difference suggest that this peak corresponds to the phosphate peak in solution. This peak is assigned to an in-phase stretching vibration of the γ-phosphate group ([83]). The fact, that this band appeared at the same position when complexed with Mg^{++} in solution as when the nucleotide binds to the protein, can be interpreted as that the interactions of the γ-phosphate with protein are not very different than with Mg^{++} in water, and the GTP•Mg^{++} complex inside p21 has the similar conformation as in water. Binding studies on GTP binding to *ras*-p21 seems to support this conclusion. The affinity of GTP to *ras*-p21 is only about twice that of GDP, while the affinity of GDP to ras-p21 is a factor of 10^6 stronger than that of GMP ([44]). Although an x-ray study ([11]) showed that the phosphate binding site is characterized by large number of protein residues that can form hydrogen bonding with the oxygen atoms on the phosphate, the effective binding of the phosphate motif with protein residues seems focused on β-phosphate and the slight increasing in the protein affinity to GTP may come from the interactions of protein residues with Mg^{++} ion.

E. Nucleotide Binding in the Active Form of *ras*-p21

In the last section, the phosphate binding to the active form of *ras*-p21 was discussed. It is possible that the guanine binding motif may also be influenced by the changes from GDP binding form to GTP binding form. This possibility was investigated with difference Raman spectroscopy by incorporating into p21 GTP or GTP analogs that are isotopically labeled or chemically modified at guanine base .

Figure 7.9 shows the difference Raman spectra of GTP minus 8D-GTP in solution (a) and p21 (b). The spectra of p21•GDP minus p21•8D-GDP is also plotted in Figure 7.9c for comparison. Data were collected for 10 hours period at 4°C. The GTP and 8D-GTP contents of the complexes were decreased from 90% before Raman measurement to 60% after. The hydrolysis of GTP is a result of the intrinsic GTPase activity of the protein.

There are very few differences when comparing spectrum of p21•GTP minus p21•8D-GTP (Figure 7.10b) with that of p21•GDP minus p21•8D-GDP (Figure 7.10c). This suggest that the same interactions between nucleotide and protein are exerted on the guanine ring of GTP and GDP. The bands at 1300 cm^{-1} to 1400 cm^{-1} region are nearly identical, indicating the guanosine motif of GTP binds to the active site in the same conformation, namely *c2'-endo anti*, as GDP. This is a known result of x-ray studies ([22, 23]).

ITP was also incorporated into p21 to investigate nucleotide binding. Figure 7.10 shows the difference spectra of the GTP minus ITP in solution (a) and in p21 (b). Comparing to the difference of p21•GDP and p21•IDP (Figure 5.2c), two bands at 1461 cm^{-1} and 1315 cm^{-1} of the inactive form of protein did not show up in the difference of active protein complex. The band at 1315 cm-1 may corresponding to the band at 1322 cm-1 of the free spectrum, while the band at 1461 may come from the protein. The reasons that these difference do not appear in the difference spectrum of IDP and ITP complexes need to be further investigated. The major nucleotide bands at 1350 cm^{-1} to 1700 cm^{-1} region remain the same for the two forms, which may reflect the fact that the interactions that protein act upon guanine ring are not much different for the protein active and inactive forms, and it is not the puring ring portion of the nucleotide that controls the activity of the protein.

Figure 7.1: The hydrolysis of GTP in *ras*-p21. The relative amount of GTP and GDP were determined by RP-HPLC. The ratio of $[p21 \bullet GTP]/[p21]_0$ is equivalent to the nucleotide concentration ratio of [GTP]/([GDP]+[GTP]) after the free nucleotides were washed out. The curves do not extrapolate to 100% GTP content at time t=0, since some of the bound GTP was already hydrolyzed during the 3 hours of sample preparation. P21 complex was at ca. 3 mM in buffer R. The curve fittings gave the GTP hydrolysis rate of $k_{RT} = 9.4 \times 10^{-3}$ min^{-1} at room temperature and $k_{0°C} = 2.9 \times 10^{-4}$ min^{-1} at 0°C.

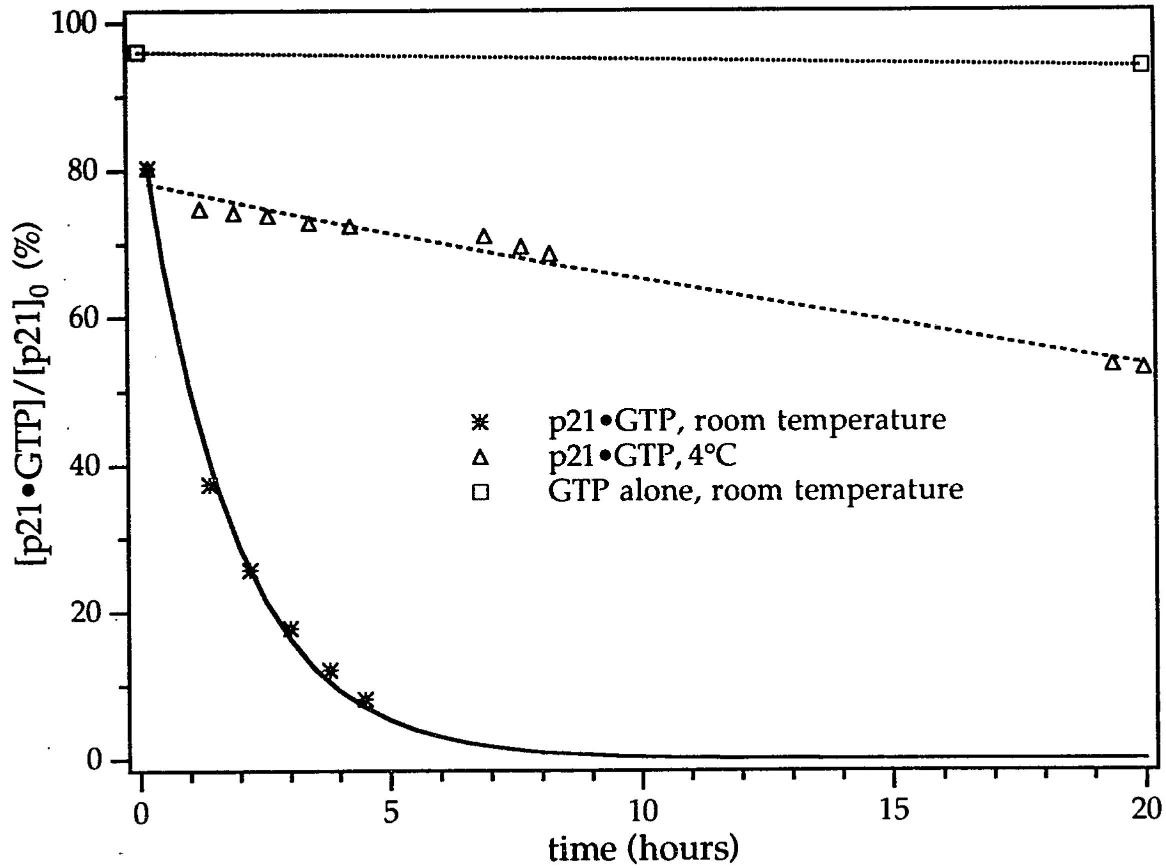
100
80
60
40
20
0
[p21•GTP]/[p21]0 (%)
0
5
10
15
20
time (hours)
p21•GTP, room temperature
p21•GTP, 4°C
GTP alone, room temperature

Figure 7.1

Figure 7.2: Raman spectra of GDP (a), GTP (b) , GMP-PNP (c) and GMP-PCP (d). The excitations were with the 488 nm line from an Argon laser. The nucleotides were all at concentrations of about 0.1 mM and pH 7.0. The vibrations from phosphate group are labeled with (p).

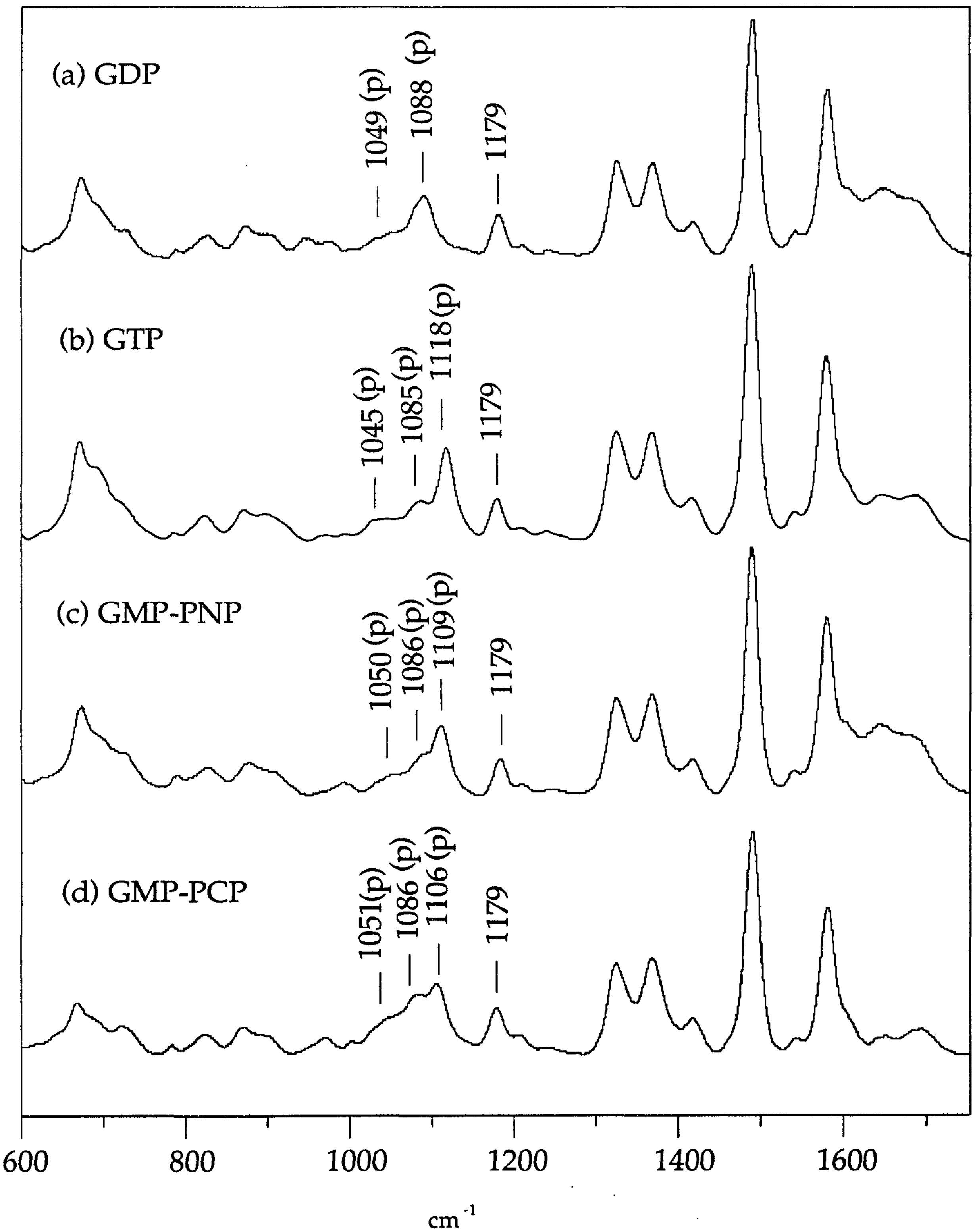
(a) GDP
1049 (p)
1088 (p)
1179
(b) GTP
1045 (p)
1085 (p)
1118 (p)
1179
(c) GMP-PNP
1050 (p)
1086 (p)
1109 (p)
1179
(d) GMP-PCP
1051(p)
1086 (p)
1106 (p)
1179
600
800
1000
1200
1400
1600
cm-1

Figure 7.2

Figure 7.3: The Phosphate region of the Raman spectra of GDP (a), GDP + $MgCl_2$ (b), GTP (c), GTP + $MgCl_2$ (d). Phosphate vibrations are labeled with (p). The excitation was with the 530 nm line from an Kr^+ ion laser. The nucleotides were all at concentrations about 0.05 M and pH 7.0, and the ratio of Mg^{++} to nucleotides was 1:1.

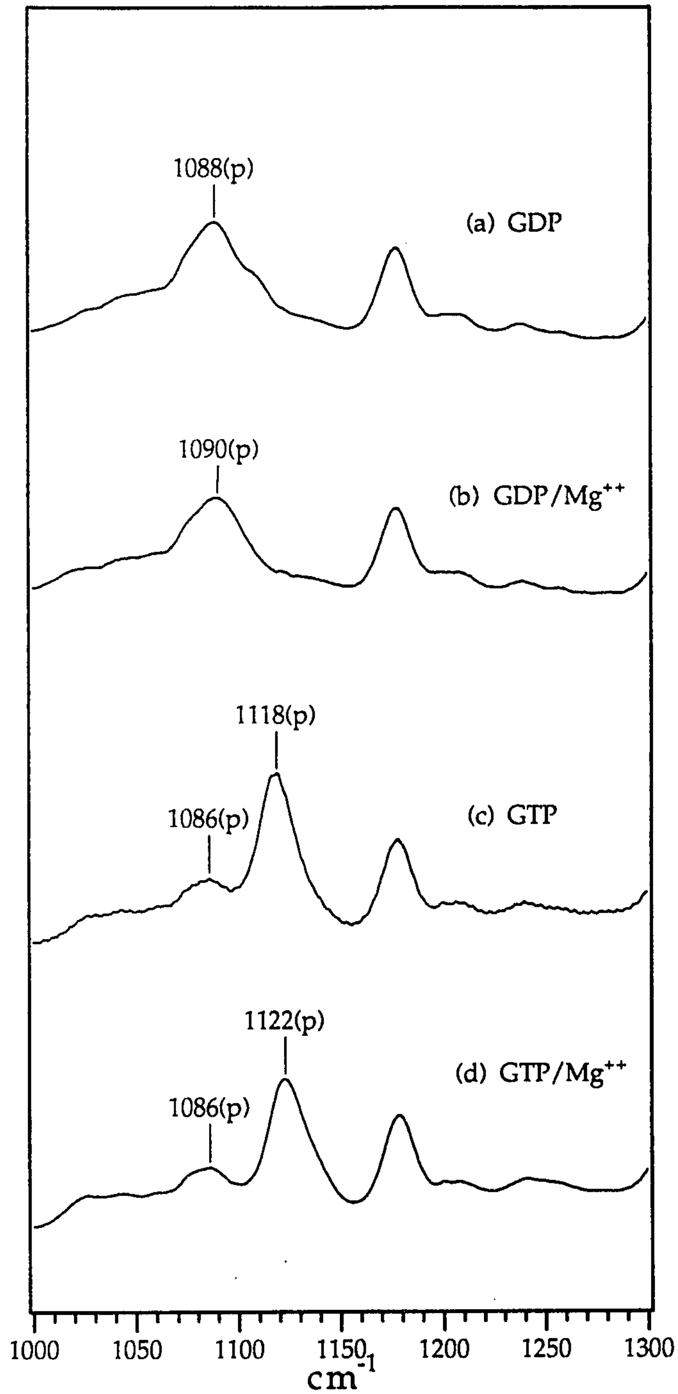
1088(p)
(a) GDP
1090(p)
(b) GDP/Mg++
1118(p)
1086(p)
(c) GTP
1122(p)
(d) GTP/Mg++
1086(p)
1000
1050
1100
1150
1200
1250
1300
cm-1

Figure 7.3

Figure 7.4: Raman difference spectra of GDP minus GMP-PNP in solution (a) and in EF-Tu (b). GDP and GMP-PNP were at ca. 0.1 M, pH 7.4 and excited with 180 mW of 488 nm argon laser light. EF-Tu complexes were at 2 mM in buffer R and excited with 100 mW of 488 nm argon laser light.

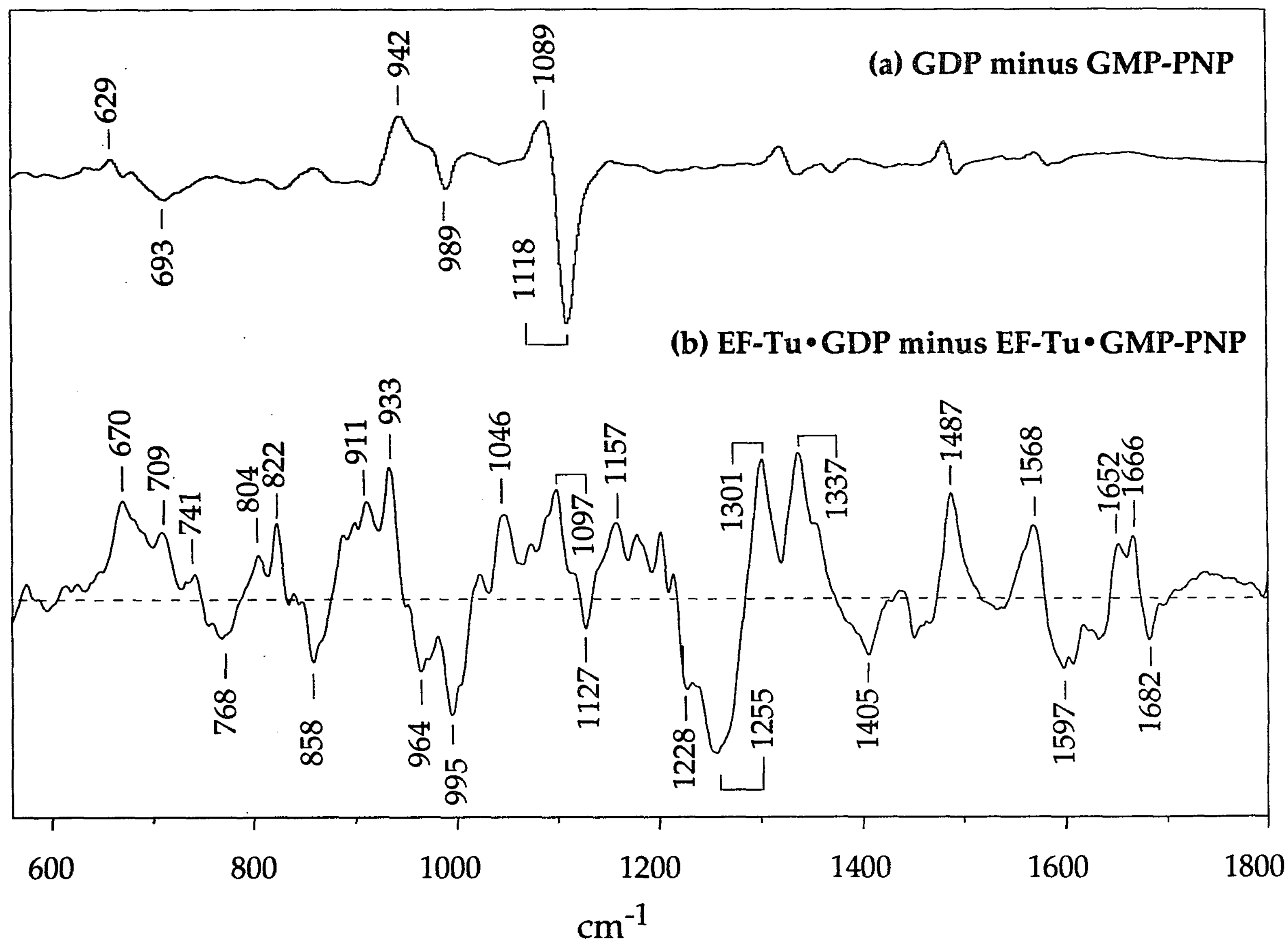
(a) GDP minus GMP-PNP
(b) EF-Tu•GDP minus EF-Tu•GMP-PNP
629
693
942
989
1089
1118
670
709
741
768
804
822
858
911
933
964
995
1046
1097
1127
1157
1228
1255
1301
1337
1405
1487
1568
1597
1652
1666
1682
600
800
1000
1200
1400
1600
1800
cm-1

Figure 7.4

Figure 7.5: The S-H stretching region of EF-Tu•GDP (a) and EF-Tu•GMP-PNP (b). The experimental conditions were same as those in Figure 7.4. The peaks at 2622 cm^{-1}, 2681 cm^{-1}, 2727 cm^{-1} and 2766 cm^{-1} are the vibrations of protein CH-containing groups ([90]). These bands remain the same for both active and inactive forms of EF-Tu.

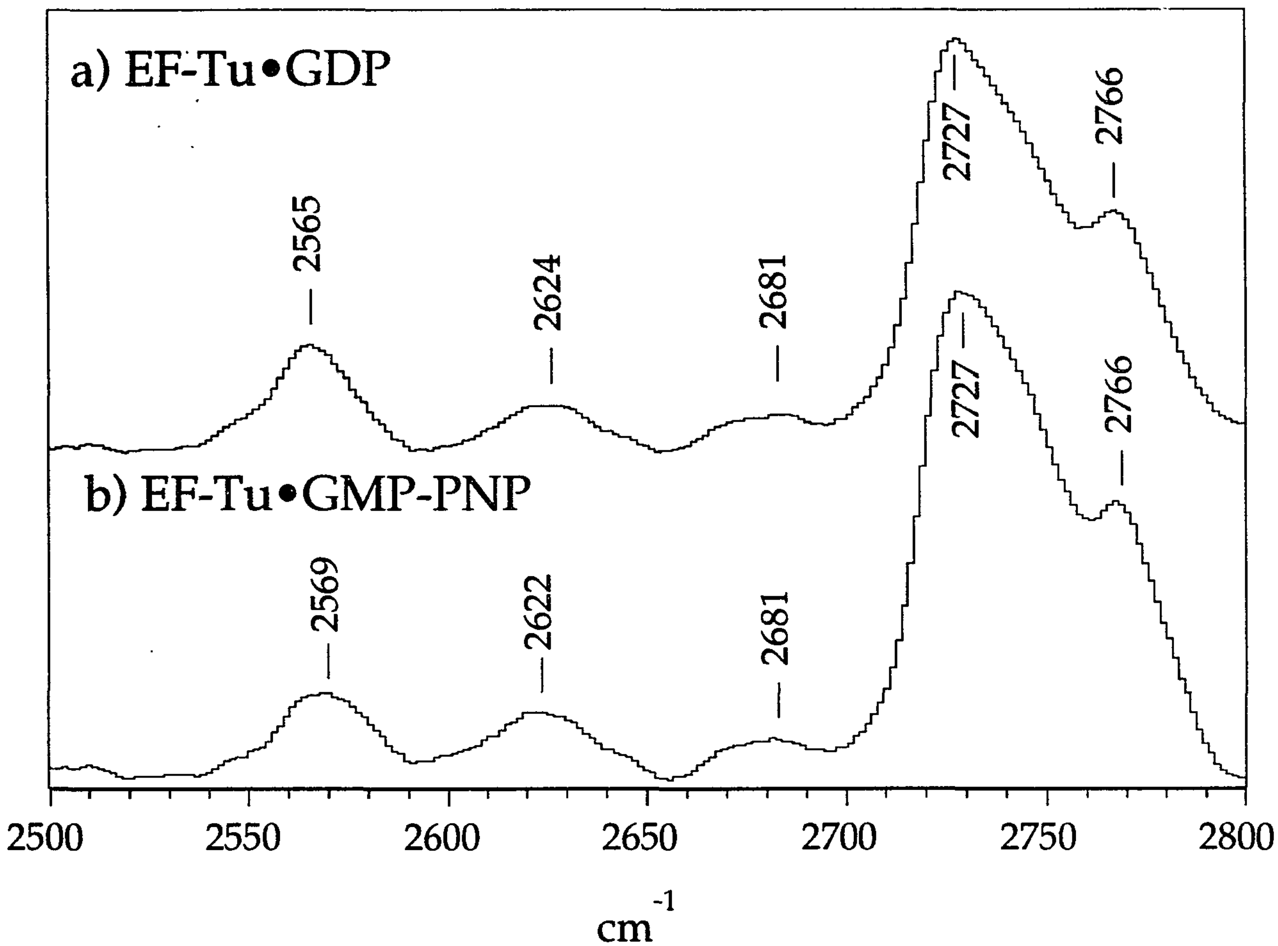
a) EF-Tu•GDP
2565
2624
2681
2727
2766
b) EF-Tu•GMP-PNP
2569
2622
2681
2727
2766
2500
2550
2600
2650
2700
2750
2800
cm-1

Figure 7.5

Figure 7.6: A blow up view of S-H stretching bands. The peaks are fit to three Gaussian bands.

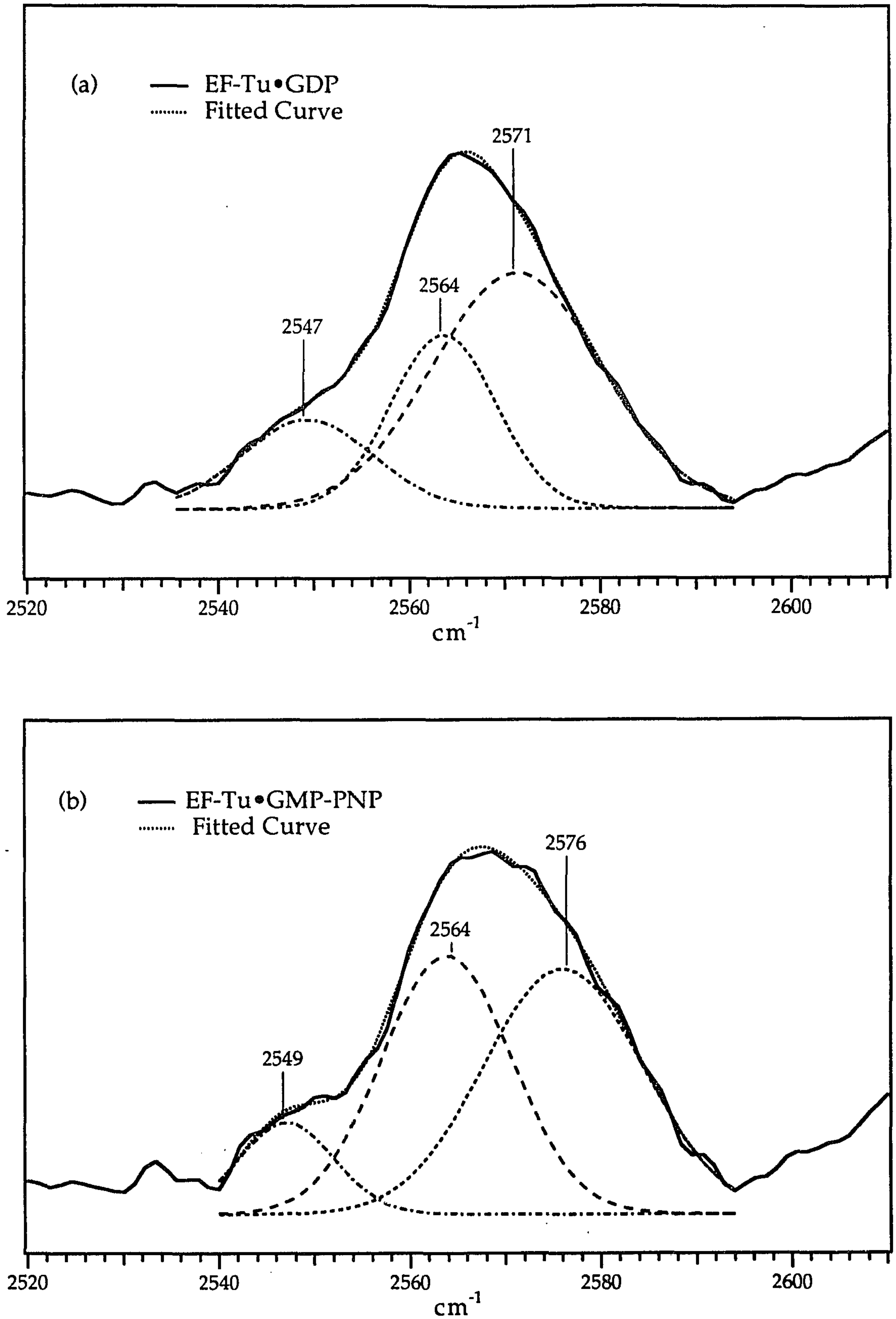
(a)
EF-Tu•GDP
Fitted Curve
2571
2564
2547
2520
2540
2560
2580
2600
cm-1
(b)
EF-Tu•GMP-PNP
Fitted Curve
2576
2564
2549
2520
2540
2560
2580
2600
cm-1
Figure 7.6

Figure 7.7: The Raman difference spectra of p21•GDP minus p21•GTP at (a) t=1 hour; (b) t=4 hours; (c) t=8 hours after the complexes were made. The Raman measurement was started at t=0, 85% p21•GTP. After 8 hours, GTP complex dropped to 50%. P21 complexes was at 3 mM in buffer R and excited with 100 mW of 568 nm Kr^+ ion laser light.

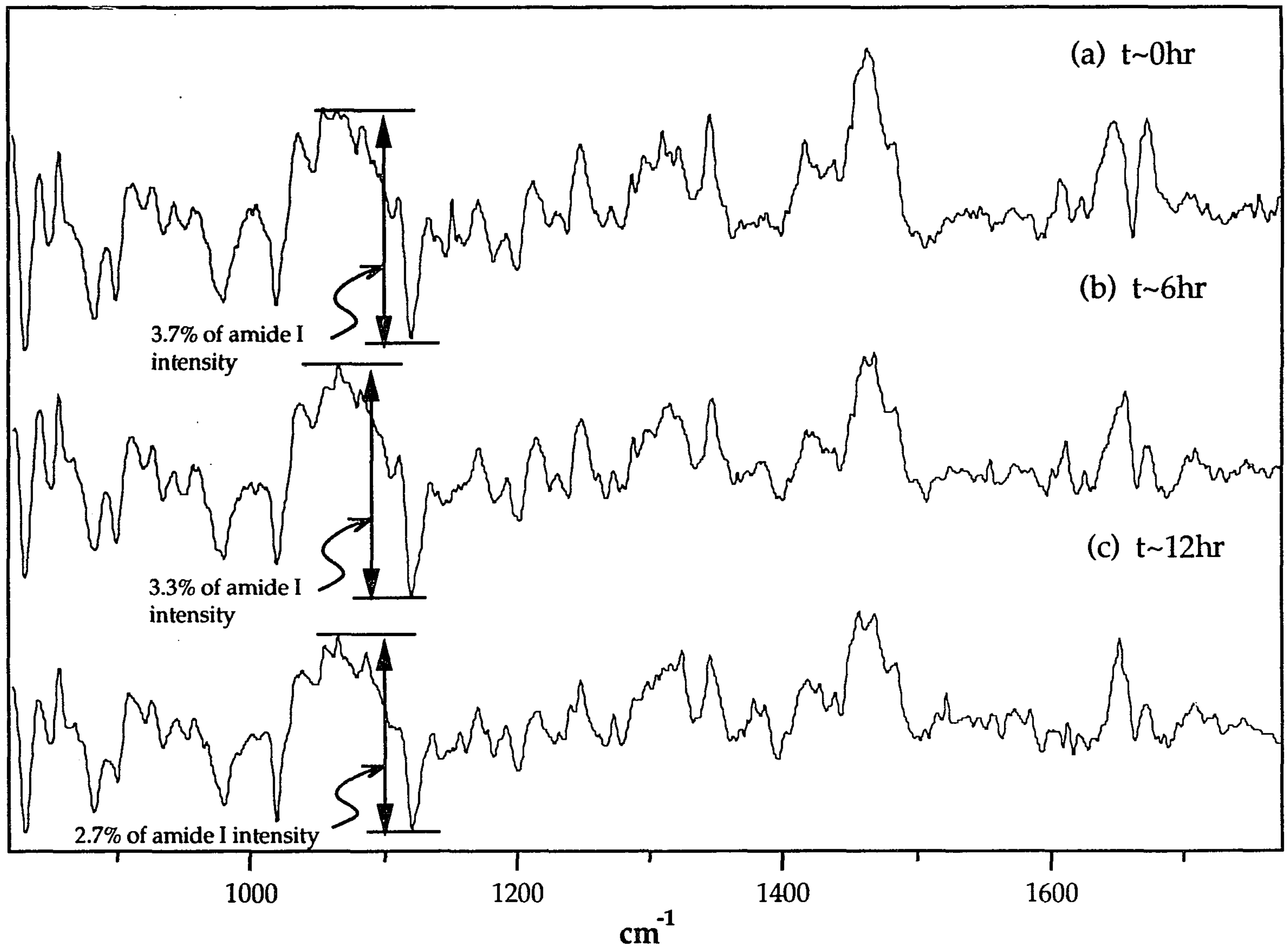
(a) t~0hr
(b) t~6hr
(c) t~12hr
3.7% of amide I intensity
3.3% of amide I intensity
2.7% of amide I intensity
1000
1200
1400
1600
cm-1

Figure 7.7

Figure 7.8: The difference spectra of GDP minus GTP in solution contained $MgCl_2$ in 1:1 ratio to the nucleotides (a), the concentration of the nucleotides were ca. 0.05 M, pH 7.2, and in p21 (b), the experimental conditions were the same as indicated in Figure 7.7.

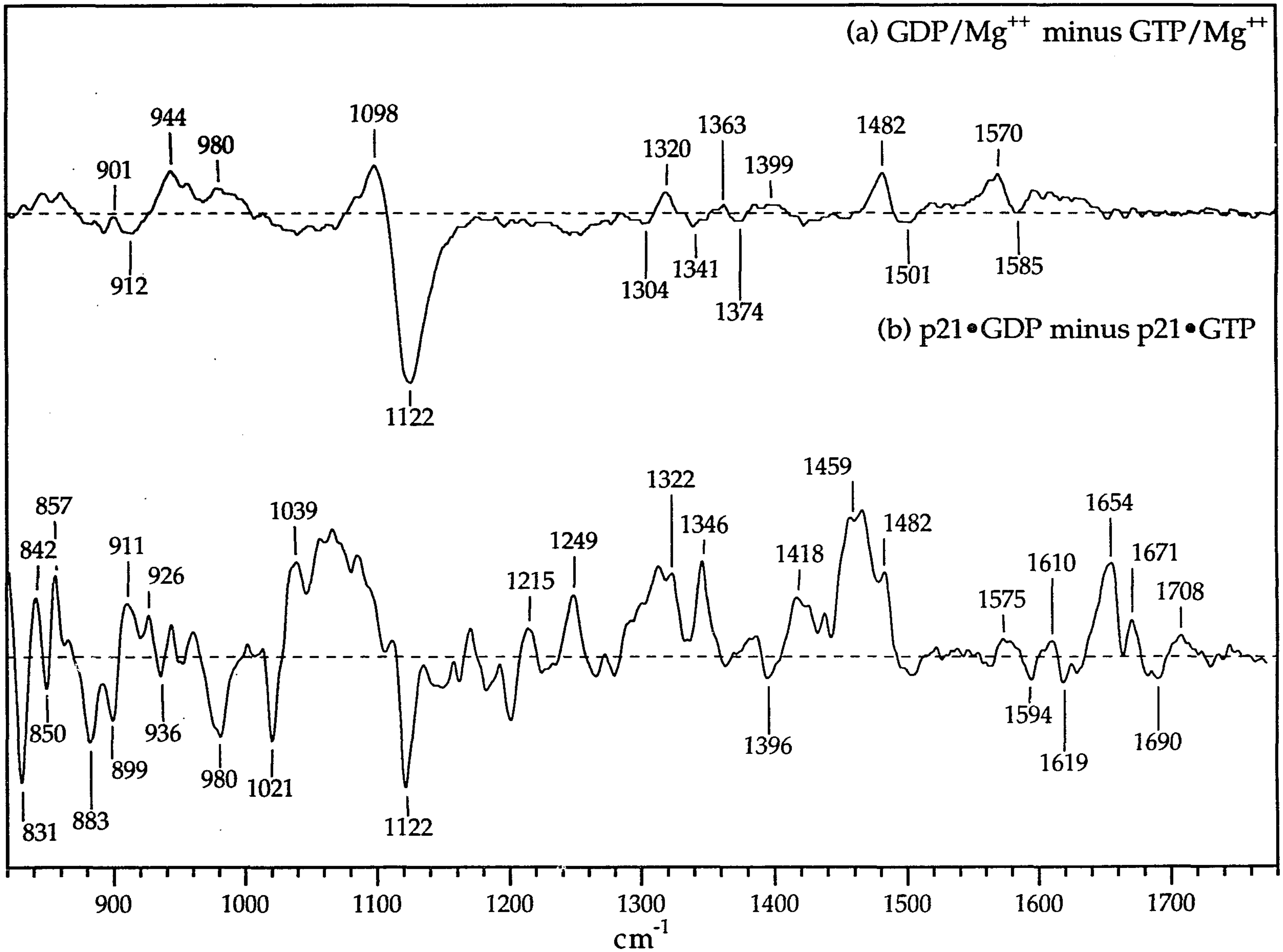

(a) GDP/Mg++ minus GTP/Mg++
(b) p21•GDP minus p21•GTP
944
980
901
1098
1320
1363
1399
1482
1570
912
1122
1304
1341
1374
1501
1585
857
842
911
926
1039
1215
1249
1322
1346
1459
1418
1482
1575
1610
1654
1671
1708
850
899
936
980
1021
831
883
1122
1396
1594
1619
1690
900
1000
1100
1200
1300
1400
1500
1600
1700
cm-1

Figure 7.8

Figure 7.9: The Raman difference spectra of GTP minus 8D-GTP in solution (a), and in p21 (b). The spectrum of p21•GDP minus p21•8D-GDP is also plotted (c) for comparison. The nucleotide spectra were excited with 180 mW of 568 nm Kr^+ ion laser light. P21 complexes were at 3 mM in buffer R and excited with 100 mW of same laser line.

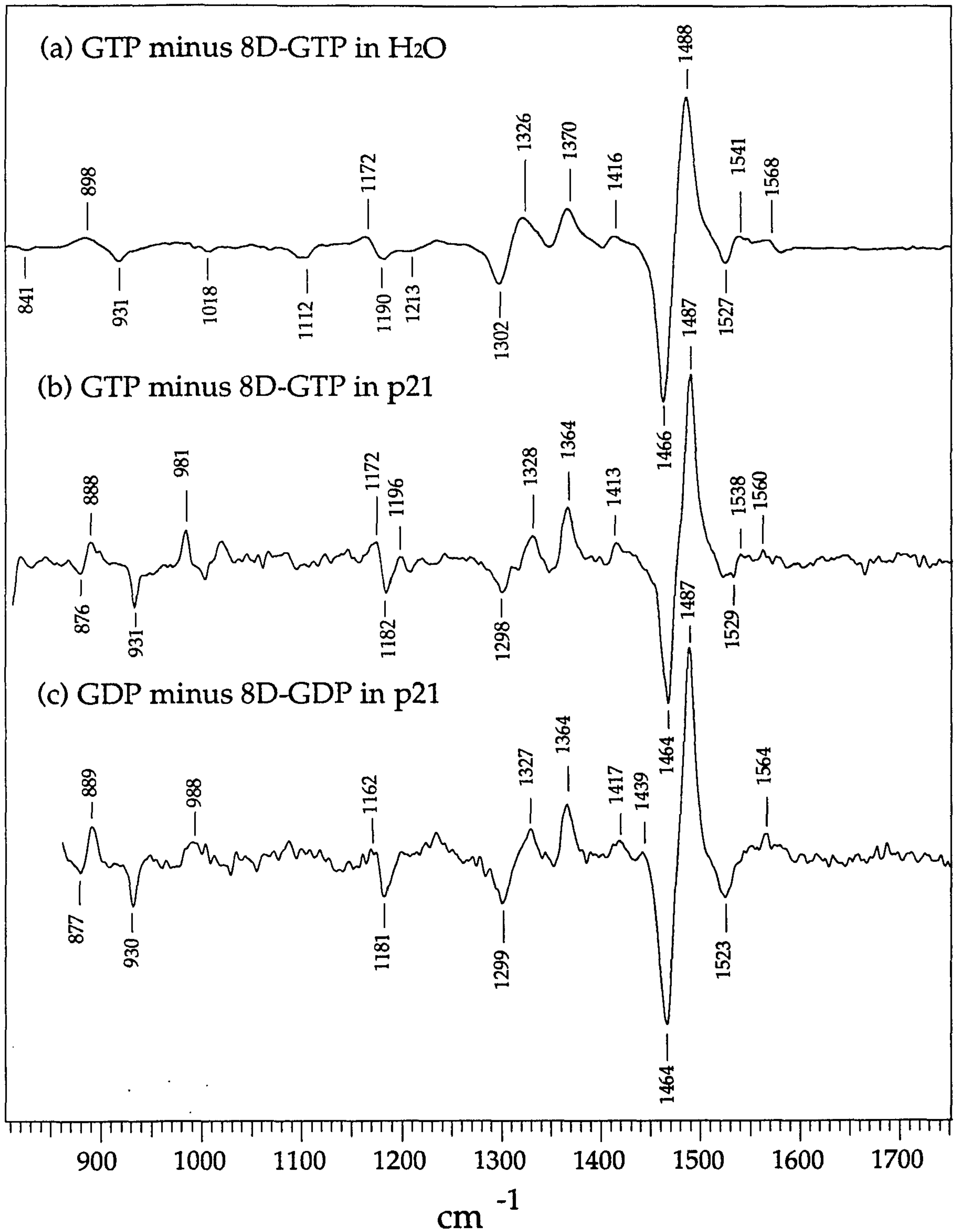
(a) GTP minus 8D-GTP in H2O
(b) GTP minus 8D-GTP in p21
(c) GDP minus 8D-GDP in p21
841
898
931
1018
1112
1172
1190
1213
1302
1326
1370
1416
1466
1488
1527
1541
1568
876
888
931
981
1172
1182
1196
1298
1328
1364
1413
1464
1487
1529
1538
1560
877
889
930
988
1162
1181
1299
1327
1364
1417
1439
1464
1487
1523
1564
900
1000
1100
1200
1300
1400
1500
1600
1700
cm -1

Figure 7.9

Figure 7.10: The Raman difference spectra of GTP minus ITP in solution (a), and in p21 (b). The spectrum of p21•GDP minus p21•IDP is also plotted (c) for comparison. The nucleotide spectra were excited with 180 mW of 568 nm Kr^{+} ion laser light. P21 complexes was at 3 mM in buffer R and excited with 100 mW of same laser line.

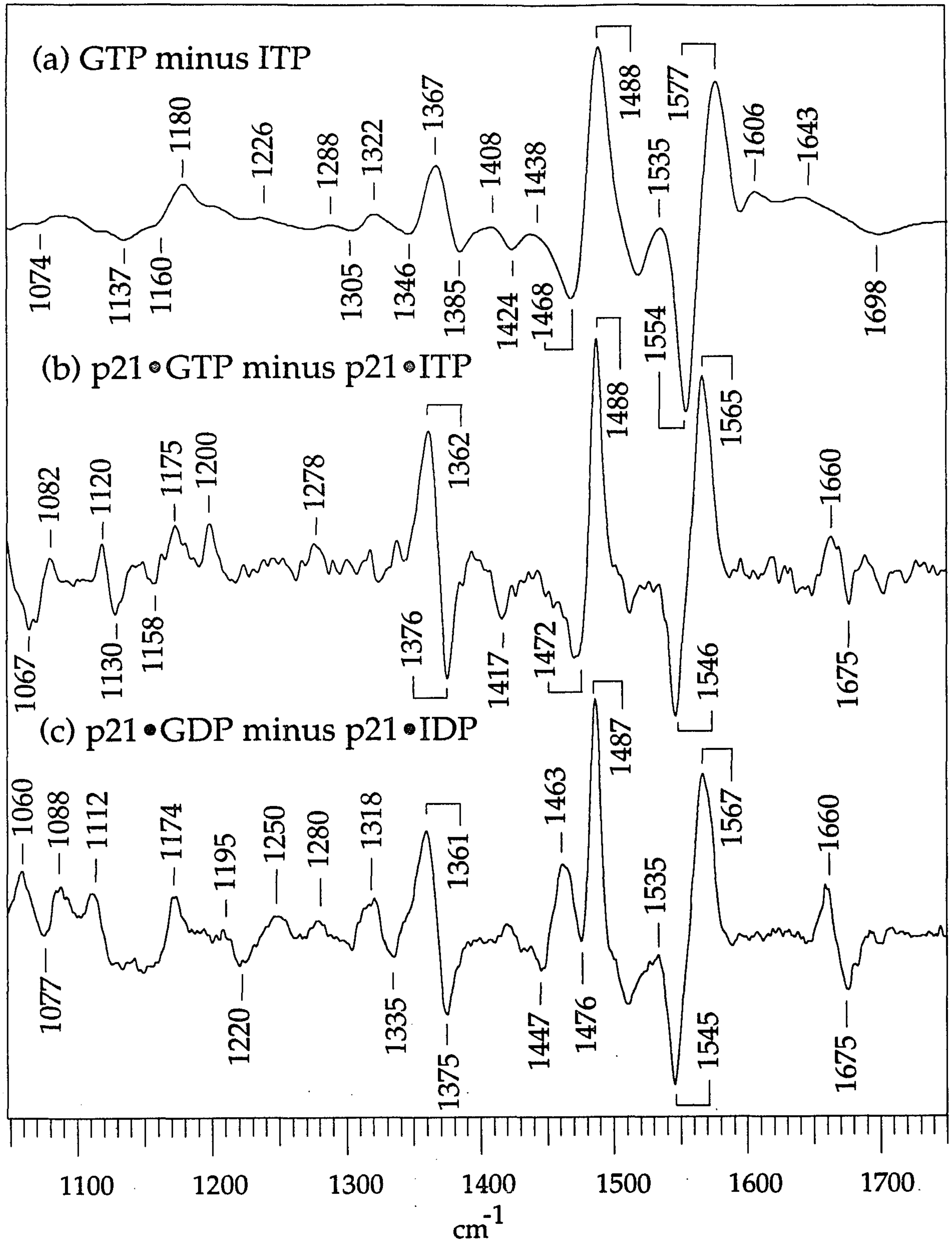
(a) GTP minus ITP
(b) p21•GTP minus p21•ITP
(c) p21•GDP minus p21•IDP
1100
1200
1300
1400
1500
1600
1700
cm^{-1}

Figure 7.10

Chapter VIII

HYDROGEN-DEUTERIUM EXCHANGE IN PROTEINS

A. Evidence for the different hydrogen exchanging rate in different protein-nucleotide complexes.

It has been known for a long time that hydrogen atoms attached to nitrogen and oxygen in proteins, as well as those exchangeable hydrogens on ligands, are replaced by deuterium when a protein-ligand complex is dissolved in D_2O solution. Raman measurements in D_2O buffer for protein-nucleotide complexes were carried out to get additional support to the conclusions derived from experiments performed in H_2O buffer.

When protein is dissolved in D_2O buffer, the amide III bands in the 1200 cm^{-1} to 1300 cm^{-1} region, arising from in-plain vibration of the peptide N-H group, shifts down to ~980 cm^{-1} (Figure 8.1). This shift to a lower frequency, approximately by the factor of $\sqrt{2} = 1.4$ (the square root of the mass ratio of D/H) reflects the fact that the major contribution to the amide III is the N-H band. Other bands in the spectrum originated form methylene group, tyrosine, tryptophan and phenylalanine side chains remain virtually unchanged upon deuteration. In amide I bands of EF-Tu and p21, at ~1668 cm^{-1} and 1662 cm^{-1}, shift down 7 cm^{-1} and 2 cm^{-1} respectively to 1660 cm^{-1} upon deuteration, showing a different extend of the correlations of N-H bending with C=O stretching mode for these two proteins.

Figure 8.2a shows the difference spectrum of GDP minus IDP in D_2O. Vibrations from purine ring dominate the 1300 cm^{-1} to 1600 cm^{-1} region of this spectrum. These ring vibrations are not much affected when the nucleotides bind to protein (Figure 8.2b). In the higher frequency region (1600 cm^{-1} ~ 1700 cm^{-1}), the pattern is drastically different between the solution difference spectrum (8.2a) and the protein bound ones (8.2b, 8.2c). Instead of the simple derivative-like feature observed in solution, the protein difference spectra bands in this region are broad, at different positions and have much higher intensity. It is hard to draw any correspondence between the bands in solution difference spectrum with the protein differences spectrum.

It was the observation that these bands in carbonyl stretch region diminish with time (Figure 8.3), that lead us to the idea that these bands may represent a different deuteration extent of the two protein-nucleotide complexes. Since our experiments are designed to detect a single group vibration of a bound ligand, it is quite possible that the differences of a few unexchanged hydrogens may obscure the weak nucleotide bands we were looking for. To test this idea further, the difference spectrum between EF-Tu•GDP samples incubated in D_2O buffer for different lengths of time were taken. Figure 8.4a shows the difference spectrum formed between EF-Tu•GDP samples incubated in D_2O buffer for 4 hours and for 72 hours. Initially the intensity of the bands in amide I region are about 1.6% of the amide I peak. The fact that this derivative-like feature is relatively small indicates that most of the exchangeable hydrogens were replaced by deuterium within 4 hours. The association of the lower frequency band with the sample that was incubated in D_2O buffer longer is also consistent with that the species which is deuterated in higher degree has amide I peak with lower frequency. We expect that this difference would reduce in intensity if the incubation in D_2O for both samples was longer, which was indeed the case (Figure 8.4b). The amide I difference reduce to 0.4% after both samples were incubated in D_2O buffer further for another three days. The attempt to see the complete diminishing of the differences failed because prolonged incubation in D_2O buffer disrupted the protein structure; the difference spectrum for the samples incubated in D_2O longer than 6 days showed dramatic protein changes.

B. The origins of the different hydrogen-deuterium exchange rates

The bands in the amide I region of the difference spectra (Figure 8.2, 8.5 and 8.6) are very similar, all of them have a negative band at ~1635 cm^{-1} and a positive band around 1665 cm^{-1}. If these bands are truly the result of different extent of deuterium-hydrogen exchange, it seems that the exchange rate is always slower in proteins complexed with GDP than complexed with other nucleotide analogs, i.e. IDP, GDPβS and 6-thioGDP. Results of exchange studies performed by tritium out-exchange ([91]), NMR spectroscopy ([92]) and theoretical modeling ([93]), which concludes that the deuterium-hydrogen exchanging rate is determined by the accessibilities of the catalysis ions (H^+, OH^- or H_2O) in water solution and by the strength of the hydrogen bonding between exchangeable hydrogens and hydrogen bond acceptors of the protein. In this later case, hydrogen bonds must be broken temporarily to allow the exchange to occur. Replacement of the natural ligand by GDP analogs in the active site of EF-Tu reduces protein-nucleotide affinity dramatically, and this may affect the hydrogen bonding between the ligand and protein and between protein hydrogen and protein acceptor groups. In contrast to the case of EF-Tu, which binds GTP one hundred times weaker than it binds GDP, *ras*-p21 has about two fold higher affinity for GTP than for GDP. Perhaps by checking the deuterium-hydrogen exchange characters of these different protein-nucleotide complexes, we may get an idea whether the differences in the affinities originate form hydrogen bonding and, if it is, how many hydrogen bonds are involved.

The first attempt to correlate the deuterium-hydrogen exchange rate with strength of hydrogen bonding performed on EF-Tu did not give a conclusive result. G-proteins are not quite suitable to begin such studies because of their high cost and low stabilities. A better choice might be ribonuclease. Raman spectroscopy has a special advantage to this type of study since the strength of hydrogen bonding is directly correlated with vibrational frequencies.

Sample preparation for Raman measurements usually takes more than five hours. The difference bands in amide I region were relatively small, usually 1 to 5 area percentage of the whole amide I peak. This may indicate that the hydrogen exchange rates for the two protein-nucleotide complexes differ only for very small amount (probably 4 to 20 hydrogens after 5 hours for a protein with about 400 residues, such as EF-Tu). When samples are incubated in the D_2O buffer, the spectroscopic effects of these very slowly exchangeable hydrogens may show up in a process that last for few days. This time range is very suitable for Raman studies.

Hydrogen-deuterium exchange experiments carried out previously by other more complicated methods have provide very useful information in understanding protein folding and protein dynamic structures ([91, 94, 95]). Raman technique has also been used to study such exchanges ([96]). Raman difference technique may turn out to be a more powerful tool to pursuing this type of research, if the idea discussed above can somehow be proved on a more solid basis. The difference Raman technique may have higher sensitivity than all the techniques used to date and also may provide conformational information of the slowly exchanging protons.

Figure 8.1: Raman spectra of EF-Tu•GDP and p21•GDP in H_2O buffer and in D_2O buffer. EF-Tu complex was at 2 mM in buffer R and excited with 100 mW of 488 nm argon laser light. *Ras*-p21 complex was at 3 mM in buffer R and excited with 100 mW of 530 nm argon laser light.

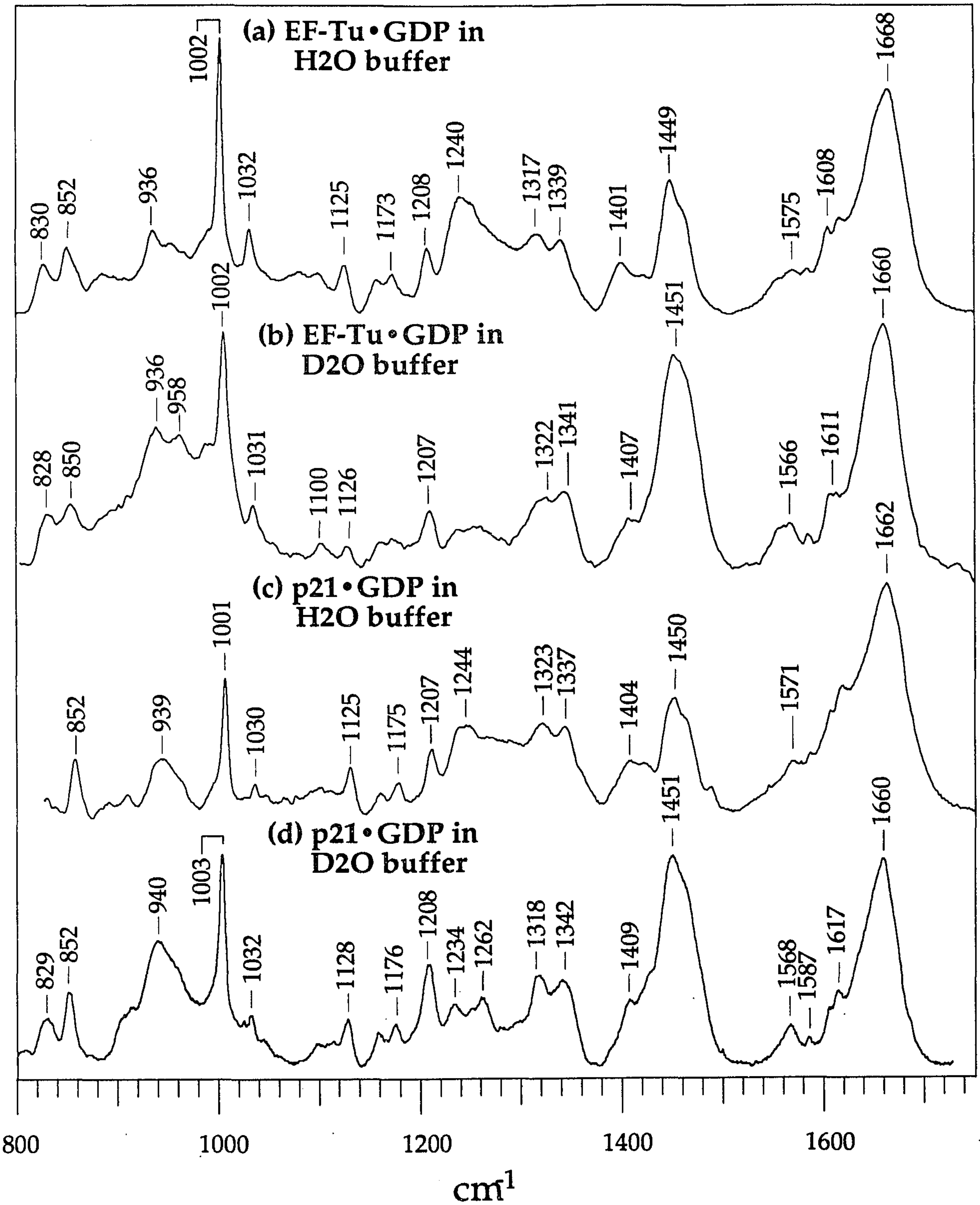
(a) EF-Tu•GDP in H2O buffer
(b) EF-Tu•GDP in D2O buffer
(c) p21•GDP in H2O buffer
(d) p21•GDP in D2O buffer
830
852
936
1002
1032
1125
1173
1208
1240
1317
1339
1401
1449
1575
1608
1668
828
850
936
958
1031
1100
1126
1207
1322
1341
1407
1451
1566
1611
1660
852
939
1001
1030
1125
1175
1207
1244
1323
1337
1404
1450
1571
1662
829
852
940
1003
1032
1128
1176
1208
1234
1262
1318
1342
1409
1451
1568
1587
1617
1660
800
1000
1200
1400
1600
cm-1

Figure 8.1

Figure 8.2: Raman difference spectra of GDP minus IDP in D_2O (a), in EF-Tu (b), and in p21 (c). The nucleotides were at ca. 100 mM, pH 7.4 and excited with 180 mW of 488 nm argon laser light. EF-Tu complex was at 2 mM in deuterated buffer R and excited with 100 mW of 488 nm argon laser light. *Ras*-p21 complex was at 3 mM in deuterated buffer R and excited with 100 mW of 530 nm argon laser light.

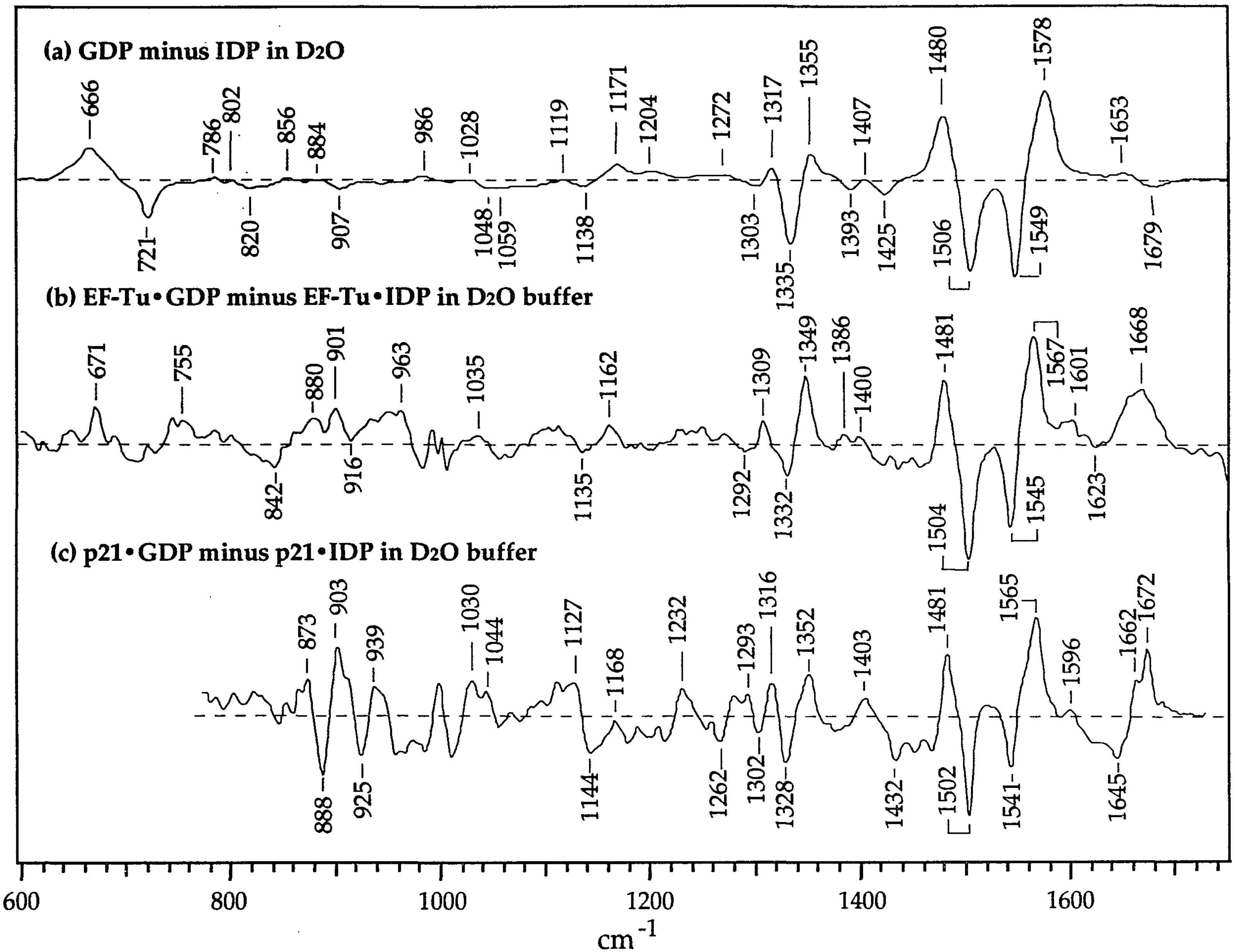
(a) GDP minus IDP in D2O
666
721
786
802
820
856
884
907
986
1028
1048
1059
1119
1138
1171
1204
1272
1303
1317
1335
1355
1393
1407
1425
1480
1506
1549
1578
1653
1679
(b) EF-Tu•GDP minus EF-Tu•IDP in D2O buffer
671
755
842
880
901
916
963
1035
1135
1162
1292
1309
1332
1349
1386
1400
1481
1504
1545
1567
1601
1623
1668
(c) p21•GDP minus p21•IDP in D2O buffer
873
888
903
925
939
1030
1044
1127
1144
1168
1232
1262
1293
1302
1316
1328
1352
1403
1432
1481
1502
1541
1565
1596
1645
1662
1672
600
800
1000
1200
1400
1600
cm -1

Figure 8.2

Figure 8.3: Raman difference spectra of GDP minus IDP in EF-Tu after incubated in deuterated buffer R for 4 hours (a), overnight (b), and for three days (c). The samples were at 2 mM and excited with 180 mW of 488 nm argon laser light.

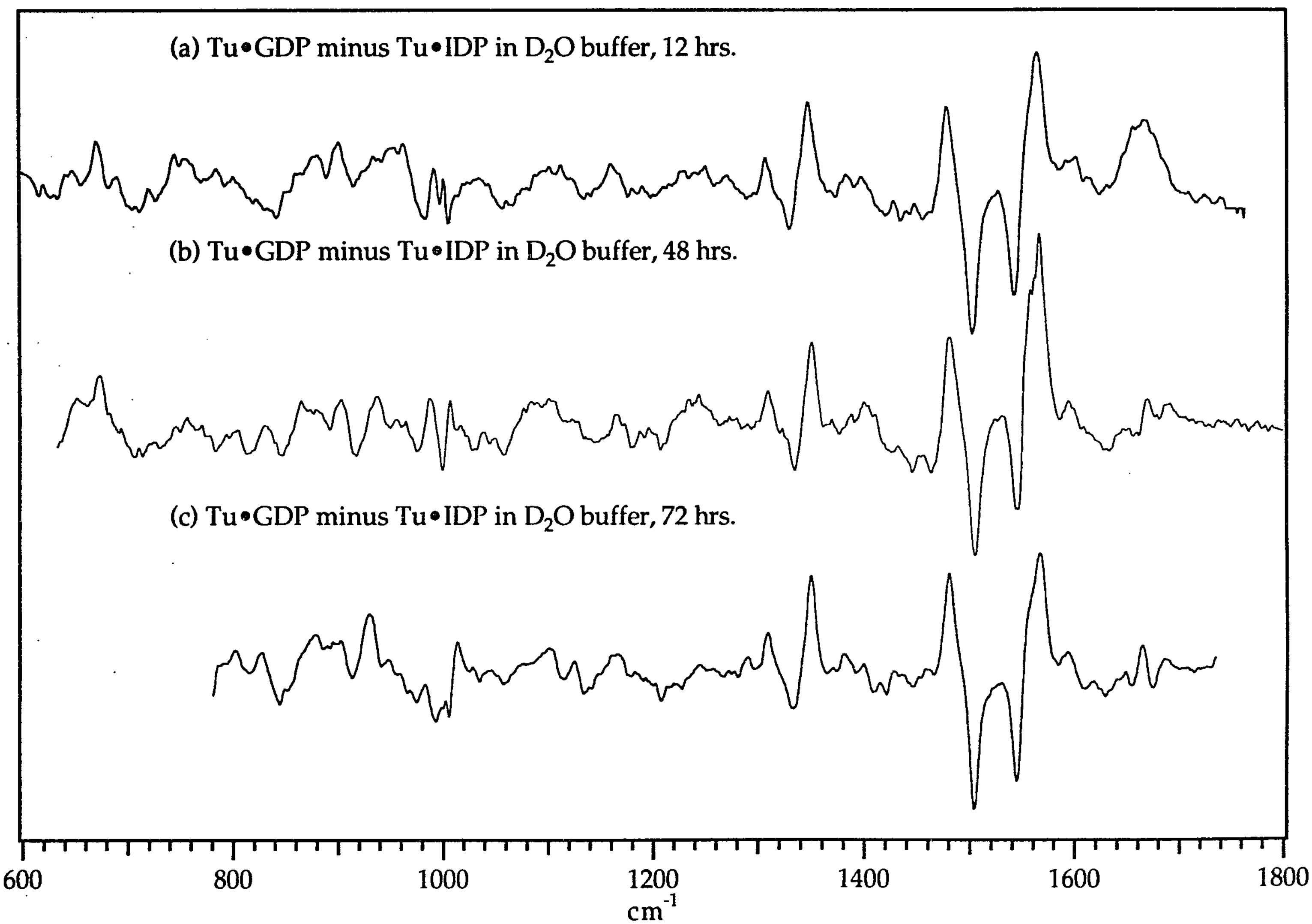
(a) Tu•GDP minus Tu•IDP in D_2O buffer, 12 hrs.
(b) Tu•GDP minus Tu•IDP in D_2O buffer, 48 hrs.
(c) Tu•GDP minus Tu•IDP in D_2O buffer, 72 hrs.
600
800
1000
1200
1400
1600
1800
cm^{-1}

Figure 8.3

Figure 8.4: Raman difference spectra formed between EF-Tu•GDP incubated in deuterated buffer R for different length of time. The samples were at 2 mM and excited with 100 mW of 488 nm argon laser light.

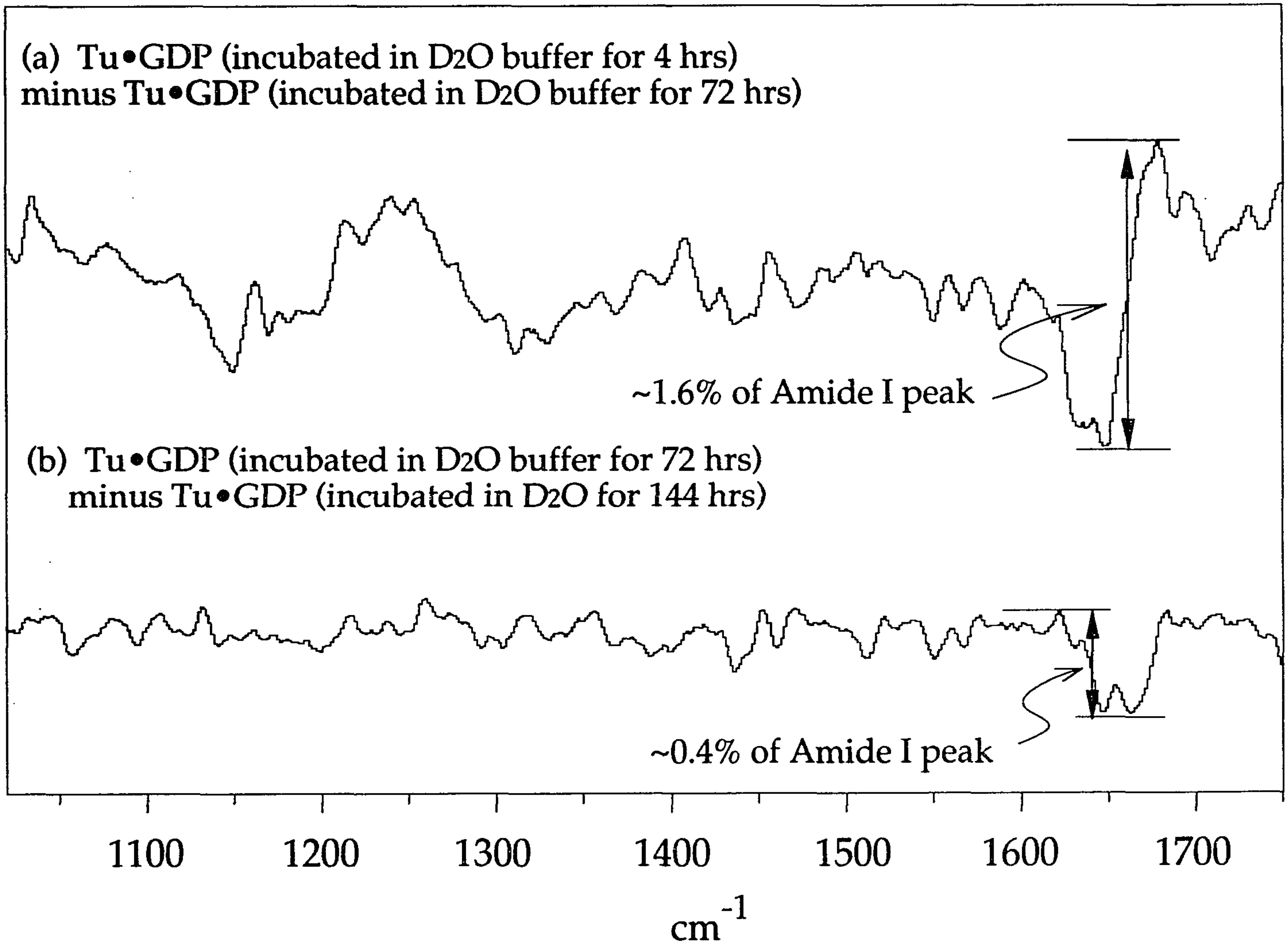
(a) Tu•GDP (incubated in D2O buffer for 4 hrs)
minus Tu•GDP (incubated in D2O buffer for 72 hrs)
~1.6% of Amide I peak
(b) Tu•GDP (incubated in D2O buffer for 72 hrs)
minus Tu•GDP (incubated in D2O for 144 hrs)
~0.4% of Amide I peak
1100
1200
1300
1400
1500
1600
1700
cm-1

Figure 8.4

Figure 8.5: Raman difference spectra of GDP minus GDPβS in D_2O (a) and in EF-Tu with deuterated buffer R (b). The nucleotides were at ca. 100 mM, pH 7.4 and excited with 180 mW of 488 nm argon laser light. EF-Tu complexes were at 2 mM in deuterated buffer R and excited with 100 mW of 488 nm argon laser light.

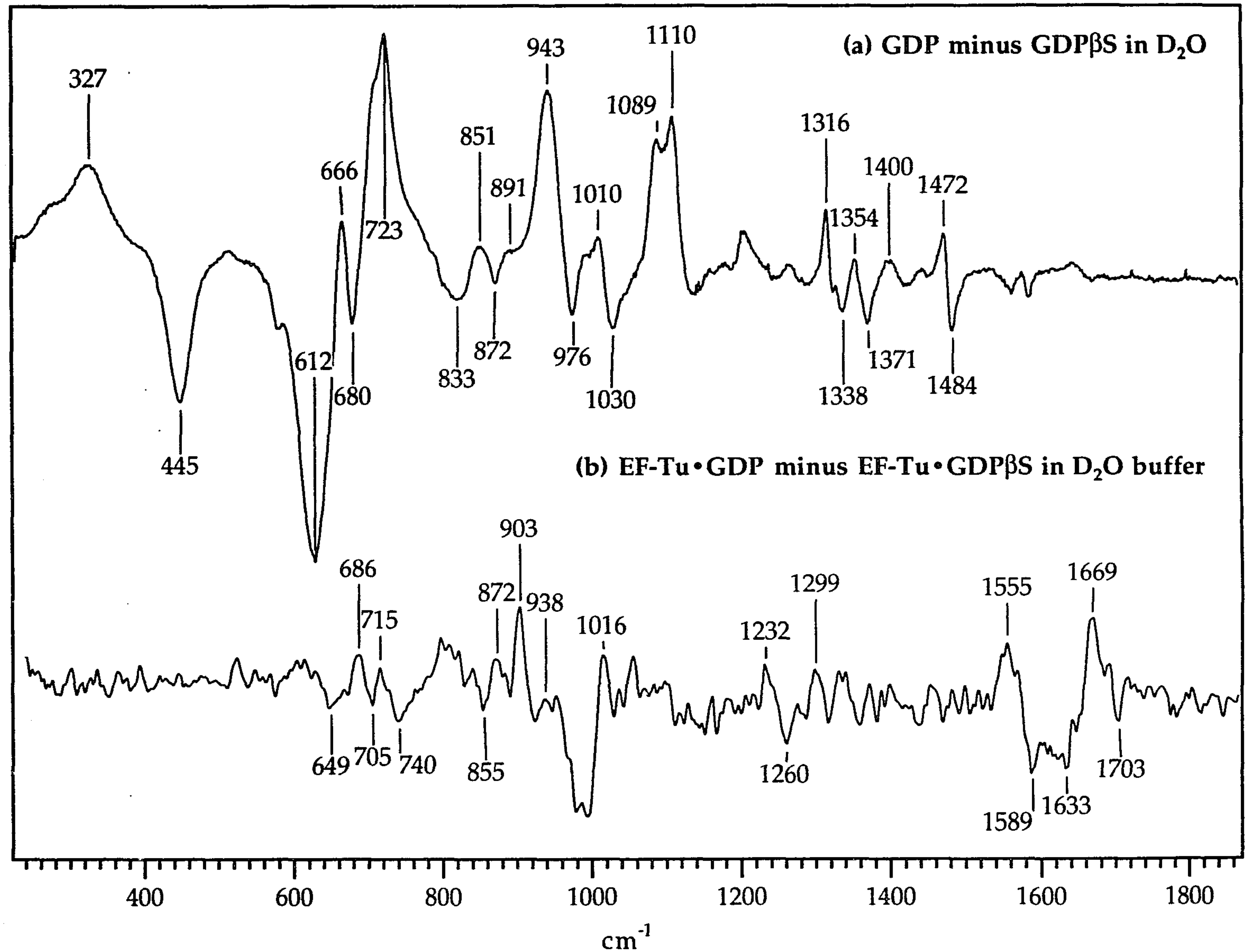
(a) GDP minus GDPβS in D₂O
327
445
612
666
680
723
833
851
872
891
943
976
1010
1030
1089
1110
1316
1338
1354
1371
1400
1472
1484
(b) EF-Tu•GDP minus EF-Tu•GDPβS in D₂O buffer
649
686
705
715
740
855
872
903
938
1016
1232
1260
1299
1555
1589
1633
1669
1703
400
600
800
1000
1200
1400
1600
1800
cm-1

Figure 8.5

Figure 8.6: Raman difference spectra of GDP minus 6-thio-GDP in D_2O (a), in EF-Tu with deuterated buffer R (b). The nucleotides were at ca. 100 mM, pH 7.4 and excited with 180 mW of 530 nm Kr^+ ion laser light. EF-Tu complexes were at 2 mM in deuterated buffer R and excited with 100 mW of 530 nm Kr^+ ion laser light.

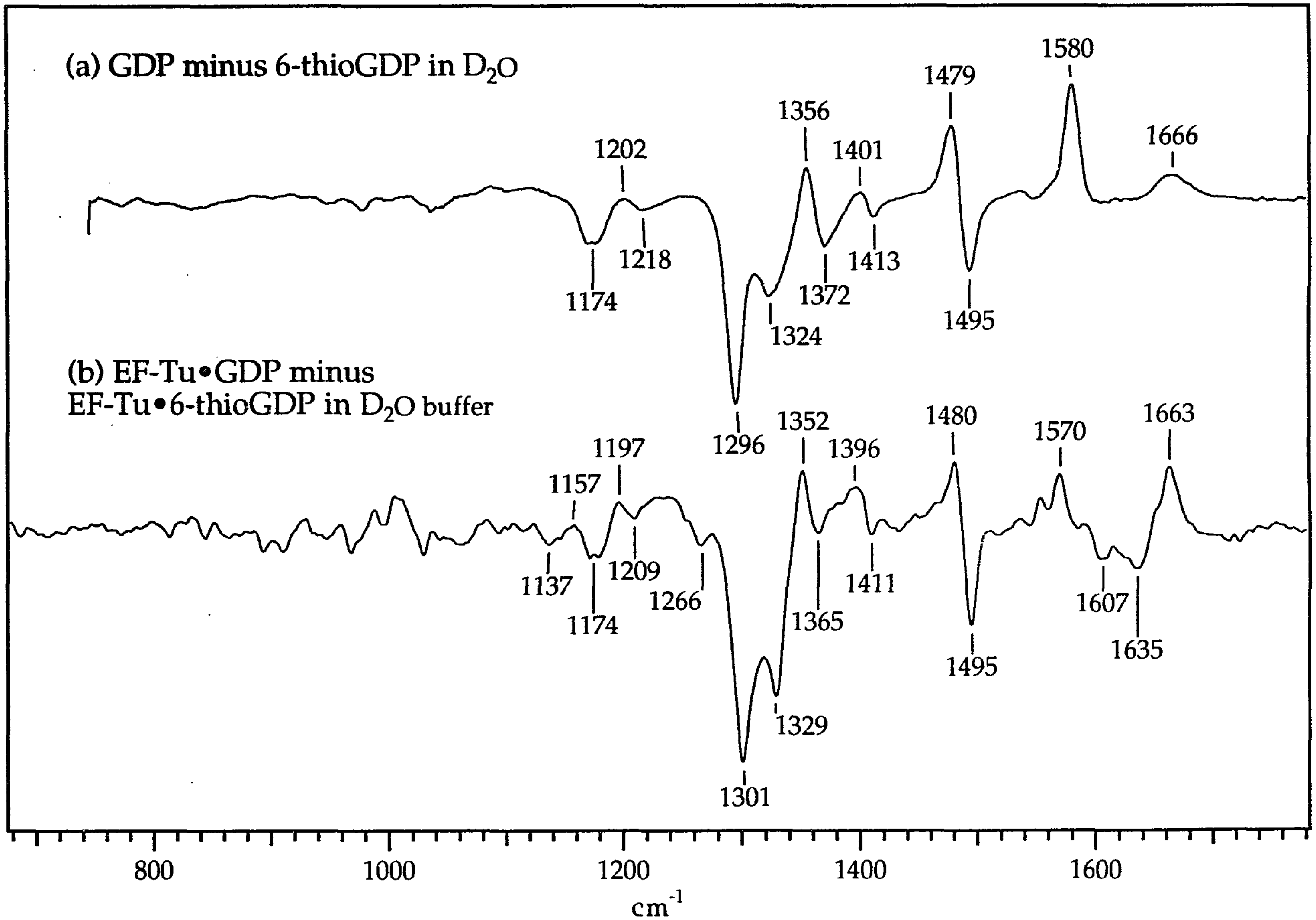
(a) GDP minus 6-thioGDP in D2O
1580
1479
1356
1202
1401
1666
1218
1174
1372
1413
1495
1324
1296
(b) EF-Tu•GDP minus
EF-Tu•6-thioGDP in D2O buffer
1352
1480
1663
1197
1396
1570
1157
1137
1209
1174
1266
1411
1365
1607
1635
1495
1329
1301
800
1000
1200
1400
1600
cm-1

Figure 8.6

Chapter IX

APPENDIX

A. Protein Activity Assays

The assays for EF-Tu and *ras*-p21 are based upon their binding ability to GDP. The activities of the proteins are measured by examining the extent of binding of ^{3}H-GDP to the proteins absorbed on to a cellulose nitrate filter.

Materials

Radioactive Mix: ^{3}H-GDP, 250ul (1.0mCi/ml, 22.5mCi/mg, from Amersham); 1mM GDP, 187µl; distilled water, 7813µl and absolute ethanol, 1.5ml. The absorption of the Mix at 260 nm is around 0.25.

Binding Buffer: 0.2 M $(NH_4)_2SO_4$; 0.2 M Tris-HCl, pH 7.4; 5 mM DTT; 1 mM NaN_3; 1 mM $MgCl_2$; 3 mM EDTA (for p21 assay only).

Wash Buffer: 10 mM Tris-HCl, pH7.4; 10 nmM $MgCl_2$.

Cellulose nitrate filters: 25 mm diameter (Millipore Corp, type HA or Schleicher and Schuell type C-5).

EF-Tu or p21: Absorption at 280 nm should be between 0.01 to 0.1 OD.

Method

An aliquot of 20 µl protein is added to a 10x20 mm test tube in a total volume of 200 µl, containing 50 µl binding buffer, 20 µl radioactive mix. The reaction mixture is allowed to equilibrate for 30 min room temperature, and is then diluted with 2 ml of wash buffer, filtered, and washed three times with 3-ml portions of the same buffer. The filters are dissolved in 4 ml of scintillation fluid

(Filtron-X, National Diagnostic Inc.), and radioactivity is measured in a scintillation counter.

Radioactive labeled GDP is expensive. The amount used can be determined by the accuracy required from the assay. To assay column fractions, 10 μl mix for each assay would be enough.

To assay EF-Tu, the incubation time can be reduced to 15 min. by increasing the temperature to 37°C.

B. Isolation of Plasmid DNA - Mini Prep

The following procedure is used to isolate multicopy plasmids from small cultures. It is one of a number of procedures developed to enable researchers to screen and characterize plasmids from large numbers of different strains.

Procedure:

1) Pellet cells from 5 ml overnight cultures with a GSA rotor, 6000 rpm for 10 minutes and re suspend each in 50 ml of 25% sucrose in H_2O.

2) Add 300 µl of M-STET (5% triton X-100, 50 mM EDTA, 50 mM Tris pH 8.0, 5% sucrose and mix well.

3) Transfer mixtures to 1.5 µl Eppendorf tubes and add 25 ml of 10 mg/ml lysozyme.

4) Heat tubes in boiling H_2O bath for 1 minuet and immediately chill on ice.

5) Centrifuge for 15 min. in microfuge and remove supernatant (about 200 µl) to a new Eppendorf tube.

6) Add 200 ml of ice cold isopropanol to precipitate nucleic acids. Freeze in dry ice-ethanol bath for 20 minutes.

7) Centrifuge for 15 min. in microfuge and drain supernatant on paper towel.

8) Dry pellets in vacuum system.

9) Resuspend pellets in 200 µl TE buffer (10 mM Tris pH 7.4, 1 mM EDTA).

10) Run the samples on 0.7% argrose gel.

C. Fermentation

High density fermentor (Lab-Line Instruments, Inc.) was used for growing cell in large quantities. The media is made up of two solutions, A and B.

solution A: Tryptone, 43 g; Yeast extract, 93 g; Glycerol, 20 ml; NaCl, 20 g; add water to 3,000 ml.

solution B: KH_2PO_4, 7.19g; K_2HPO_4, 60.48g; add water to 1.000 ml. The pH of solution B should be between 7.5 - 8.5.

The two solutions are autoclaved separately and mixed together after they cool down. 20 ml of 0.1 M $CaCl_2$, 20 ml of 1 M $MgSO_4$, and ampiciline (100 μg/ml) are filter-sterilysed and added to the culture.

Inoculum is grown in a 500 ml cell culture overnight and then added to the fermentor with the rest of media. The fermentation conditions are set to 37°C and air pressure 15 psi. After 2 hours growth, the cells are induced with 50 μM IPTG, 100 μg/ml of ampiciline and 50 ml of 50% glycerol are also added to the culture. The cells are harvested after further 8 hours.

Harvested cells are pelleted down by centrifugation and washed with buffer A for one to three times and then stored at -70°C.

D. The conformation of nucleotides

The free bases adenine, guanine, cytosine, uracil and thymine bear a hydrogen atom at positions 9 (purine) or 1 (pyrimidine) which in the nucleosides is replaced by the sugar moiety. A nucleotide is a nucleoside phosphorylated at one of the free sugar hydroxyls, generally the 5' position.

Relative to the sugar moiety, the base can adopt two main orientations about the glycosl C1'-N link, called *syn* and *anti* (Figure 9.1b).

The five-membered furanose ring is generally nonplanar. It can puckered in an envelope (E) from with four atoms in a plane and the fifth atom is out by 0.5 Å; or in a twist (T) form with two adjacent atoms displaced on opposite sides of a plane through the other three atoms. Two envelope conformations, $C_{2'}$-*endo* and $C_{3'}$-*endo* are shown in Figure 9.1c.

Figure 9.1: (a) The chemical structure of GDP.

(b) Definition of *anti* and *syn* conformational ranges according to ref ([97]). χ is defined as torsional angle $O_{4'}$-$C_{1'}$-N_9-C_4 for purine nucleoside, and torsional angle $O_{4'}$-$C_{1'}$-N_1-C_2 for pyrimidine nucleosides. In the figure, base is toward the viewer; the base is rotated relative to the sugar. In anti, the bulk of the hetercycles, is pointing away from the sugar, and in *syn* it is over or toward the sugar.

(c) Two envelope form of sugur puckering modes. In $C_{3'}$-*endo* conformation, $C_{2'}$-$C_{1'}$-$O_{4'}$-$C_{4'}$ are in a plane. In $C_{2'}$-*endo* conformation, $C_{1'}$-$O_{4'}$-$C_{4'}$-$C_{3'}$ are in a plane. Views in the figure are with this plane perpendicular to the paper.

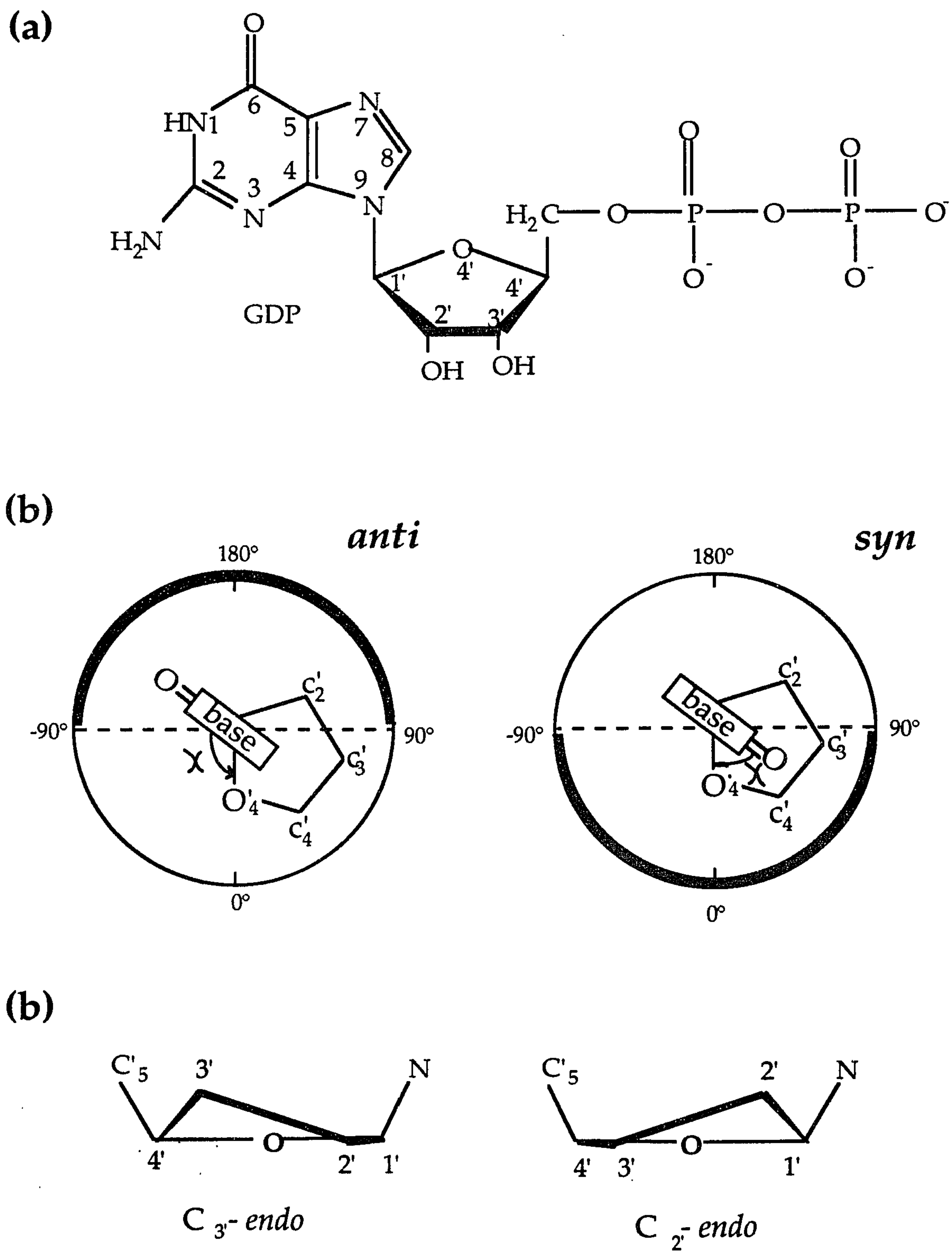

Figure 9.1

Chapter X

REFERENCES

1. Masters, S.B., R.M. Stroud, and H.R. Bourne, *Family of G Protein a- Chins: Amphiphatic Analysis and Predicted Structure of Functional Domains*. Prot. Engin., 1986. **1**: p. 47-54.

2. Wooley, P. and B.F.C. Clark, *Homologies In the Structure of G Binding Proteins: An Analysis Based On Elongation Factor Tu*. Bio/technology, 1989. **7**: p. 913-920.

3. Bourne, H.R., D.A. Sanders, and F. McCormick, *The GTPase Superfamily: Conserved Structure and Molecular Mechanism*. Nature, 1991. **349**: p. 117-127.

4. Bourne, H.R., D.A. Sanders, and F. McCormick, *The GTPase Superfamily: a Conserved Switch for Diverse Cell Functions*. Nature, 1990. **348**: p. 125-131.

5. Stryer, L., *Biochemistry*. 3th Edition ed. 1988, New York: W. H, Freeman and Company.

6. Parmegiani, A., *et al.*, *Properties of a Genetically Engineered G Domain of Elongation Factor Tu*. Proc. Natl. Acad. Sci. USA, 1987. **84**: p. 3141-3145.

7. Trahey, M. and F. McCormick, *A Cytoplasmic Protein Stimulates Normal N-ras p21 GTPase, But Does Not Affect Oncogenic Mutants*. Science, 1987. **238**: p. 542-545.

8. Pai, E.F., *et al.*, *Structure of the Guanine Nucleotide Binding Domain of the Ha-Ras Oncogene Product p21 in the Triphosphate Conformation*. Nature, 1989. **341**: p. 209-214.

9. Wolfman, A. and I.G. Macara, *A Cytosolic Protein Catalyzes the Release of GDP from p21ras*. Science, 1990. **248**: p. 67-69.

10. Tsai, *A Cytoplasmic Protein Inhibits the GTPase Activity of H-Ras in a Phospholipid-Dependent Manner*. Science, 1990. **250**: p. 982-985.

11. Pai, E.F., *et al., Refined Crystal Structure of the Triphosphate Conformation of H-ras p21 at 1.35 Å Resolution: Implication for the Mechanism of GTP Hydrolysis*. EMBO J., 1990. **9**: p. 2351-2359.

12. Spiro, T.G., ed. *Resonance Raman Spectra of Polyenes and Aromatics*. Biological Applications of Raman Spectroscopy, Vol. 2. 1987, Wiley & Sons: New York. 1-367.

13. Spiro, T.G., ed. *Resonance Raman Spectra of Heme and Metalloproteins*. Biological Applications of Raman Spectroscopy, ed. T.G. Spiro. Vol. 3. 1988, Wiley & Sons: New York. 1-565.

14. Chen, D., *et al., Classical Raman Spectroscopic Studies of NADH and NAD^+ Bound to Liver Alcohol Dehydrogenase by Difference Techniques*. Biochem., 1987. **26**: p. 4776-4784.

15. Deng, H., *et al., Classical Raman Spectroscopic Studies of NADH and NAD^+ Bound to Lactate Dehydrogenase by Difference Techniques*. Biochem., 1989. **28**: p. 1525-1533.

16. Yue, K.T., *et al., A Raman Study of Reduced Nicotinamide Adenine Dinucleotide Bound to liver Alchohol Dehydrogenase*. Biochem., 1984. **23**: p. 6480-6483.

17. Yue, K.T., H. Deng, and R. Callender, *Raman Difference Spectroscopy in Measurements of Molecules and Molecular Groups Inside Proteins*. J. Raman Spec., 1989. **20**(8): p. 541-546.

18. Deng, H., *et al., Hydrogen Bonding and Reaction Specificity in Lactate Dehydrogenase Studied by Raman Spectroscopy*. J. Phys. Chem., 1989. **93**: p. 4710-4713.

19. Yue, K.T., *et al., The Determination of the pK_a of Histidine Residues in Proteins by Raman Difference Spectroscopy*. Biochim. Biophys. Acta, 1991. **1078**: p. 296-302.

20. Deng, H., *et al., Molecular Properties of Pyruvate Bound to Lactate Dehydrogenase: a Raman Spectroscopic Study*. Proc. Nat'l. Acad. Sci. (USA), 1989. **86**: p. 4484-4488.

21. de Vos, A.M., *et al., Three-Dimensional Structure of an Oncogene Protein: Catalytic Domain of Human c-H-ras p21*. Science, 1988. **239**: p. 888-893.

22. Milburn, M.V., *et al., Molecular Switch for Signal Transduction: Structural Differences Between Active and Inactive Forms of Protooncogenic ras Proteins*. Science, 1989. **247**: p. 939-945.

23. Schlichting, I., *et al., Time Resolved X ray Crystallographic Study of The Conformational Changes in Ha-Ras p21 Protein On GTP Hydrolysis*. Nature, 1990. **345**: p. 309-315.

24. Jurnak, F., *et al., Three-dimentional Models of the GDP and GTP Forms of the Guanine Nucleotide Domain of E. Coli Elongation Factor Tu*. Biochim. Biophys. Acta, 1990. **1050**: p. 209-214.

25. Jurnak, F., *Structure of the GDP Domain of EF-Tu and Location of the Amino Acids Homologous to ras Oncogene Proteins*. Sci., 1985. **230**: p. 32-36.

26. la Cour, T.F.M., *et al., Structural Details of the Binding of Guanosine Diphosphate to Elongation Factor Tu from E. coli as Studied by X-ray Crystallography*. EMBO J., 1985. 4(9): p. 2385-2388.

27. Kaziro, Y., *The Role of Guanosine Triphosphate in Polypeptide Chain Elongation*. Biochim. Biophys. Acta, 1978. **505**: p. 95-127.

28. Clark, B.F.C., *et al., Structural Determination of the Functional Sites of E. coli Elongation Factor Tu*. Biochim. Biophys. Acta, 1990. **1050**: p. 203-208.

29. Wittinghofer, A., *et al., Three-Dimensional Structure of p21 in the Active Conformation and Analysis of an Oncogenic Mutant*. Envirom. Hlth. Perspec., 1991. (93): p. 11-15.

30. Valencia, A., *et al., GTPase domains of ras p21 oncogene protein and elongation factor Tu: Analysis of three-dimensional structures, sequence families, and function sites*. Proc. Natl. Acad. Sci. USA, 1991. **88**: p. 5443-5447.

31. Tu, A.T., *Raman Spectroscopy in Biology, Principles and Application*. 1982, John Wiley &Sons.

32. Yue, K.T., *et al., Raman Spectroscopy of Liver Alchohol Dehydrogenase.* Biochem. Biophys. Res. Comm., 1984. **122**: p. 225-229.

33. Eccleston, J.F. and D.R. Trentham, *The Interaction of Chromophoric Nucloetides with Subfragment 1 of Myosin.* Biochem. J., 1977. **163**: p. 15-29.

34. Breter, H. and H. Mertes, *The quantitative determination of metabolites of 6-mercaptopuring in biological meterials. VII, chemical synthesis by phosphorylation of 6-thioguanosine 5'-monophosphate, 5'-diphosphate and 5'-triphosphate and their purification and identification by reversed-phase/ion-pair high-performance liquid chromatography and by various enzymatic assays.* Biochimica et Biophysica Acta, 1990. **1033**: p. 124-132.

35. Fox, J., *et al., Thiation of Nucleosides. I. Synthesis of 2-Amino-6-mercapto-9-b-D-ribofuranosylpurine ("Thioguanosine") and Related Purine Nucleosides.* J. Amer. Chem. Soc, 1958. **80**: p. 1669-1675.

36. Sowa, T. and S. Ouchi, *The Facile Synthesis of 5'-Nucleotides by the Selective Phosphorylation of a Primary Hydroxyl Group of Nucleoside with Phosphoryl Chloride.* Bulletin of the Chemical Society of Japan, 1975. **48**: p. 2048-2090.

37. Leberman, R., *et al., A simplified Procedure for the Isolation of Bacterial Polypeptide Elongation Factor EF-Tu.* Anal. Biochem., 1980. **104**: p. 29-36.

38. Tucker, J., *et al., Expression of p21 Proteins in E. coli and Stereochemistry of the Nucleotide Binding Site.* EMBO J., 1986. **5**(6): p. 1351-1358.

39. Block, W. and A. Pingoud, *The Identification and Analysis of Nucleotide Bound to the Enlongation Factor Tu from Escherichia coli.* Anal. Biochem, 1981. **114**: p. 112-117.

40. Miller, D.L. and H. Weissbach, *Elongation Factor Tu and the Aminoacyl-tRNA:EFTu:GTP Complex.* Adv. Enzymol., 1974. **30**: p. 219-232.

41. Bradford, M.M., *A Rapid and Sensitive Method for the Quantitation of Microgram Quantities of Protein Utilizing the Principle of Protein-Dye Binding.* Anal. Biochem., 1976. **72**: p. 248-254.

42. Hall, A. and A.J. Self, *The Effect of Mg2+ on the Guanine Nucleotide Exchange Rate of p21 n-ras*. J. Biol. Chem., 1986. **261**(24): p. 10963-10965.

43. Mistou, M., R. Cool, and A. Parmeggiani, *Effects of ions on the intrinsic activities of c-H-ras protein p21. A comparison with elongation factor Tu.* Eur. J. Biochem., 1992. **204**: p. 179-185.

44. John, J., *et al.*, *Kinetics of Interaction of Nucleotides With Nucleotide- Free H-ras-p21*. Biochem., 1990. **29**: p. 6058-6065.

45. Darwish, A.A. and R.K. Prichard, *Analysis of Ribonucleotides by Reverse Phase HPLC Using Ion Pairing on Radially Compressed or Stainless Steel Columns*. J. Liq. Chromat., 1981. **4**(9): p. 1511-1524.

46. Bellamy, L.J., *The Infrared Spectra of Complex Molecules: Advances in Infrared Group Frequencies*. 2 ed. Vol. 2. 1980, London: Chapman and Hall. 1-299.

47. Eccleston, J.F., *Spectroscopic Studies ofthe Nucleotide Binding Site of Elongation Factor Tu from Escherichia coli. An Approach to Characterizing the Elementary Steps of the Elongation Cycle of Protein Biosynthesis*. Biochem., 1981. **20**: p. 6265-6272.

48. Noonan, T., *et al.*, *Interaction of GTP Derivative with Cellular and Oncogenic ras-p21 Proteins*. J. Med. Chem., 1991. **34**: p. 1302-1307.

49. Tsuboi, M., *et al.*, *Resonance Raman Spectroscopy and Normal Modes of the Nucleic Acid Bases*, in *Biological Application of Raman Spectroscopy*, T.G. Spiro, Editor. 1987, John Wiley & Sons:

50. Peticolas, W.L., *et al.*, ed. *Nucleic Acids*. Biological Applications of Raman Spectroscopy: Raman Spectra and the Conformations of Biological Molecules, ed. T. Spiro. Vol. 1. 1987, John Wiley and Sons: New york. 81-133.

51. Lane, M.J. and G.J. Thomas, *Kinetics of Hydrogen-Deuterium Exchange in Guanosine 5'-Monophosphate and Guanosine 3':5'-Monophosphate Determined by Laser Raman Spectroscopy*. Biochem., 1979. **18**(18): p. 3839-3846.

52. Nishimura, Y., *et al.*, *Conformation-Sensitive Raman Lines of Mononucleotides and Their Use in a Structure Analysis of Polynucleotides: Guanine and Cytosine Nucleotides*. J. Mol. Struct., 1986. **146**: p. 123-153.

53. Small, E.W. and W.L. Peticolas, *Conformational Dependence of the Raman Scattering Intensities from Polynucleotides. III. Order-Disorder Changes in Helical Structures*. Biopolymers, 1971. **10**: p. 1377-1416.

54. Lord, R.C. and N.T. Tu, *Laser Excited Raman Spectroscopy of Biomolecules: I. Native Lysozyme and its constituent amino acids*. J. Mol. Biol., 1970. **50**: p. 509-524.

55. Hwang, Y.-W. and D.L. Miller, *A Mutation that Alters the Nucleotide Specificity of Elongation Factor Tu, a GTP Regulatory Proteins*. J. Biol. Chem., 1987. **262**: p. 13081-13085.

56. Latajka, Z. and S. Scheiner, *Correlation Between Interaction Energy and Shift of the Carbonyl Stretching Frequency*. Chem. Phys. Letts., 1990. **174**(2): p. 179-184.

57. Wittinghofer, A., W.F. Warren, and R. Leberman, *Structural Requirements of The GDP Binding Site of Elongation Factor Tu*. FEBS Lett., 1977. **75**(1): p. 241-243.

58. Eccleston, J.F., *et al.*, *The Application of Fluorescent and Photosensitive Analogues of Guanine Nucleotides to the Function and Structure of G-binding Proteins*, in *The Guanine Nucleotide Binding Proteins*, L. Bosch, B. Kraal, andA. Parmeggiani, Editor. 1989, Plenum Press: New York. p. 87-97.

59. Delaria, K. and F. Jurnak, *Preparation of Escherichia coli Elongation Factor Tu - Guanosine 5'-Triphosphate Analogs*. Anal. Biochem., 1989. **177**: p. 188-193.

60. Thomas, J.G. and B. Prescott, *Structure Similiarity, Difference and Variability in the Filamentous Viruses fd, If1, IKe, Pf1, and Xf: Investigation by Laser Raman Spectroscopy*. J. Mol. Biol., 1983. **165**: p. 321-356.

61. Otto, C., F.F.M. De Mule, and J. Greeve, *A Raman Spectroscopic Study of the Interaction Between Nucleotides and the DNA Binding Protein gp32 of Bacteriophage T4*. Biopolymers, 1987. **26**: p. 1667-1689.

62. Thomas, J.G. and B. Prescott, *Studies of Virus Structure by Laser Raman Spectroscopy*. J. Mol. Biol., 1976. **102**: p. 103-124.

63. Ferreira, A.S. and J.J.G. Thomas, *Kinetics of Hydrogen-Deuterium Exchange and Kinetic Isotope Effects in Inosine-5'-Monophosphate and Inosine-3'5'-Monophosphate Determined by Laser Raman Spectroscopy*. 1981. **11**: p. 508-514.

64. Sheina, G.G., *et al.*, *IR Spectra of Guanine and Hypoxanthine Isolated Molecules*. J. Molec. Str., 1987. **158**: p. 275-292.

65. Medeiros, C.G. and J.J.G. Thomas, *Raman Studies of Nucleic Acids IV: Vibrational Spectra and Associative Interactions of Aqueous Inosine Derivatives*. Biochem. Biophys. Acta, 1971. **247**: p. 449-462.

66. Medeiros, G.C. and G.J. Thomas, *On the Tautomeric Structure of Inosine*. Bichim. Biophys. Acta, 1971. **238**: p. 1-4.

67. Psoda, A. and D. Shugar, *Spectral Studies on Tautomeric Forms of Inosine*. Biochim. Biophys. Acta, 1971. **247**: p. 507-513.

68. Tajmir-Riahi, H.A. and T. Theophamides, *A Fourier Transformatiom Infrared Study of the Electrophilic Attack at the N7-site of guanosine-5'-monophosphate*. Can. J. Chem., 1984. **62**: p. 266-272.

69. Colthup, N.B., L.H. Daly, and S.E. Wiberley, *Introduction to Infrared and Raman Spectroscopy*. 3rd ed. 1990, San Diego: Academic Press. 1-547.

70. Manor, D., *et al.*, *An Isotope Edited Classical Raman Difference Spectroscopic Study of the Interactions of Guanine Nucleotides With Elongation Factor Tu and H-ras p 21*. Biochem., 1991. **30**: p. 10914-10920.

71. Majoube, M., *Vibrational Spectra of Guanine. A normal Coordinate Analysis*. J. Mol. Struct., 1984. **114**: p. 403-406.

72. Kjeldgaard, M. and J. Nyborg, *Refined Structure of Elongation Factor EF-Tu from Escherichia Coli*. J. Mol. Biol, 1992. **223**: p. 721-742.

73. Joesten, M. and L.J. Schaad, *Hydrogen Bonding*. 1974, New York: Marcel Dekker, Inc. 1-622.

74. Thijs, R. and T. Zeegers-Huyskens, *Infrared and Raman Studies of Hydrogen Bonded Complexes involving Acetone, Acetophenone, and Benzopenone-I. Thermodynamic Constants and Frequency Shifts of the vOH and vC=O stretching Vibrations*. Spectrochemica Acta., 1984. **40A**(3): p. 307-313.

75. Delabar, J.-M. and W. Guschlbauer, *raman Spectroscopic study of 2H- and 15N- Substituted Guanosines: Monoers, Gels, and Polymers*. Biopolymers, 1979. **18**: p. 2073-2089.

76. Deng, H., *et al.*, *Resonance Raman Studies of the HOOP Modes in Octopus Bathorhodopsin with Deuterium Labeled Retinal Chromophores*. Biochem., 1991. **30**: p. 4495-4502.

77. Vinogradov, S.N. and R.H. Linnel, *Hydrogen Bonding*. 1971, New York: Van Nostrand Reinhold Company. 47-81.

78. Kaziro, Y., *et al.*, *Structure and Function of Signal-Transducing GTP-Binding Proteins*. Ann. Rev. Biochem., 1991. **60**: p. 349-400.

79. Deng, H., J. Burgner, and R. Callender, *Raman Spectroscopic Studies of NAD Coenzymes Bound to Malate Dehydrogenases by Difference Techniques*. Biochem., 1991. **30**: p. 8804-8811.

80. Grand, R.J.A. and D. Owen, *The Biochemistry of ras p21*. Biochemistry Journal, 1991. **279**: p. 609-631.

81. Sigal, I.S., *et al.*, *Mutant ras - Encoded Proteins With Altered Nucleotide Binding Exert Dominant Biological Effects*. Proc. Natl. Acad. Sci. USA, 1986. **83**: p. 952-956.

82. Wierenga, R.K., M.C.H. De Mayer, and W.G.J. Hol, *Interaction of pyrophosphate moieties with a-helices in dinucleotide binding proteins.* Biochem, 1985. **24**: p. 1346-1357.

83. Takeuchi, H., H. Murata, and I. Harada, *Interaction of Adenosine 5'-Triphosphate with Mg2+: Vibrational Study of Coordination Sites by Use of 18O-Labeled Triphosphates*. J. Am. Chem. Sco, 1988. **110**: p. 392-397.

84. Neal, S.E., *et al.*, *Kinetic Analysis of the Hydrolysis of GTP by p21N-ras*. The Journal of Biological Chemistry, 1988. **263**: p. p19718-19722.

85. Yu, N. and B.H. Jo, *Comparison of protein structure in crystals and in solution by laser Raman scattering. II. Ribonuclease A and carboxypeptidase A*. J. Am. Chem. Sco., 1973. **95**: p. 5033.

86. Yu, N.-T. and B.H. Jo, *Comparison of protein structure in crystals and in solution by laser Raman scattering*. Arch. Biochem. Chem., 1973. **250**: p. 2196.

87. Furano, A.V., *Content of elongation factor Tu in Escherichia coli*. Proc. Nat. Acad. Sci., 1975. **72**(12): p. 4780-4784.

88. Jonak, J., *et al.*, *N-Tosil-L-Phenylalanylchloromethane reacts with Cysteine 81 in the Molecule of Elongation Factor Tu from E. coli*. FEBS Lett., 1982. **150**: p. 485-488.

89. Li, H. and G. Tomas J. Jr., *Cysteine Conformation and Sulfhydryl Interactions in Proteins and Viruses. 1. Correlation of the Raman S-H Band with Hydrogen Bonding and Intramolecular Geometry in Model Compounds*. J. Am. Chem. Soc., 1991. **113**: p. 456-462.

90. Tu, A.T., *et al.*, *Laser Raman scattering of alph- and beta-methyl-D-glucosides*. Carbohydr. Res., 1977. **67**: p. 239.

91. Mallikarachchi, D., D.S. Burz, and N.M. Allewell, *Effects of ATP and CTP on the conformation of the Regulatory Subunit of Escherichia coli Aspartate Transcarbamylase in Solution: A Medium-Resolution Hydrogen Exchange Study*. Biochem., 1989. **28**: p. 5386-5391.

92. Patel, J.D. and L.L. Canuel, *Nucleor magneticd resonance studies of slowly exchanging peptide protons in cytochrome C in aqueous solution*. Proc. Natl. Acad. Sci. USA, 1976. **73**(5): p. 1398-1402.

93. Ellis, M.L., *Models for hydrogen exchange from folded proteins. II*. Biophys. J, 1978. **23**: p. 79-87.

94. Louie, G., *et al.*, *Allosteric Energy at the Hemoglobin Beta Chain C Terninus Studied by Hydrogen Exchange*. J. Mol. Biol., 1987. **201**: p. 755-764.

95. Kaminsky, S.M. and F.M. Richards, *Differences in hydrogen exchange behavior between the oxidized and reduced forms of Escherichia coli thioredoxin*. 1992. **1**(1): p. 10-21.

96. Thomas, G.J.J. and J. Livramento, *Kinetics of Hydrogen-Deuterium Exchange in Adenosine 5'-Monophosphate, Adenosine 3':5'-Monophosphate, and Poly(ruboadenylic acid) Determined by Laser-Raman Spectroscopy*. Biochem., 1975. **14**: p. 5210-5218.

97. Saenger, W., *Principles of Nucleic Acid Structure*. 1984, Springer-Verlag.